AD 443158

NA-64-603

North American Aviation, Inc.

SPECTRAL EMISSIVITY OF FLASH
COMBUSTION REACTION
FINAL TECHNICAL REPORT
(1 JUNE 1963 TO 31 MAY 1964)
CONTRACT Nonr 4236(00)

International Airport, Los Angeles 9, California
LOS ANGELES DIVISION

SERIAL NO.

NA-64-608

SPECTRAL EMISSIVITY OF FLASH COMBUSTION REACTION STUDY PROGRAM

FINAL TECHNICAL REPORT

CONTRACT Nonr 4236(00)

NR 012-505/4-24-63

PROGRAM CODE NO. 3730 1 JUNE 1963 to 31 MAY 1964

Dr. J. M. Gerhauser, Principal Investigator

ARPA Order No. 306-62

PREPARED BY

Avionic's Group

APPROVED BY

J. J. Pierro
Project Manager

DATE 6 July, 1964
NO. OF PAGES 152 + i thru viii

NORTH AMERICAN AVIATION, INC. / LOS ANGELES DIVISION
INTERNATIONAL AIRPORT • LOS ANGELES CALIFORNIA 90009

TABLE OF CONTENTS

LIST OF ILLUSTRATIONS

LIST OF ILLUSTRATIONS (Continued)

LIST OF ILLUSTRATIONS(Continued)

LIST OF ILLUSTRATIONS(Continued)

LIST OF TABLES

FOREWORD

As required by contract Nonr-4236 (00), this is the final report of the program for the study of spectral emissivity of flash combustion reactions. It covers the period 1 July 1963 to 31 May 1964 and is part of Project DEFENDER under the joint sponsorship of the Advanced Research Projects Agency, the Office of Naval Research, and the Department of Defense. The general objective of this study is the investigation of the factors that control the duration, brightness temperature, and spectral distribution of the radiant energy produced by chemical flashes.

The study is being carried out by North American Aviation as a joint program between the Avionics Department, Los Angeles Division, and the Research Department, Rocketdyne Division. The prime contract is with the Los Angeles Division.

The program contributors are Mr. J. J. Pierro, Mr. J. A. Macken, and Mr. P. N. Palanos of the Los Angeles Division and Dr. J. M. Gerhauser and Dr. G. R. Schneider of the Rocketdyne Division. Mr. D. Dickson of the Los Angeles Division is the report editor.

SECTION I

INTRODUCTION AND SUMMARY

Soon after the advent of lasers it was recognized that many applications would require high energy density laser devices. It was also obvious that the pumping subsystem presented one of the major obstacles in achieving high energy density. This prompted NAA/LAD to explore chemical reactions for pumping lasers because their high energy density indicated a great potential for filling this need. The first order feasibility of chemical pumping was established by NAA in October 1963 when a neodymium laser was successfully pumped by an aluminum-oxygen flash reaction. However, the information on basic radiation characteristics that was needed to evaluate the ultimate potential of chemical pumping was not available.

This study was initiated to provide the additional data required on maximum intensity, spectral distribution, duration, and efficiency of radiation emitted by high energy metal-oxygen reactions and the degree of control that might be achieved over these characteristics. The study has been carried out in four parts: 1) A detailed theoretical analysis of candidate reactions to select those with most promise from an energy per pound and intensity standpoint; 2) An experimental investigation of candidate reactions selected from step 1 to measure radiation intensity, spectral distribution, duration and efficiency; 3) A theoretical and experimental study of techniques to control these with emphasis on maximum intensity in the absorption bands of neodymium and ruby; and 4) an analysis of the inter-relationship of the chemical reaction and the laser

system to re-examine the potential of chemical pumping in the light of results from the above studies.

In brief, the study has shown: (a) several reactions produce brightness temperatures (1) above the approximate threshold temperatures for neodymium (3500°K to 5000°K) and ruby (5200°K) with a maximum of 6500°K (2) achieved; (b) the brightness temperatures are a strong function of pressure with highest temperatures achieved between 2000 psi and 50,000 psi; (c) except in the early stages of unpressurized reactions where line and band emission are present, the spectral distribution is a continuum, but not necessarily a black body distribution; (d) the time duration of the flash can be controlled to within 1/2 to 3 milliseconds; (e) that these reactions can be effectively used to pump high energy density laser systems.

A computer program, originally directed towards predicting adiabatic flame temperature in evaluating rocket propellant performance, was adapted to find potentially high flame temperature chemical reactions. The results of this program was the disclosure of several reactions that proceed at a temperature greater than 5500°K. Those reactions that were selected for experimental investigation were the oxidation of: (1) Aluminum, (2) Zirconium, (3) Hafnium, (4) Thorium, (5) Beryllium, and (6) Cyanogen. The last two were eliminated without testing due respectively to toxicity and low heat of combustion.

(1) Brightness Temperature: The temperature of a black body radiator which would produce an equivalent intensity at the portion of the spectrum being observed.

(2) See Section III for details of temperature measurement.

The experimental combustion phase was aimed at producing the highest possible temperature by varying the metal, the oxidizer, and the pressure of the reaction. It was found, both theoretically and experimentally, that higher temperatures were achieved with higher pressures. Two techniques were used to achieve higher pressures: (a) Dynamic pressurizing(3) of metal powder and solid oxidizer; and (b) pre-pressurizing metal wool with gaseous oxygen. The results achieved with these two techniques are shown graphically in Figure 1. This shows that the pressurized oxygen system produces brightness temperatures equivalent to those of dynamic pressurization, but at lower pressures. The highest brightness temperature, 6500°K, was obtained by the reaction of hafnium powder and potassium perchlorate under a pressure of approximately 40,000 psi. However, it can be seen from Figure 1 that temperatures greater than 6000°K are achieved at the much lower pressure of 1450 psi by pressurized oxygen. Some uncertainties exist in the value of maximum brightness temperatures measured at high pressure due to window clouding that occurs during the high temperature reaction. Results from several different tests have provided the basis for an estimate of the effect on light intensity measured and this was used to determine the brightness temperature of 6500°K inside the chamber.

The spectral distribution of these pressurized reactions are essentially black body with relatively constant brightness temperatures across the spectrum from 3660 Å to 6700 Å as shown in Figure 2. The extremely high pressures (20,000 to 60,000 psi) generated in the dynamic pressurization chamber was found to entirely suppress line and band emission from excited species present in the reaction zone.

(3) Dynamic Pressurization - Pressurization generated by containment of the chemical reaction.

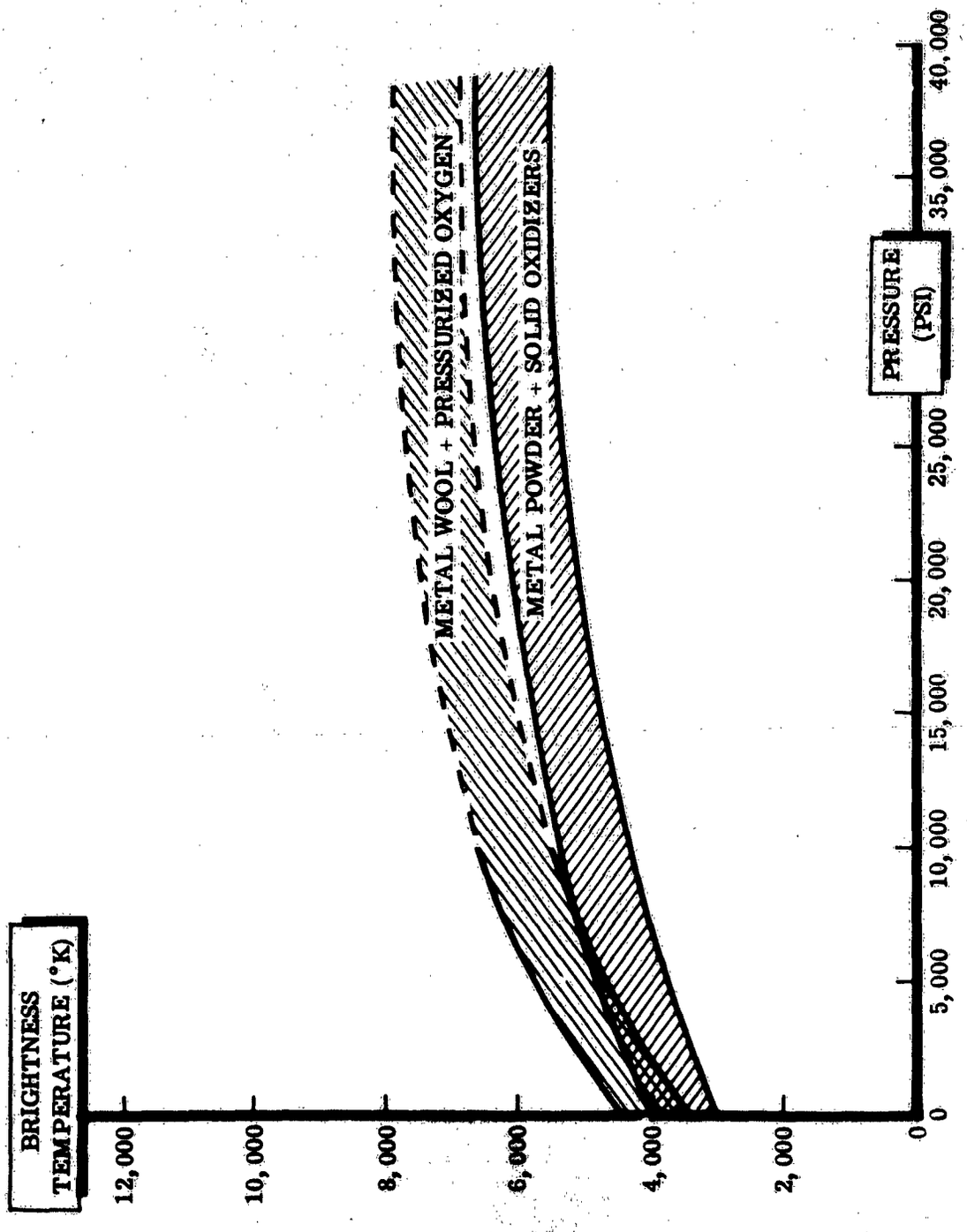

Figure 1. Brightness Temperatures Available From Chemical Reactions at Various Pressures

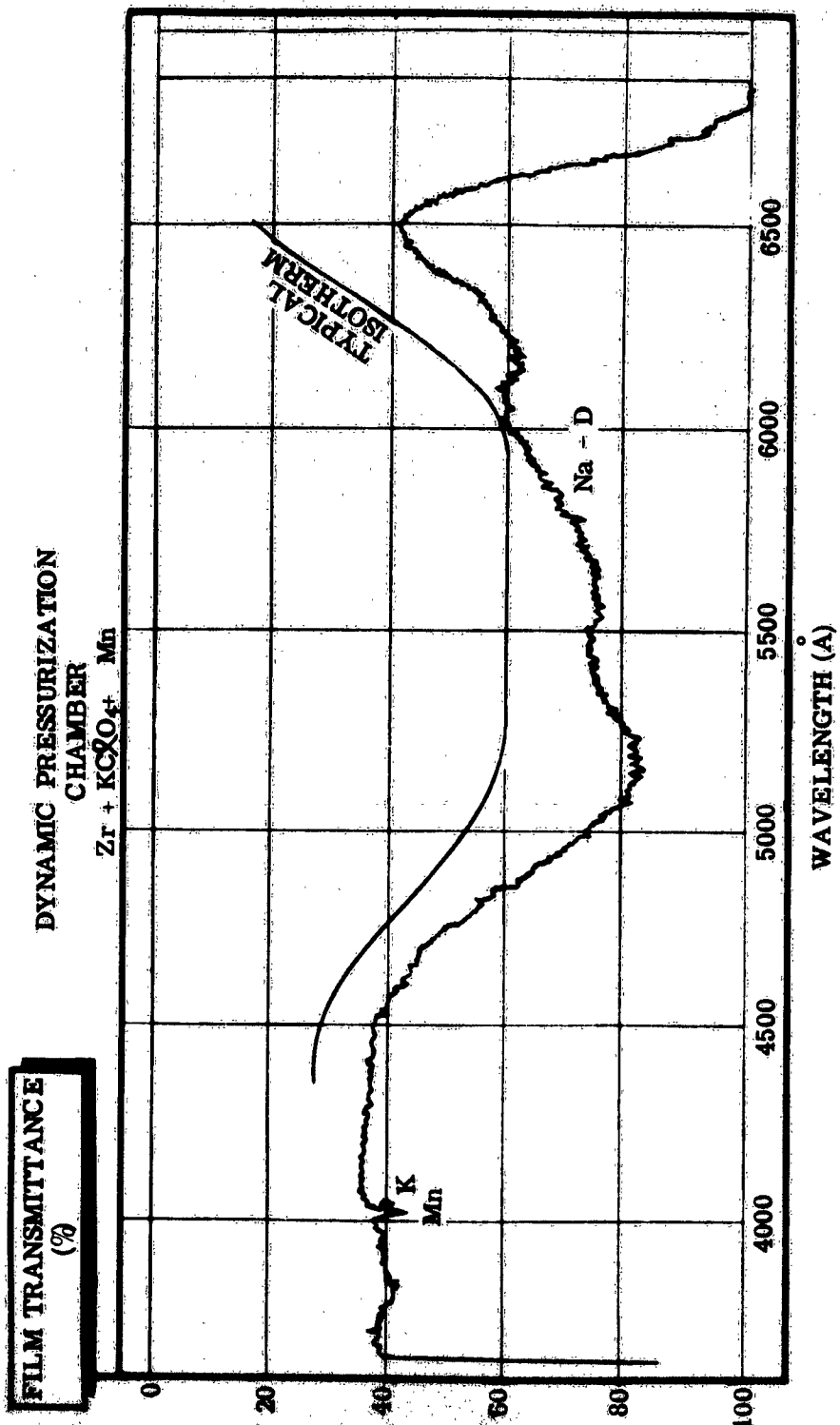

Figure 2 Densitometer Readout of Spectrographic Plate for $Zr + KClO_4 - Mn$

An important objective of the study was shaping the spectrum for more efficient use of the energy for pumping lasers. This was to be attempted through the use of dopants or non-equilibrium reactions. Non-equilibrium radiation was not observed in any of the experiments tried. Dopants produced some spectral shaping in the lower temperature reactions (below 4000°K) but gradually faded into continuum black body radiation as the pressure and temperature increased.

Studies of unpressurized solid oxidizer systems were conducted to determine the basic parameters controlling spectral distribution of the radiated energy and to determine the effect of dopants on the basic reactions. A series of basic reactions, including Zr + $KClO_4$, Hf + $KClO_4$, Th + $KClO_4$, Al + $KClO_4$, Mg + Al + $KClO_4$ and Mg + Al + $NaClO_3$, were studied intensively. The spectra of these reactions (Appendix II) show that major emission is continuum, characteristic of condensed species present in the flame, with line and band emission from vaporized oxide and metal species observable above the continuum background. An Al + $KClO_4$ time resolved spectrum is shown in Figures 3 & 4. The brightness temperatures observed were considerably below the adiabatic flame temperatures, indicating that emissivities were low and that considerable cooling was taking place. The cooling effect is also indicated by the strong line reversal observed in the sodium and potassium doublets.

Addition of dopants (salts, metals, and phosphors) produced no evidence of non-equilibrium radiation in the 3600 Å to 6700 Å interval. If non-equilibrium radiation was present, it could have escaped detection if it occurred in pulses much less than the 2 millisecond per frame exposure time used in taking the time resolved spectra, or if the emissivity

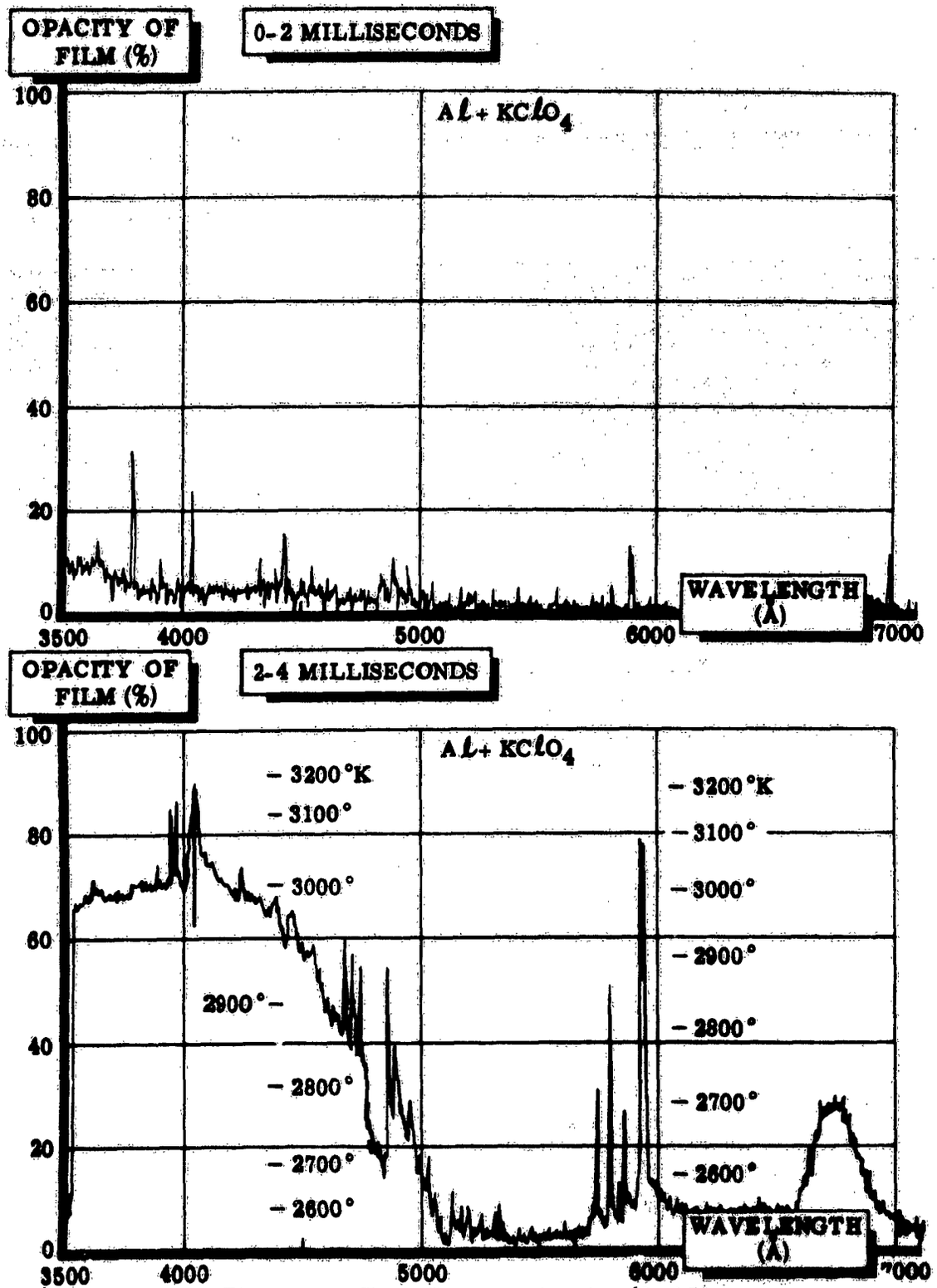

Figure 3. Time Resolved Spectra (1 & 2)

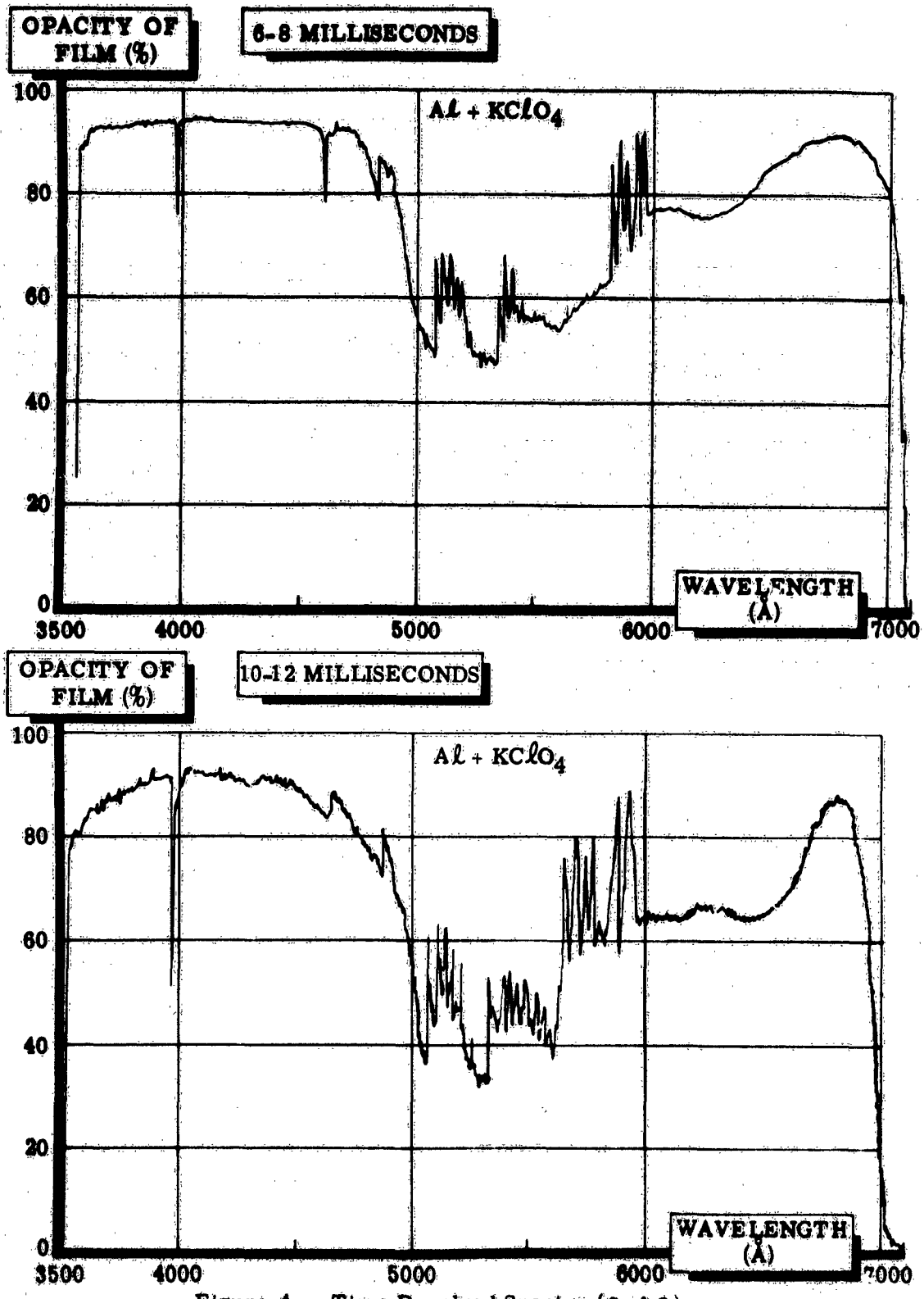

Figure 4 . Time Resolved Spectra (2 of 2)

of the non-equilibrium radiation was low.

Many of the additives tested with Al + $KClO_4$ formed radiative gaseous species that served to increase the energy radiated in certain spectral regions to levels achieved more slowly by the continuum; often these species would appear in absorption later in the flash. In Figure 5 for example, brightness temperature vs. wavelength plots are given for a flash at 2 to 4 msec. (early in the flash) and at 14-16 msec. (late). The BaCl band appears first in emission, then in absorption. Thus, if the radiation is required quickly or the continuum emissivity is low, dopants will prove useful for "spectral shaping".

Reaction duration has been observed to vary from 0.1 milliseconds to over 100 milliseconds. However, flash durations from 1/2 to 3 milliseconds are quite feasible. Several variables have been found to decrease reaction duration. These include pressurization, finer particle size, excess oxidizer, and increased packing density. Typical light pulses for the several reaction studies are shown in Figure 6 .

The efficiency of conversion of chemical energy to radiated energy was determined to be 25% for mixtures of aluminum and gaseous oxygen at one atmosphere pressure, while zirconium and oxygen converts about 40% of its energy into radiation. This amounts to about 1.6 million joules of radiated energy per pound of zirconium-oxygen mixture and 1.9 million joules radiated per pound of aluminum and oxygen. The brightness temperature for these reactions is about 4000°K for the zirconium and 3800°K for the aluminum. Increasing the brightness temperature by pressurizing the reaction is usually accompanied by a decrease in radiation efficiency to less than 10%.

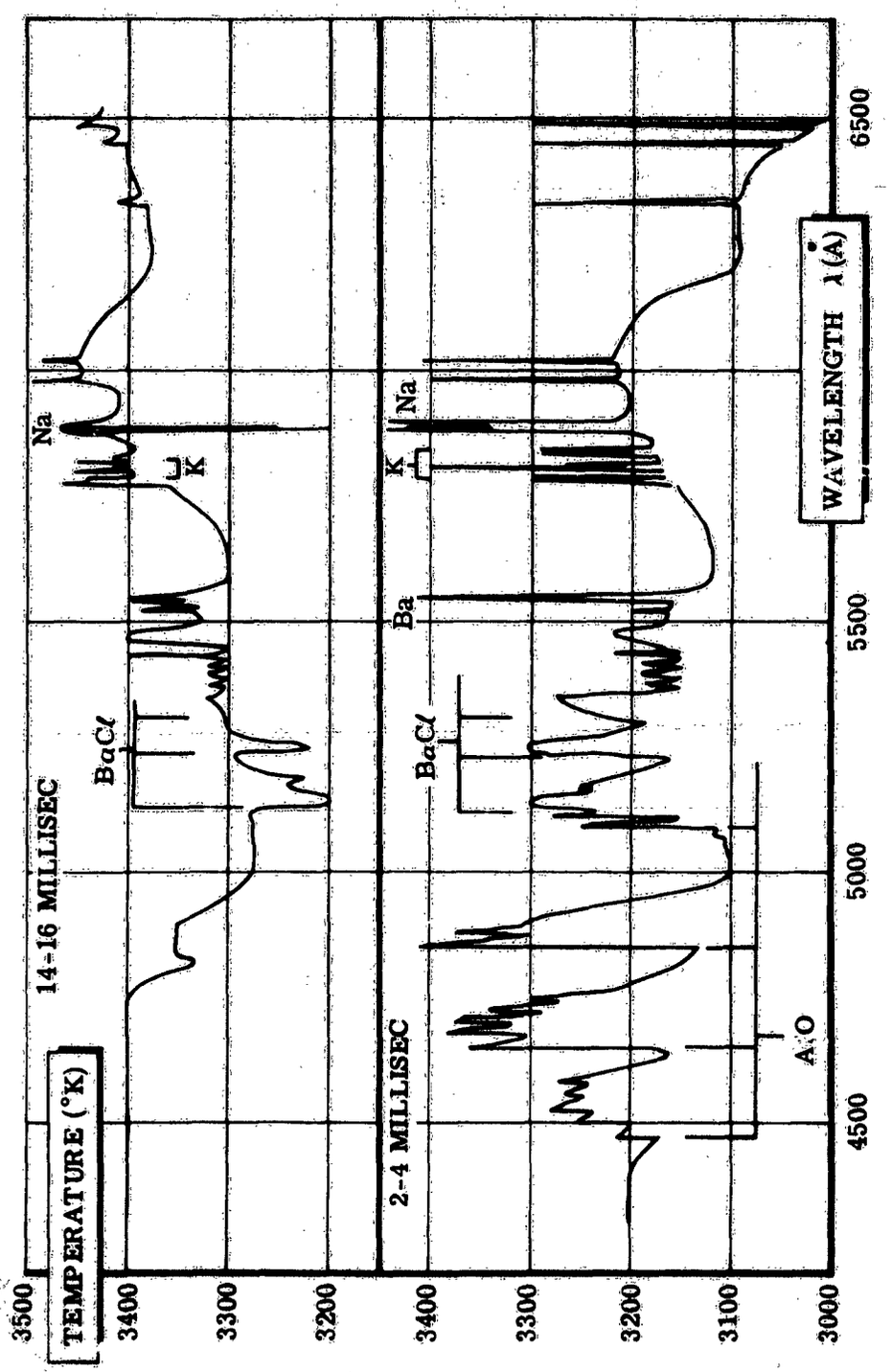

Figure 5 Temperature Versus Wavelength 40% Al + 30% $KClO_4$ + 30% $Ba(NO_3)_2$

$Mg + A\ell + Ba\,(C\ell O_3)_2$ 1 ATM

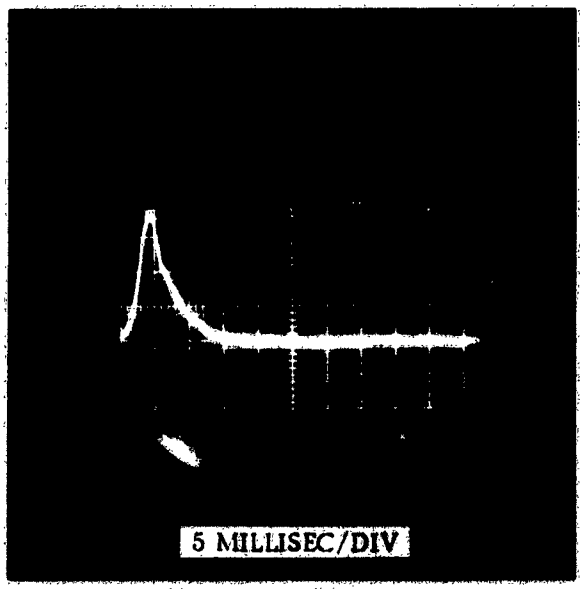

$Zr + O_2$ 625 PSI

Figure 6. Typical Intensity Per Time Pulse

The temperatures being produced are adequate to pump both ruby and neodymium lasers. For light weight high energy laser systems, several approaches appear interesting, but the one that offers the most promise is a neodymium oscillator amplifier with the amplifier pumped by unpressurized chemical reactions at 4400°K. The oscillator can be pumped by higher temperature pressurized oxygen reactions. This system offers high conversion efficiency from chemical energy to radiation and operates in the most efficient spectral region for neodymium. Also, it avoids possible weight penalties caused by pressurized reaction chambers.

While neodymium laser rods can be pumped by some of the unpressurized reactions it is necessary to achieve a higher pumping intensity to pump ruby because threshold pumping temperature is about 5250°K. To pump ruby there appears to be three possible approaches:

(1) Increase the temperature of the reaction through pressurization. Zirconium and hafnium reactions can produce temperatures significantly above the threshold temperature.

(2) Increase the intensity on the laser by cladding the rod. An intensity increase of up to a factor of three can be achieved by proper cladding.

(3) Provide an external fluorescent device to increase the brightness temperature in the pumping bands. Such a device can increase the intensity of the useful parts of the spectrum by greater than a factor of 10.

Combinations of these methods for increasing the intensity also appears feasible.

The experimental studies performed during the past year have served to delineate the expected operation of relatively simple chemical light sources. The characteristics and potential of the most promising reactions are well understood. The immediate future effort should be directed towards system applications and improvements.

It is recommended that the scope of the study contract be extended to include exploration of four areas: 1) basic laser system performance using a chemically pumped cavity; 2) oscillator - amplifier laser system; 3) laser cladding; and 4) fluorescent conversion. The object of the first area is to: 1) explore system problems and develop techniques and criteria of system design; 2) determine performance, particularly total system efficiency; and 3) optimize the design parameters through experiment. The objectives of the other three study areas are primarily to improve efficiency and reduce overall system weight. Unpressurized reactions can be used to pump neodymium laser amplifiers quite efficiently and at very high energy-to-weight ratios. Cladding the laser rod will increase the light intensity seen by the laser, thus increasing laser output and efficiency. Also, it appears that the proper application of fluorescent converters could further increase efficiency and decrease weight. This is expected to lead to the first practical portable high energy density laser system.

Section II

METAL BURNING MECHANISM SURVEY

Metal burning has been used for quite some time as a means of producing high luminosity flashes. Many metal oxidations are suited for this role as light sources by virtue of the high flame temperatures, the availability at the boiling point of the oxide of most of the chemical energy released, and the high emissivities of the burning metal-metal oxide particles.

Much of the recent literature on metal oxidation has been devoted to the details of the over-all physical processes involved. The reason for this interest is, of course, due to the use of metal powders in solid propellant formulations. There appears to be little controversy about the steps involved in the combustion processes of different metals. The observed behavior of the oxidation is correlated fairly well with the physical properties of the metal and its oxide. Pertinent physical properties are the size of the particle, the volatility of the metal relative to the oxide, and the solubility of the oxide in the metal. When the metal boils at a lower temperature than the oxide, the reaction is observed to take place in the vapor phase (e.g., Mg, Li, Ca, K, Na). The diffusion flame surrounding the particle feeds heat back to the particle to keep the metal boiling and diffusing into the reaction zone. With less volatile metals, such as Zr, Ti, Be and Al the metal oxides are formed on or very near the surface of the metal particle. A deposit of the metal oxide forms around the particle and, depending on the rate of heat loss from this object, it can (a) shatter into smaller burning droplets from the pressure generated by the boiling metal interior, (b) burn slowly as

oxygen diffuses in or metal vapor diffuses out of the liquid oxide layer, or (c) extinguish if heat losses cause the metal oxide film to solidify and reduce oxygen and metal diffusion rates.

Metals such as Si and B have oxides that boil at temperatures lower than the metal boiling points, and one would expect no oxide film over the particle. Whether the metal evaporation or oxygen diffusion would limit the combustion process would depend on the surface temperature of the exposed metal.

Fassel, Papp, Hildenbrand and Serrika (1) have examined the combustion of metal powders, paying particular attention to the Al-Mg alloys with slight additions (2%) of Li, Ti, B, V, Zr, Mo, Cr, Ni, and Mn. The additives were observed to decrease the burning rate of the Al-Mg alloys by about a factor of six. The particles were burnt in a natural gas torch and solid combustion products were trapped for analysis. Many of the large oxide particles were found to be hollow shells of oxide sometimes containing a smaller spherical droplet of the metal alloy. Based on their results, the authors have proposed a model for the combustion process that is quite similar to that presented above.

Gordon (2) reported studies being conducted on burning metals, alloys, metal hydrides, carbides, nitrides and borides. The particles were carried in an oxygen stream using an annular natural gas - air pilot flame for ignition. Streak photos taken of single burning particles were used to determine burning rates, ignitability and the physical processes of importance. Nebulous streaks and high burning rates were taken as evidence

of a diffusion flame (e.g., MgH_2, LiH and CaH_2) while sharply defined streaks of considerable length indicated surface burning (e.g., Ti, Zr, TiC, TiAl, TiB_2 and ZrN). Components of alloys having widely different volatilities were found to burn serially - the most volatile being distilled off first and burned (e.g., LiAlH -- hydrogen first, then Li leaving the burning Al particle behind). The size of the particles burnt by Gordon ranged around 44 microns.

Boron combustion was studied by Talley (3). This metal is of interest here because its oxide boils at a lower temperature than the metal. Interpreting the data obtained from burning boron rods in oxygen, Talley defines two possible rate limiting steps at temperatures above the ignition point, evaporation rate of B_2O_3 at 2000°K and diffusion of O_2 through B_2O_3 vapor to the B surface at T = 2480°K. These results again fit into the mechanism initially outlined.

Wood (4) has taken photos of burning metal particles in 0.4 mm x 5 mm ribbons of solid propellant. His observations are that Zr and Si do not burn with diffusion flames while Al and Mg do. The burning Al and Mg particles were sometimes seen to terminate in a flash or burst, suggesting that a boiling metal surrounded by an oxide coating is not always needed for droplet shattering.

Metal combustion processes have been analyzed using spectroscopic techniques by Brzustowski and Glassman (5). Spectra were taken of burning magnesium ribbons at low pressures in various oxidizing media and of burning Al and Zr foils in commercial flashbulbs containing O_2. The spectra

of Mg combustion taken as a function of pressure clearly indicated the MgO vapor exists at the highest temperature of the system. Higher pressures led to increased MgO condensation in the neighborhood of the high temperature reaction zone, and thus a rise in intensity of continuum radiation. This is in agreement with the work of Coffin (6) who burnt Mg ribbons in various gas compositions. The flame around the ribbon was noted to have a definite structure; the light intensity was greatest a short distance from the ribbon, suggesting reaction in the vapor phase. The flash reactions of Al, investigated by Brzustowski and Glassman using time resolution spectroscopy, showed the presence of AlO, Al and a continuum attributed to solid Al_2O_3. The lines of Al appear in emission early in the flash and in about 5 milliseconds reverse in the increasing continuum intensity. AlO bands appear early and at peak flash intensity are seen to merge with the continuum. Near the end of the flash the bands of AlO and Al are again seen in emission. The Zr foil flash shows Zr and ZrO lines in emission throughout the reaction. Brzustowski and Glassman state that Zr, ZrO, and AlO always appear in emission because they exist near the peak flame temperature as decomposition products of Al_2O_3 and ZrO_2. An analysis of the combustion products shows much of the Al_2O_3 to be about 5 microns in size while the ZrO_2 consists of spherical particles ranging from 15 to 700 microns. Because of the particle sizes in the oxide residue, the authors are of the opinion that Al burnt in the vapor phase while Zr burnt on the surface of the particles. Reference is made to unpublished data of Ratenberg and Johnson (G.E. Company) consisting of Fastax moving pictures of the flash. The movies, according to the

authors, clearly shows particle burning of Zr and a nearly homogeneous volume of light for the Al flash bulb.

Using photographic photometry Markstein (7) measured reaction rates in diffusion flames of magnesium. The data are reported to favor a first order rate expression independent of O_2 concentration. Spectra taken of the luminescence of growing MgO deposits and of the flame showed a similar blue continuum at low pressures. This information coupled with a study of possible homogeneous kinetic mechanisms producing MgO has lead Markstein to suggest the possibility of a heterogeneous reaction on the surface of the MgO particles.

Aluminum particle burning studies have been published recently by Friedman and Macek (8, 9). It was found that aluminum particles injected into a hydrocarbon flame would ignite at temperatures corresponding to the melting point of the oxide. Further experiments in which the aluminum was ignited and burnt using $CO-O_2-N_2$ flames lead to the conclusion that there are distinct effects of H_2O on the metal combustion. Significant amounts of H_2O are stated to impede the process by some unknown means. I. Glassman (9) has taken issue with Friedman and Macek concerning any effect of H_2O on the metal burning process. More recently, Macek, Friedman and Semple (10) have used a similar technique to study beryllium burning and to verify the fact that H_2O does affect aluminum burning. The fact that Be boils at a temperature slightly lower than the melting point of the oxide makes the determination of an ignition point somewhat tricky.

For many years A. V. Grosse of Temple University has been investigating means of producing high temperature with chemical reactions. A great deal of this work dealt with metal burning. Most of the metal burning effort by

A. V. Grosse and his co-workers has been summarized in a recent report by Grosse and Conway (11). Some thermodynamic data on metals and their oxides are presented, along with a list of adiabatic combustion temperatures computed for many metals. Although the rare earths were ignored in this compilation (undoubtedly because of a lack of thermodynamic data on them), their position in the periodic table suggests they might hold promise as a means of producing high temperature. The list indicates the metals producing the highest temperatures would be La, Th, Hf, Al, and Be. The flame temperature is reported as effectly limited by the boiling point of the metal oxide; thus, increasing the total pressure on the system should lead to higher flame temperatures. Grosse and Conway state that combustion of Al at 10 atm. will produce a temperature of 4400°K compared to 3800°K at 1 atm. Also presented in this work were some descriptions of metal powder - oxygen torches.

A paper by Doyle, Conway, and Grosse (12) describes some special techniques used in stabilizing a Zr - O_2 flame. A temperature of 4930°K is calculated for the flame, but no actual experimental measurements of flame temperature are reported. The luminosity of a burner consuming 248 gr Zr/min and 90 liters O_2/min is reportedly about 200,000 candle power.

A report by Grosse's group summarizing work done on powdered metal flames up to 1953 gives detailed information on powdered metal torches and reports a temperature of 3280°C for the aluminum - O_2 flame determined by an optical pyrometer (14). Conway and Grosse have written a final report (13) on the work funded by ONR up to 1954. Some of this material has been covered in another paper (12).

Another report from Temple University by Grosse and Stokes (15) dwells briefly on the combustion of beryllium powder (-200 mesh) in oxygen. The metal is reported to be more difficult to ignite than aluminum powder, presumably because of its higher melting point and lower vapor pressure. The Be torch was ignited from an acetylene pilot flame when a hydrogen pilot proved insufficient. No measurements of the Be-O_2 flame temperature were made, but a rough estimate by Grosse and Stokes indicates it may be about 4500°K.

The combustion of Ti and Zr wires was studied by Harrison (16,17). The results indicated no substantial vaporization of the metal takes place--combustion takes place at the surface of the metal liquid. Combustion of the zirconium wire in gases containing less than 50% O_2 was eventually quenched by a thick ZrO_2 layer that hindered diffusion of O_2 to the metal surface. This experiment illustrates the importance of physical properties of the material in controlling burning rates. The results are probably only of very limited applicability to particle burning, since the rate limiting physical processes will undoubtedly change.

Relatively little published work is available on metal-oxygen reactions as light sources and what is available is confined primarily to Al-O_2 reactions. Some data on Zr-O_2 flashlamps is presented in a report already discussed (5).

Although earlier work by Brockman (18) on commercial Al photoflash lamps was interpreted as indicating most of the radiation was emitted from incandescent gases and 3% of the total light output over the range from 3000 A to 7000 A came from excited AlO, a more recent investigation by Rautenberg and Johnson (19) has shown the radiation to be primarily

from Al_2O_3 solid and the AlO to be thermally excited. Rautenberg and Johnson also attempted to measure brightness temperatures of the reaction in various G.E. photoflash lamps. The temperatures were close to 3800°K, suggesting a temperature limited by the boiling point of Al_2O_3.

A number of reports on photoflash lamps have been written by G.E. (e.g., 20) and by other lamp manufacturers but are not available because they contain proprietary information.

Brightness temperature "well above 3800°K" were reported as being reached in certain regions of the flash of experimental conical burster T86E5 aluminum metal dust photoflash bombs during the first 2 milliseconds. Temperatures of other photoflash bombs were also measured. The method used involved high speed photographic pyrometry with a claimed accuracy of 25°K (21).

Eppig and Hart (22) reported measurements on spectra of Mg and Mg-Al alloy flash bombs. The emitters were identified as oxide bands and solid particles. A temperature of 3500°K was reported for the continuum by a black body curve fitting technique of questionable applicability.

The optimum ratios of Al, $KClO_4$, $Ba(IO_3)_2$ for maximum light output were investigated by Sarner and found to be 40%, 30%, 30% respectively (23). This photoflash composition is apparently a standard one for the military. Some tests on the Zr/$KClO_4$ system showed the 72% Zr + 28% $KClO_4$ mixture to be the most efficient zirconium containing system (25).

In other studies carried out at Picatinny data were gathered on the behavior of flash bombs at high altitudes (24,25). High altitude in general increases burning time, decreases light output (with some exceptions) and causes more ignition difficulties.

Several of the flash compositions investigated underwent only a slight decrease in light output in going from sea level to 100,000 feet.

The effect of particle size on the performance characteristics of a 40% Al, 60% $KClO_4$ flash composition has been examined (26). The conclusions were that the larger sizes degraded the light output; a particle size less than roughly 17μ was suggested for good performance.

Some of the work performed on colored pyrotechnic composition by Faurel (27) might be applicable to the present dopant study. Tests were made with tellurium and thallium additives in a search for a green light. Neither of the two was satisfactory. In further tests the best green radiator was found to be BaCl.

Hershkowitz, Schartz, and Kaufman (28) have performed various measurements on Al/$KClO_4$ burning. They reported the existence of two burning velocities and presented a possible interpretation of this result. Using photographic techniques, a temperature of 3500°K was reported for the continuum.

A recent report by Edse, Reo, Strauss, and Mickelson (29) has described the construction of an Al - O_2 flame apparatus and an investigation of the usefulness of the metal-oxygen flame as a spectroscopic source. The relative intensity of the Al-O_2 flame is reported to compare quite favorably with that of the carbon arc.

High temperature flames can, of course, result from the combustion of nonmetal fuels. The flame temperatures in homogeneous systems will be limited by the dissociation of the combustion products. There is no large amount of energy available at any single temperature as is found, for instance, at the boiling point of the metal oxide in metal-oxygen systems.

A summary of the work carried out at Temple University over a ten year period (15) includes a large amount of work on cyanogen (C_2N_2) and other related compounds of the carbon, nitrogen, and oxygen system. The following calculated flame temperatures have been reported for C_2N_2 in 1:1 mole ratios.

1 atm	4835 ± 50°K
2	4900
5	4985
6.8 (100 psia)	5015
10	5050

Conway, Smith, Liddell, and Grosse (30) reported burning premixed C_2N_2 and O_2 at 100 psia using a slight preheat to avoid condensation.

A few compounds of the N:C.(C:C)$_n$ C:N series have been produced and burnt in O_2: the flame temperatures reported, however, were calculated, not measured, but should be fairly accurate.

	1 atm	10 atm	40.82 atm (600 psi)
$(C_4N_2)_{gas} + 2O_2 \longrightarrow 4CO + N_2$	5261	5573	5743
$(C_4N_2)_{gas} + 4/3O_3 \longrightarrow 4CO + N_2$	5516	5936	6100

The combustion of C_2N_2 in NO was reported as being capable of producing higher flame temperatures than C_2N_2 with O_2 (4865 as compared with 4835°K).

Some flame temperatures have also been calculated from experiments on hydrogen cyanide - fluorine - oxygen flames by Grosse and Co-workers (15). The reaction stoichiometry $2HCN + F_2 + O_2 \longrightarrow 2HF + 2CO + N_2$ was found to be correct and the theoretical flame temperatures were calculated to be 3950°K at 1 atm, 4400°K at 10 atm, and 4860°K at 100 atm. Recently a

brief summary of the high temperature research work carried out by Grosse and co-workers has been published in "Science" (31).

Section III

COMBUSTION STUDIES

INTRODUCTION

This section is divided into three major areas, corresponding to the objectives of the contract: (1) Analytical Selection of Reactions; (2) Experimental Combustion Studies; and (3) Effects of Additives. Promising reactions selected from the analytical study were explored experimentally to obtain the highest possible temperature. The experimental study began with check-out of the test apparatus. Analytical studies revealed that pressure had a significant effect on temperature. Therefore, the reactions were tested as follows: (1) unpressurized, using solid oxidizer; (2) medium pressures, to 2000 psi; and (3) high pressures to 60,000 psi. In addition, experiments were performed with exploding wires to attain higher temperature and a special study was made to measure emissivity and true temperatures. The characteristics of these reactions, such as temperature, spectral distribution and duration for the various conditions are tabulated for comparison at the end of the experimental combustion discussion. The additives study was also divided into theoretical and experimental phases. The theoretical study was designed to select additives that were most likely to produce non-equilibrium radiation. The effects of these additives on a basic reaction were then investigated in the experimental phase.

ANALYTICAL SELECTION OF REACTIONS

To serve as a guide for choice of high temperature reactions, a theoretical adiabatic flame temperature calculation was made for several

reactions. The highest temperature reactions were selected for experimental study under various conditions.

An adiabatic flame temperature is the temperature that a system would reach at a specified pressure when there is no energy loss to the surroundings and the system has come to equilibrium. The calculations require the solution of the set of coupled equations for mass balance, and the minimization of free energy. The model used thus ignores chemical kinetics, transport properties, and environmental effects. The calculations are quite standard and are programmed for machine computation.

In the calculation of equilibrium, a table of compounds is searched and the thermodynamically preferred compounds are used for the solution. It should be noted that the compounds used in the solution include a number of highly energetic compounds (such as the gaseous oxide) that act as heat sinks and limit the upper temperature. Thus the statement is often made, legitimately, that the boiling point of the oxide is the flame temperature.

From the heat of formation of the oxides, the metals that should give the highest temperatures are thorium, hafnium, zirconium, beryllium, and aluminum. The rare earths do not have accurately known heats of formation, but are expected to have high flame temperatures. Some of the adiabatic flame temperatures are shown in Figure 7 . (The thermochemical data are from the JANAF tables.) The data for thorium, potassium, and the rare earths are not incorporated in the thermochemical data used and therefore can not be included. (For potassium, the nearly equivalent sodium is used.)

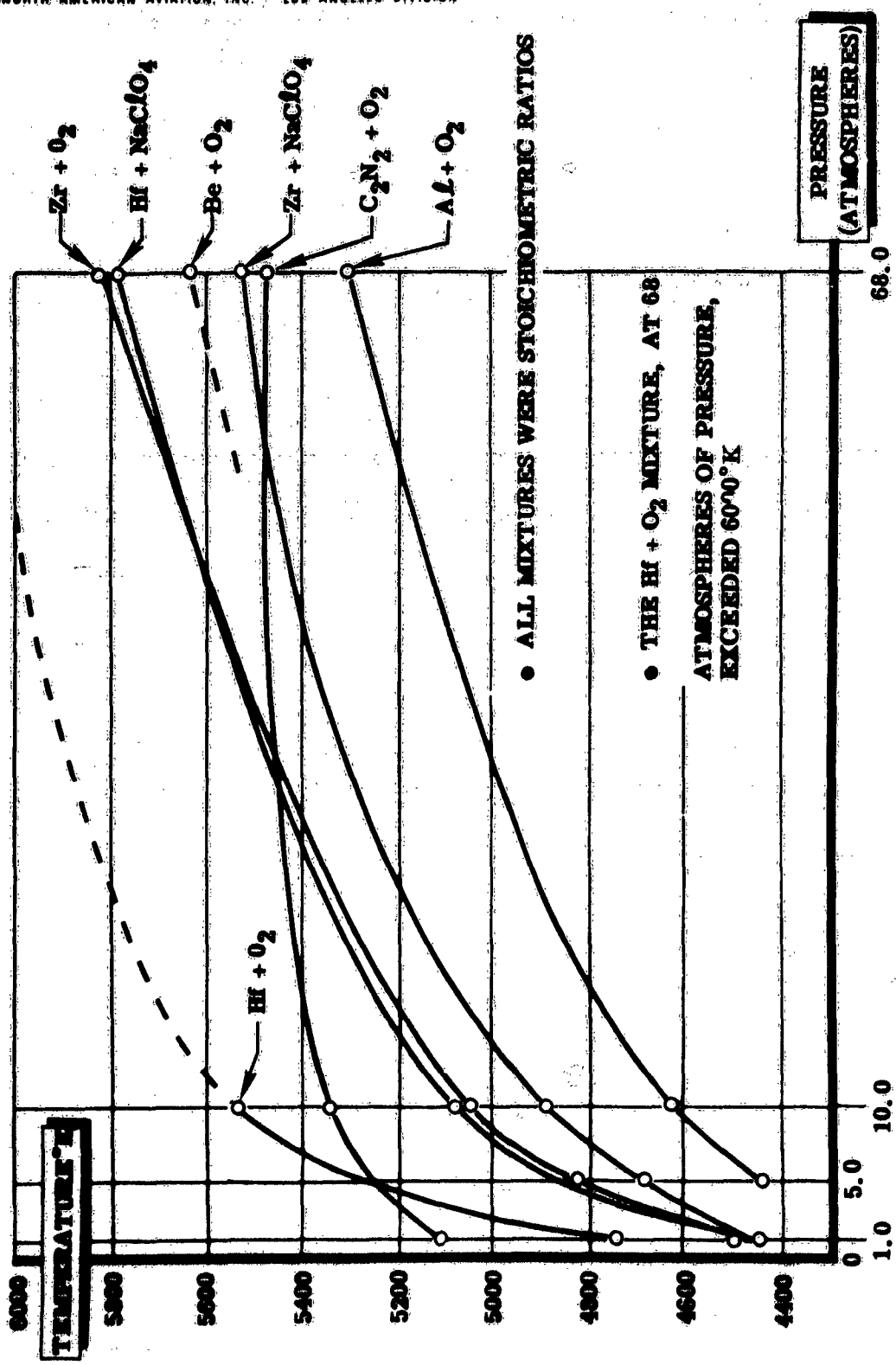

Figure 7. Theoretical Adiabatic Flame Temperature Versus Pressure

One of the variables encountered is the stoichiometry ratio. As noted in Figure 8, the stoichiometric point (the stoichiometry ratio is one) yields temperature close to the maximum. Thus, in Figure 7 the stoichiometric point is used in the calculations.

EXPERIMENTAL COMBUSTION STUDIES

System Apparatus Checkout

To facilitate checkout of equipment, it was decided to search for a basic reaction which was easy to handle and gave reproducible flashes. After checking several possible reaction mixtures, it was found that a mixture of 1/5 magnesium, 1/5 aluminum, and 3/5 sodium chlorate gave the desired results. This mixture was stable for long periods, easy to ignite, burned in less than ten milliseconds, and produced brightness temperatures close to the calibration temperatures used. Also, even after long storage, the intensity varied by less than five per cent from shot to shot.

To record short pulses, a Tektronix 535 oscilloscope was found suitable when equipped with a Polaroid oscilloscope camera. If necessary, two channels could be recorded simultaneously. Triggering was accomplished by adjusting the scope to trigger off the ignitor spike which occurs just before the chemical flash.

An intensive experimental study of possible errors was conducted with the basic reaction mixture. From this study, several sources of extraneous signals were found and eliminated. First, extensive masking

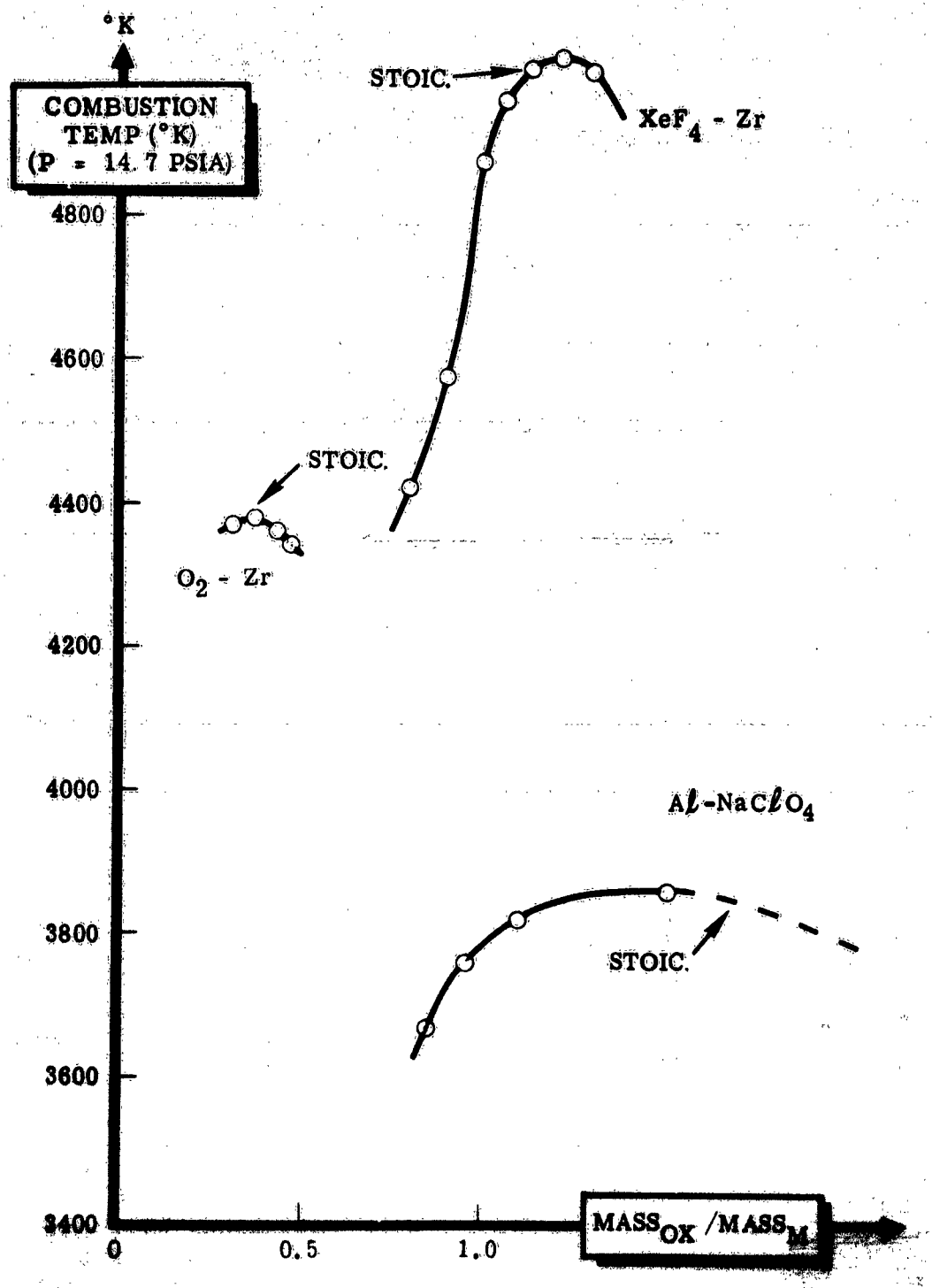

Figure 8. Oxidizer Ratio

of the reaction chamber was necessary because of the formation of a large luminous cloud above the atmospheric chamber during firing. Second, large signals from the room lights necessitated operation in the dark. Third, various signals were picked up from electrical equipment in operation in other areas of the laboratory if the output cables from the sensors were not well shielded. Fourth, the recording equipment was sensitive to shock waves produced by the faster flashes.

UNPRESSURIZED CHEMICAL REACTION EXPERIMENTS

After the preliminary experiments were completed and the system was completely checked out, an intensive study of brightness temperature variations with wavelength was undertaken. Several solid oxidizer metal mixtures were examined including:

$$Mg + Al + Ba(ClO_3)_2$$

$$Mg + Al + KClO_4$$

$$Zr + KClO_4$$

$$Hf + KClO_4$$

These reactions were performed in the atmospheric pressure chamber shown in Appendix I. Intensity measurements were made from 4500A to 11,000A with the phototube sensor unit described in Appendix I. The spectra (see Appendix II) obtained were relatively flat across the spectral region studied but large brightness temperature variations occurred in the visible region. A typical example, magnesium + aluminum + potassium perchlorate, is shown in Figure 9. Because the phototube sensor unit was inherently

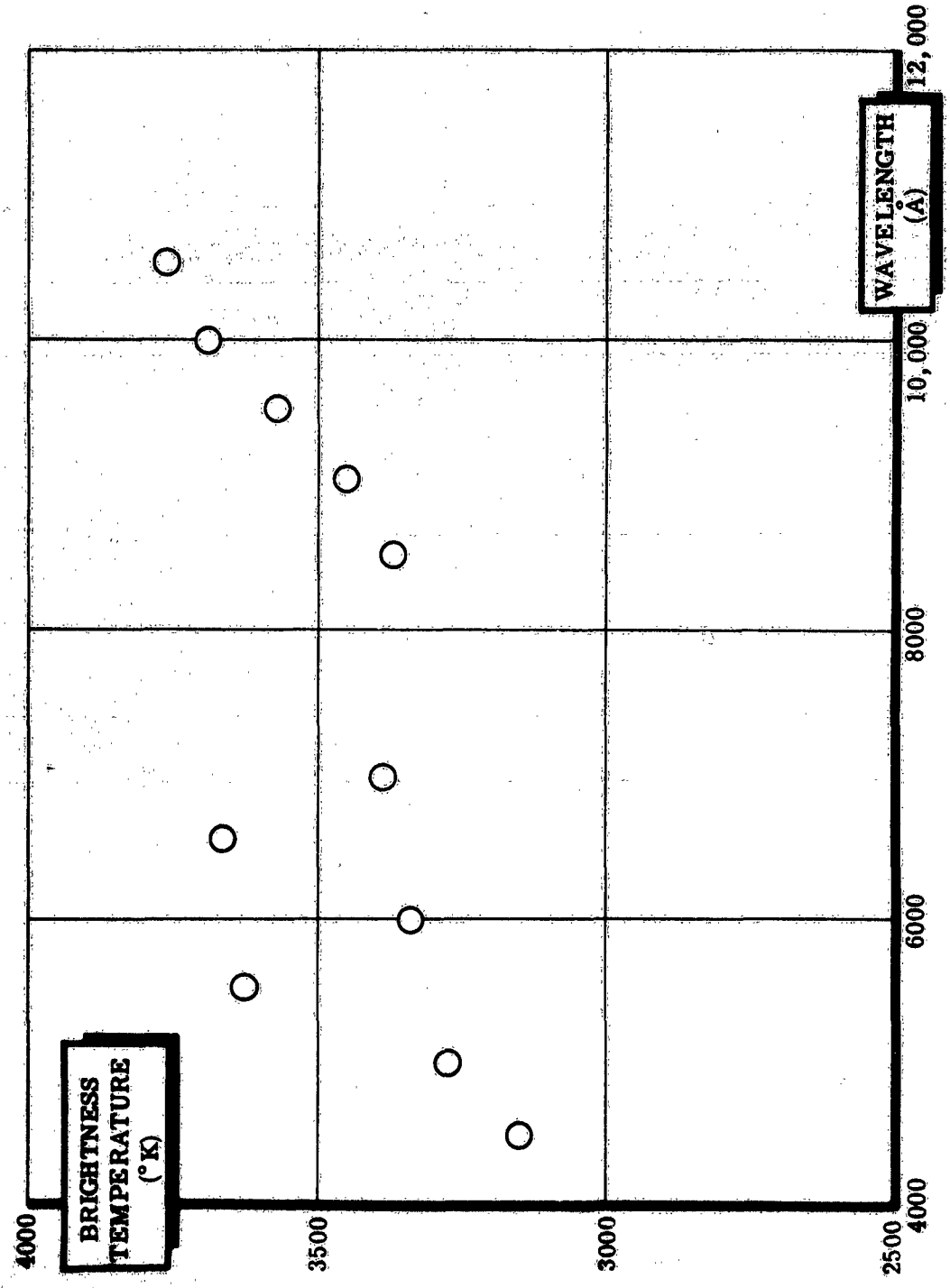

Figure 9 Brightness Temperature Versus Wavelength $Mg + Al + KClO_4$ (1-2-6)

limited to measurements at one wavelength per shot, accurate scanning of the spectrum was difficult. Therefore, further atmospheric spectral measurements were conducted on the Bausch and Lomb spectrometer system while the phototube sensors were used for duration studies with the pressurization chambers.

Reaction time profiles vary greatly depending on the mixtures used. A strong correlation was found between initial metal powder size and reaction duration. In general, the finer meshes produced shorter reactions as expected, however, little correlation was found between mesh size and brightness temperatures. With zirconium, the coarse powder (105 μ) resulted in higher temperatures than the fine mesh powder (44 μ). This effect may be due to the presence of an oxide layer on the powder which would effectively reduce the free metal concentration in the finer powders because of the larger surface areas present.

MEDIUM PRESSURE CHEMICAL REACTION EXPERIMENTS

One method of getting higher flash temperatures is to increase the pressure on the reacting system. The higher pressure raises the boiling point of the metal oxide and avoids losing the heat of vaporization plus the heat of dissociation to the monoxide.

e.g. $Al_2O_3 \rightarrow 2AlO(g) + O(g)$

$Al(g) + Al_2O_3(g) \rightarrow 3AlO(g)$

Calculated adiabatic flame temperatures for metal-oxidizer systems verified that an improvement could be made by pressurization.

Studies with pressurized oxygen were undertaken to verify the theoretically predicted adiabatic flame temperatures. At first, the metal powders were burned with oxygen, but the variation of brightness temperature with pressure always indicated a maximum. This peak can be explained by the fact that only at one pressure would the system be stoichiometric. This effect is shown with aluminum powder in Figure 10. Hafnium and zirconium behave similarly.

To correct the stoichiometry problem, studies were initiated with metal wool packed into pyrex retainer tubes. The results with aluminum wool are shown in Figure 11 with the theoretical flame temperature plotted above. If an emissivity of 0.225 is assumed for the aluminum reaction, the "actual" flame temperature is found to agree quite closely with the predicted flame temperature.

As a check on this approach, zirconium-potassium perchlorate mixtures were fired under oxygen pressurization. The results are shown in Figure 11. If the emissivity is assumed to be 0.08 fair agreement is found between the "actual" flame temperature and the predicted flame temperature.

It should be kept in mind that these experimental emissivities are subject to errors.

In another phase of this portion of the program a high pressure oxygen bomb calorimeter was modified for use by welding on two flanges to accommodate windows. A photo of the apparatus appears in Figure 12. The two windows permitted a view through the burning cloud of particles.

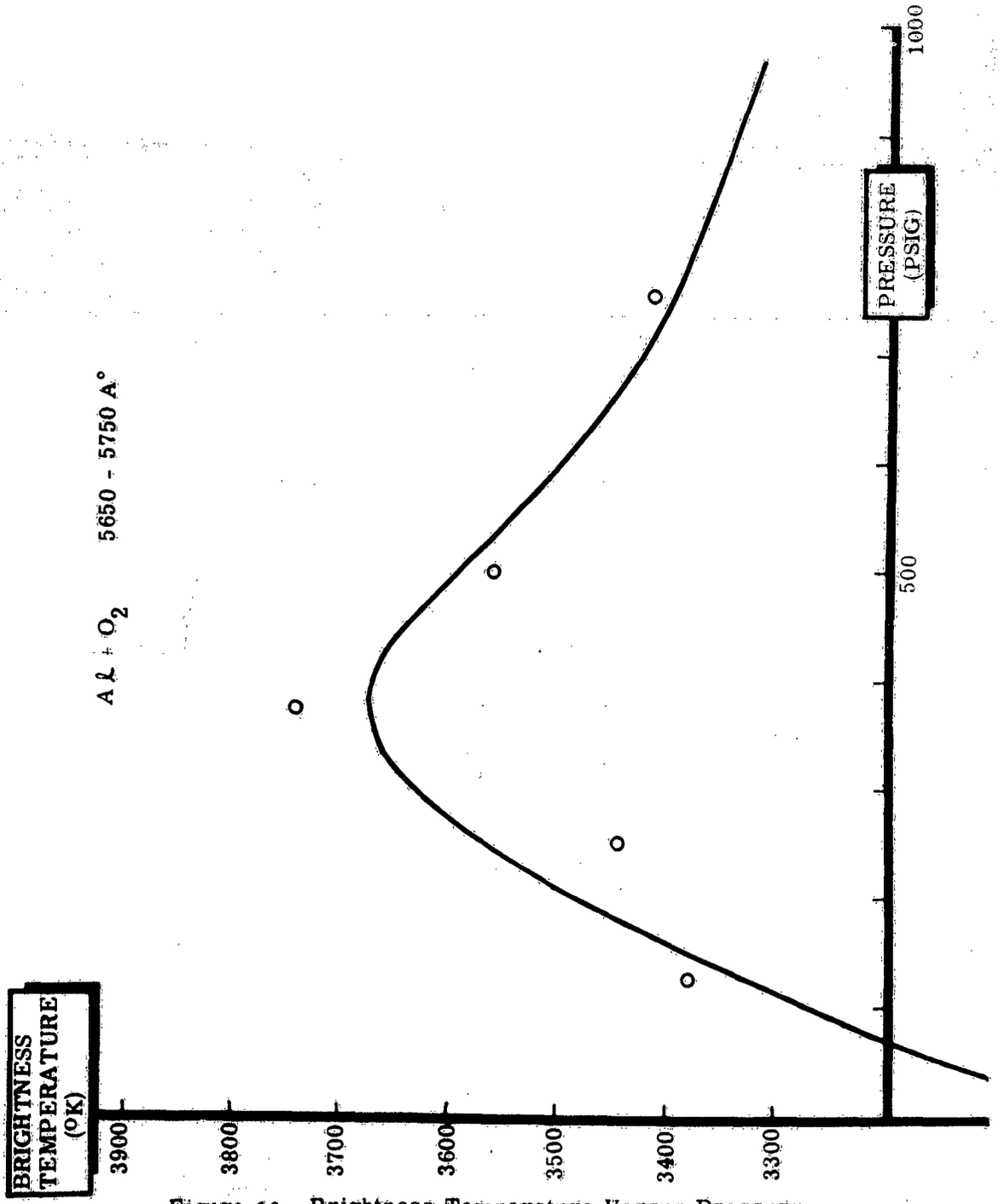

Figure 10 Brightness Temperature Versus Pressure For Flake Aluminum Powder And Gaseous Oxygen

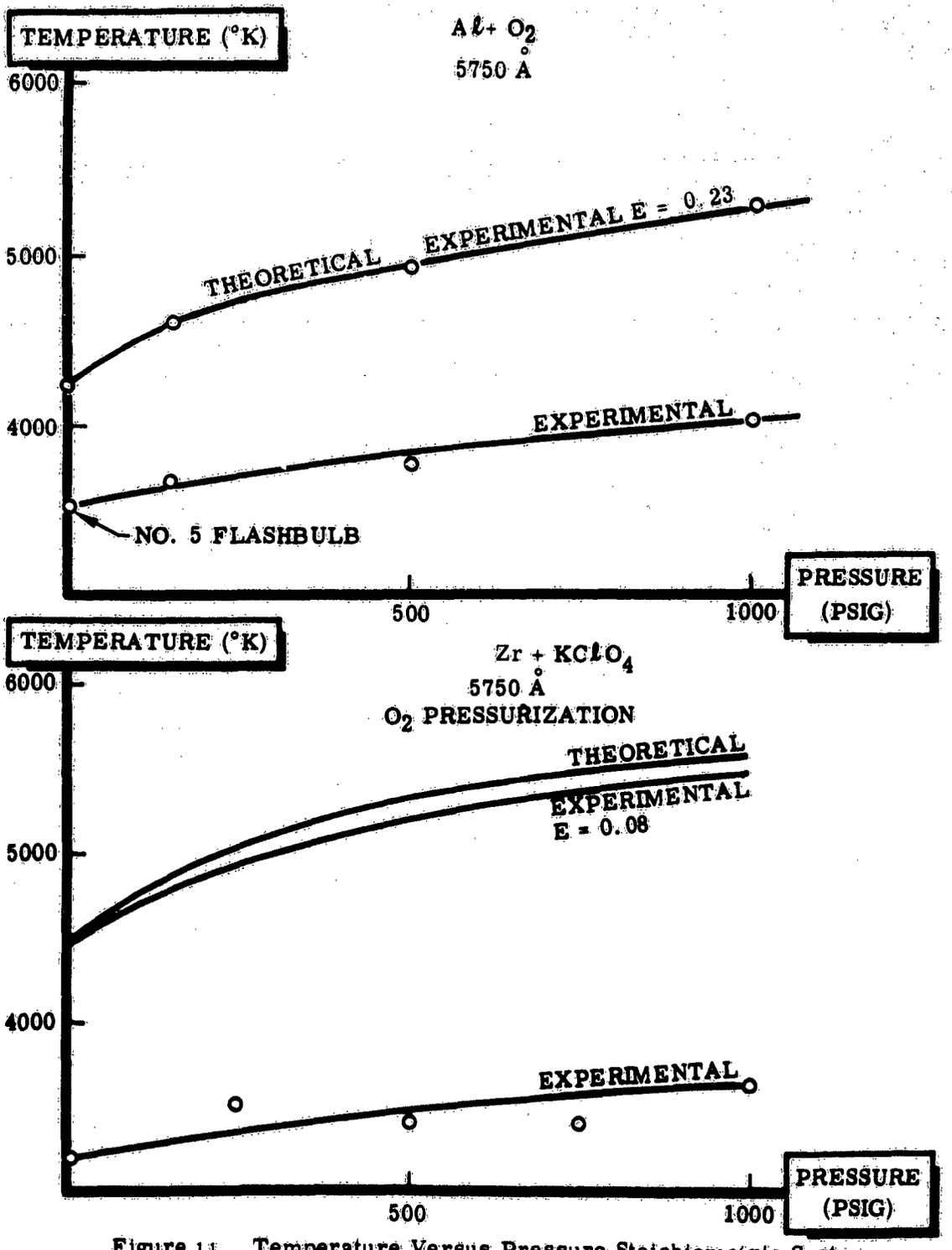

Figure 11 Temperature Versus Pressure Stoichiometric System

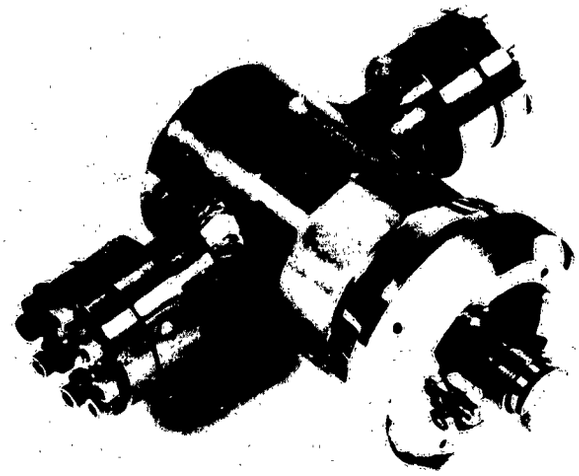

ASSEMBLED

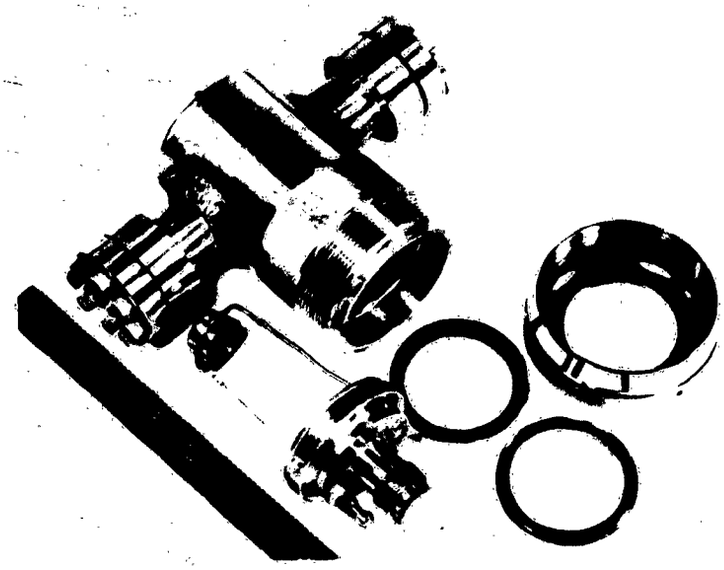

DISASSEMBLED

Figure 12. Bomb Calorimeter for Optical Studies

The recommended maximum initial pressure for this type of calorimeter is 40 atmospheres of O_2 and that is what was decided on here -- the maximum pressurization attempted was 600 psig.

Mixtures of metal powders and $KClO_4$ were placed in a cup held by the ring electrode and ignited by an electrically heated resistance wire. The windows were cleaned after every reaction to assure that light attenuation would not be a problem. Window charring or dirtying was not encountered in this pressure range. After assembly the reaction chamber was placed in the optical setup also used for taking time resolved spectra.

Experiments in the pressurized chamber were conducted with aluminum, hafnium, zirconium and thorium powders. The oxidizer in all of the tests was $KClO_4$. The data taken have been plotted as $\frac{1}{T}$ vs log P and appear in Figures 13, 14, and 15. Since the adiabatic flame temperature is equal to the boiling point of the metal oxide using the Clausius Clapeyron equation

$$\frac{d \ln P}{d\left(\frac{1}{T}\right)} = -\frac{\Delta H}{R}$$

it can be seen that with these coordinates the flame temperature, pressure function appears as a straight line.

Brightness temperatures measured for the 3% Al, 20% $KClO_4$ mixtures are at a maximum at about 100 psig when pressurized with air and indicate a broad maximum extending from 100 psig to 400 psig when pressurized with oxygen. In the vicinity of 100 psig, the measured temperatures are in

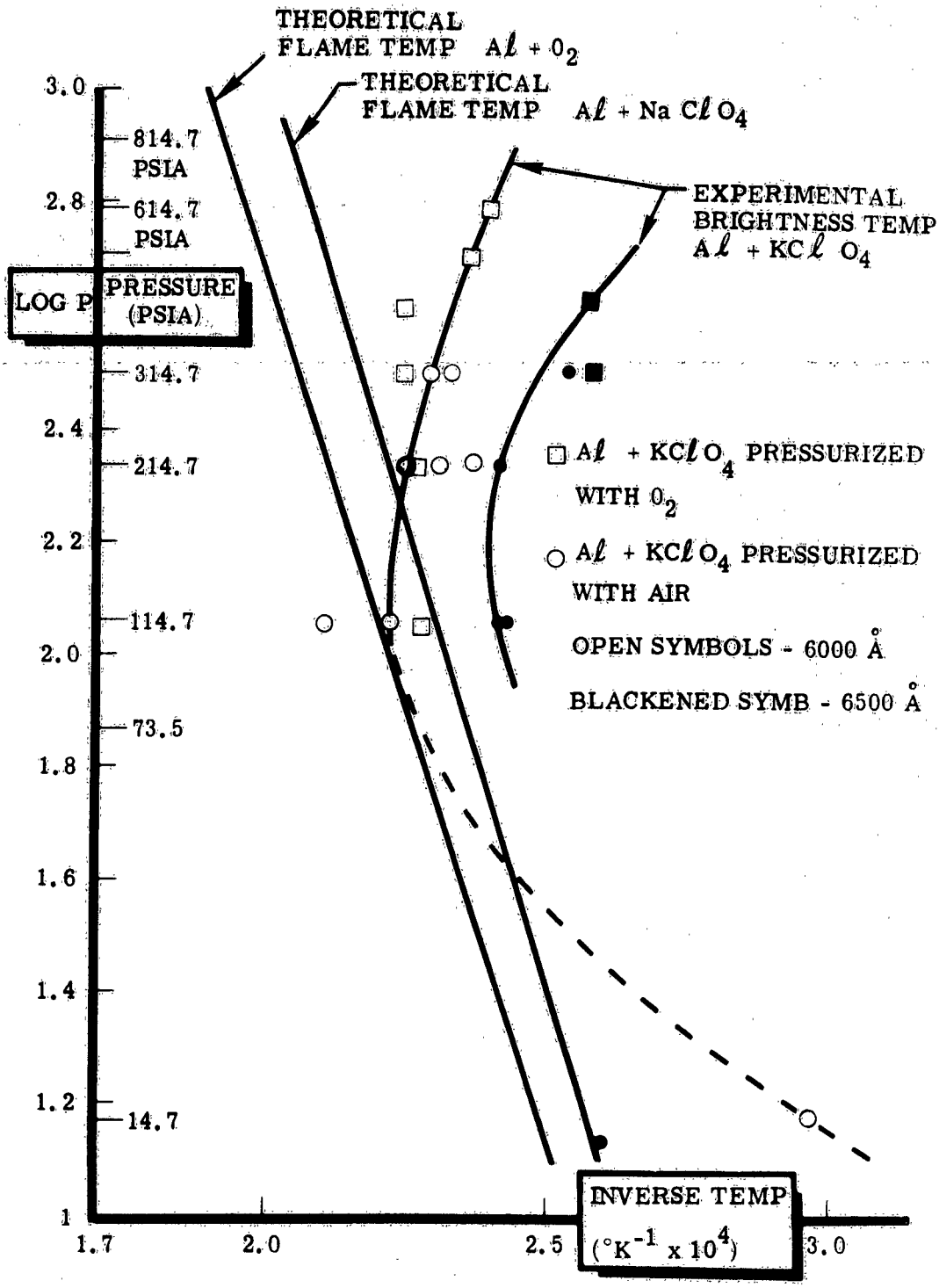

Figure 13. Pressure Versus Temperature for Aluminum Plus Perchlorates

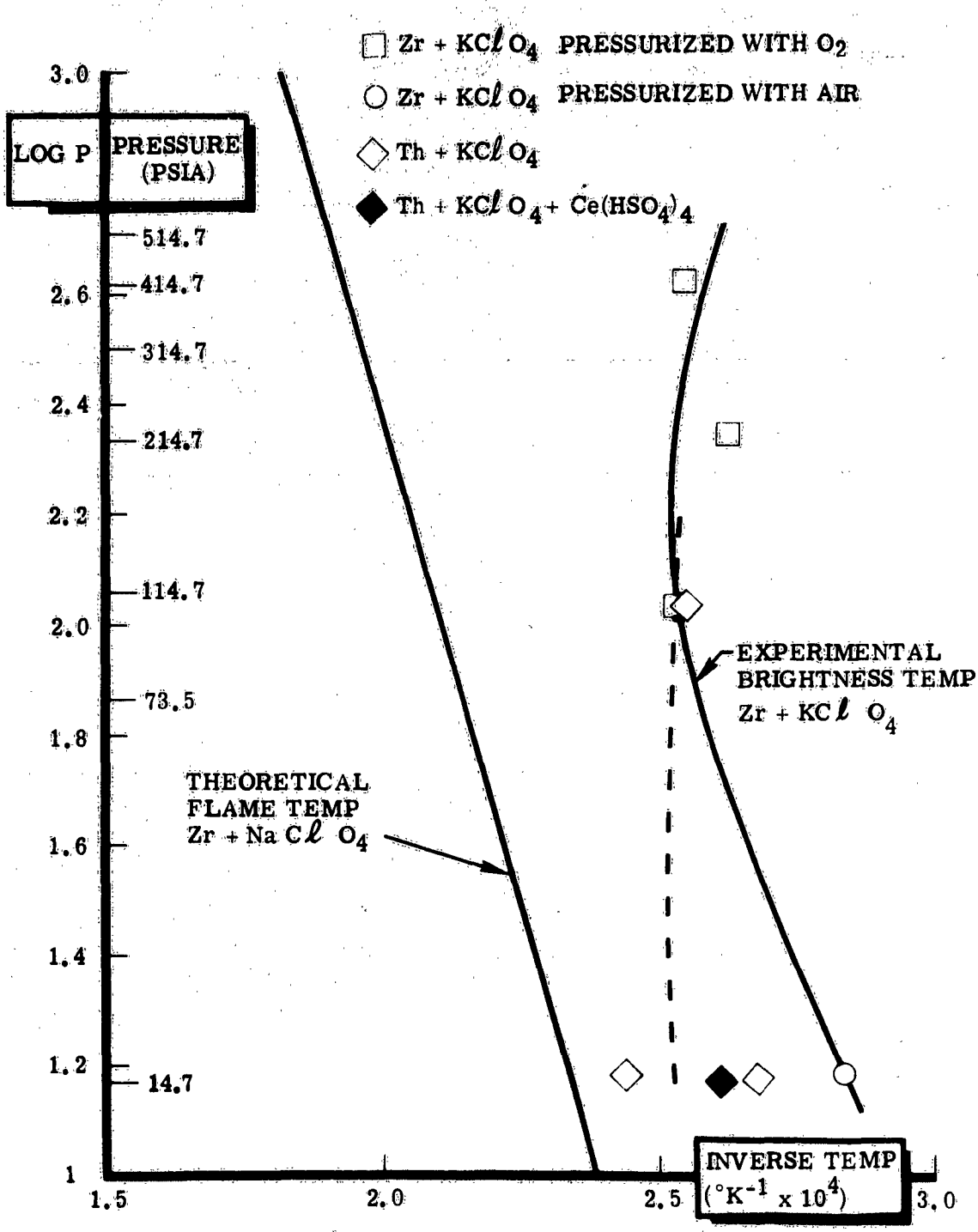

Figure 14. Pressure Versus Temperature for Thorium and Zirconium Plus Perchlorates

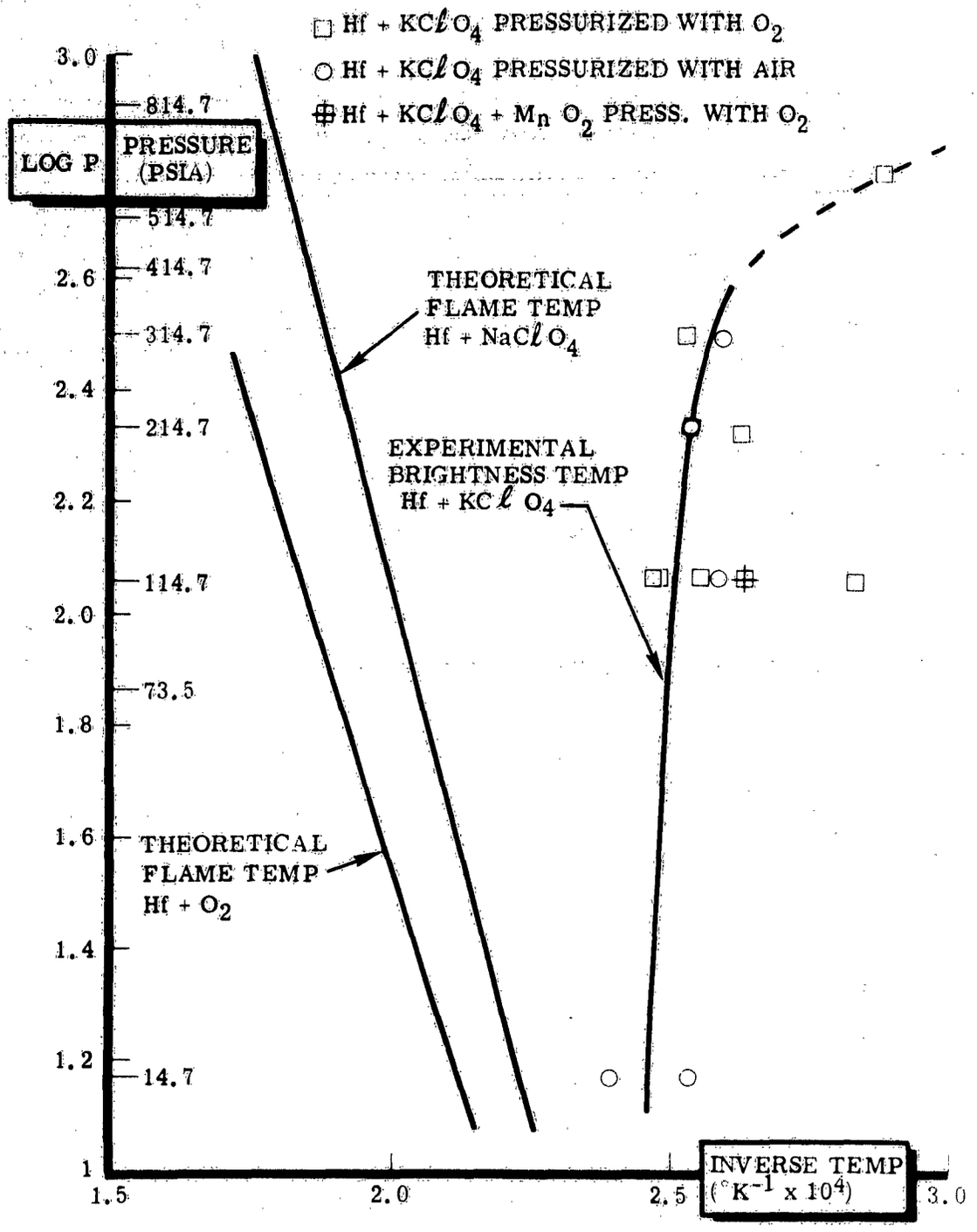

Figure 15 Pressure Versus Temperature for Hafnium Plus Perchlorates

excess of the computed adiabatic flame temperature of the $Al/NaClO_4$ reaction. Assuming the temperature measurements are not in error, a few reasonable explanations for this behavior can be given. First of all, the computed flame temperature assumes the heat of reaction to be evenly distributed among all the combustion products when in fact temperature gradients exist: there is a very hot $Al + O_2$ reaction zone in the vicinity of each burning aluminum droplet. Secondly, the chamber pressures given are the readings before a chemical reaction has been initiated. Certainly, during the explosive reaction, the transient pressure in the reactor and the pressure within the burning flash powder must be quite a bit higher.

Probably the main cause for the large increase in brightness temperature when going from 0 to 100 psig is the transition of the chemical flash from a combustion reaction to a detonation. The flash duration at 0 psig is approximately 23 milliseconds while at 100 psig the flash time ranges from 1 $\frac{1}{2}$ to 3 milliseconds. This order of magnitude reduction in flash time will result in a smaller total conduction heat loss and hence a higher flame temperature. The approximate reaction time to reach the peak brightness temperature is given in Table I. As the pressure is increased there is probably a further reduction in reaction time which more data would reveal. It is not clear why the temperature should decrease at higher pressures unless conduction heat loss was again involved. It is quite possible that the photodiodes were measuring the temperature of the colder exterior of the radiating cloud.

Oxygen and air pressurization cause slightly different results but the scatter in the data makes an analysis of this point, an academic

exercise. Since N_2 is an inert in this system, oxygen pressurization would be expected to be better.

A spectrum of the Al/$KClO_4$ flash was taken at 100 psig using the 1.5 meter Bausch and Lomb instrument. The spectrum was not time resolved; hot wire ignition made the timing too difficult and a high voltage spark could not be sed because it would arc across the thinly insulated electrode connection through the bomb calorimeter wall. The film indicated the flash consisted of continuum emission and Al, Na, and K lines in absorption; no AlO band structure was present. Mixtures of -325 mesh hafnium and potassium perchlorate exhibit the highest temperature at 0 psig. Pressurization reduced the reaction time to peak light output from 6 to 8.5 milliseconds at 0 psig to between 0.5 and 2 milliseconds, on the average, at 100 psig and higher. The change in reaction time with pressurization is not as pronounced as it was with aluminum but still one would expect a temperature rise from a reduction in conductive heat losses.

Mixtures of hafnium with 1-1/2 times the stoichiometrically required amount of $KClO_4$ did not produce flash temperatures notably different from the stoichiometric mixes. The extra heat load apparently made little difference. In other experiments about 10% by weight MnO_2 was added to the mixture, again without improving the light output. The addition of MnO_2 was reported to increase the emissivity of the metal oxide particles. If this is true, one can conclude that the emissivity of the HfO_2 particle clous is quite high, or that the lowered flame temperature, because of the added heat load of the MnO_2, is compensated for by the increase in emissivity. The results are given in Table I on Page 44.

It is strongly suspected that hafnium powder left exposed to the atmosphere will form a fair amount of oxide. Exposure of the powder to air for a period of a few days will lower the brightness temperature. There is the possibility that the Hf powder purchased already had quite a high concentration of oxide and the achievement of higher brightness temperatures with hafnium (and the other metal powders) will require oxide free metal.

The data on -325 mesh Zr and Th combustion have been plotted in Figure 14. Although only one zirconium flash was made at each pressure level, the response of the $Zr/KClO_4$ mixture to increased pressure is like the $Hf/KClO_4$ system. There is a moderate increase in temperature when the reaction is set off at 100 psig. As can be seen in Table II, the reaction time to maximum light output decreases with pressure but the effect of pressure on the total flash duration is not as great as with Al powder. The total flash duration is reduced from 17 to 8 milliseconds when the pressure is increased from 0 to 100 psig; this is not nearly as dramatic as the transition for aluminum.

One of the metals known to form a very high boiling oxide with a large heat of reaction is thorium. Thermodynamic data for thorium and its oxide were not readily available thus the flame temperature was unknown. There is then, no theoretical result to which the measured brightness temperature can be compared.

Because of the mild radioactivity of Th it was desirable to react the $Th/KClO_4$ mixture in a closed chamber. The modified bomb calorimeter was used for these measurements.

Brightness temperatures were measured at 0 and 100 psig. The maximum brightness temperature produced by stoichiometric Th/$KClO_4$ mixtures was 4115K at 1 atm. The increase in pressure didn't produce a higher flash temperature; thorium can be classed with Hf in this respect.

A mixture of thoria and 1 percent ceria is used as an active surface in the so called Welsbach mantel. The Welsbach mantel probably behaves as a catalytic surface for the recombination of free radicals which in turn serve to heat the mantle. The high emissivity of the mantel in the blue produces a white light having a high color temperature. One of the Th/$KClO_4$ flashes was doped with enough $Ce(HSO_4)_4$ to produce a proper mixture of thoria and ceria after combustion. The resultant brightness temperature of 3790K at 6000A was not promising.

TABLE I

EFFECT OF PRESSURE ON Al + $KClO_4$ REACTION

P(psig)	O_2 atm		Air		
	T_{max}(K)	t_{msec}	T_{max}(K)	t_{msec}	
0	-	-	3365	7.5	Slow Combustion
100	4410	0.7	4600	1.0	Detonation
			4515	0.4	
200	4440	0.2	4240	0.4	
			4390	0.3	
			4460	0.4	
300	4460	0.23	4320	0.25	
			4390	0.25	
400	4480	0.28	-	-	
500	4240	0.13	-	-	
600	4180	0.2	-	-	

TABLE II

EFFECT OF PRESSURE ON Hf/$KClO_4$ REACTION

	O_2		Air	
P(psig)	T(K)	T(msec)	T(K)	T(msec)
0	4180	8.5		
	3945	6		
100	3920	3.2	3880	1.8
	4015*	0.5		
	4020*	1.2		
	3820**	1.0		
	3530**	1.2		
200	3820*	0.4	3940	1.3
	3360*	1		
300	3370	1.7	3880	1.4
600	3460	0.6		

EFFECT OF PRESSURE ON Zr/$KClO_4$ REACTION

P(psig)	T (K)	$t_{(max T)}$ msec
0	3520	10
100	3980	2
200	3840	1
400	3950	0.4

* 1-1/2 times stoich. $KClO_4$
** 10% by weight MnO_2

A spectrum of the Th/$KClO_4$ system was taken at 0 psig. Besides the usual K and Na absorption lines there are emission band heads located at 5927 and 6340 A; there is no information given in Pearse and Gaydon (32) on emission from thorium compounds but it is believed that the bands belong to Th. A microphotometer trace of the film is given in Figure 59. Isotherms applicable to 2 msec. exposures and different f numbers have been drawn in on the trace. The assumptions are that the film emulsion will respond to a certain energy flux in the same manner if the exposure times are of the same order of magnitude and that the relative film darkening at various wavelengths corresponded to the highest measured brightness temperature of the flash rather than the flux level integrated somehow over the total flash duration (this last assumption is admittedly unrealistic). The measured brightness temperature at 6000A was 3740K; the film darkening at 6000A corresponded to the 3400K isotherm. A 3740K isotherm was then faired in on the trace using the ratio of flux density given by 3400K and 3740K at 6000A as a fictitious emissivity.

Zirconium wool + pressurized oxygen studies have been made under conditions of constant volume in the apparatus shown in Figure 22. The data is summarized in Figure 16. Plexiglass windows were used in these runs and a severe charring problem developed because the window was in direct contact with the hot reaction products. Consequently, the recorded brightness temperatures are considerably below the true brightness temperature of the flash. However, the 5230°K temperature obtained is above lasing threshold for ruby and near the optimum operating point for neodymium lasers.

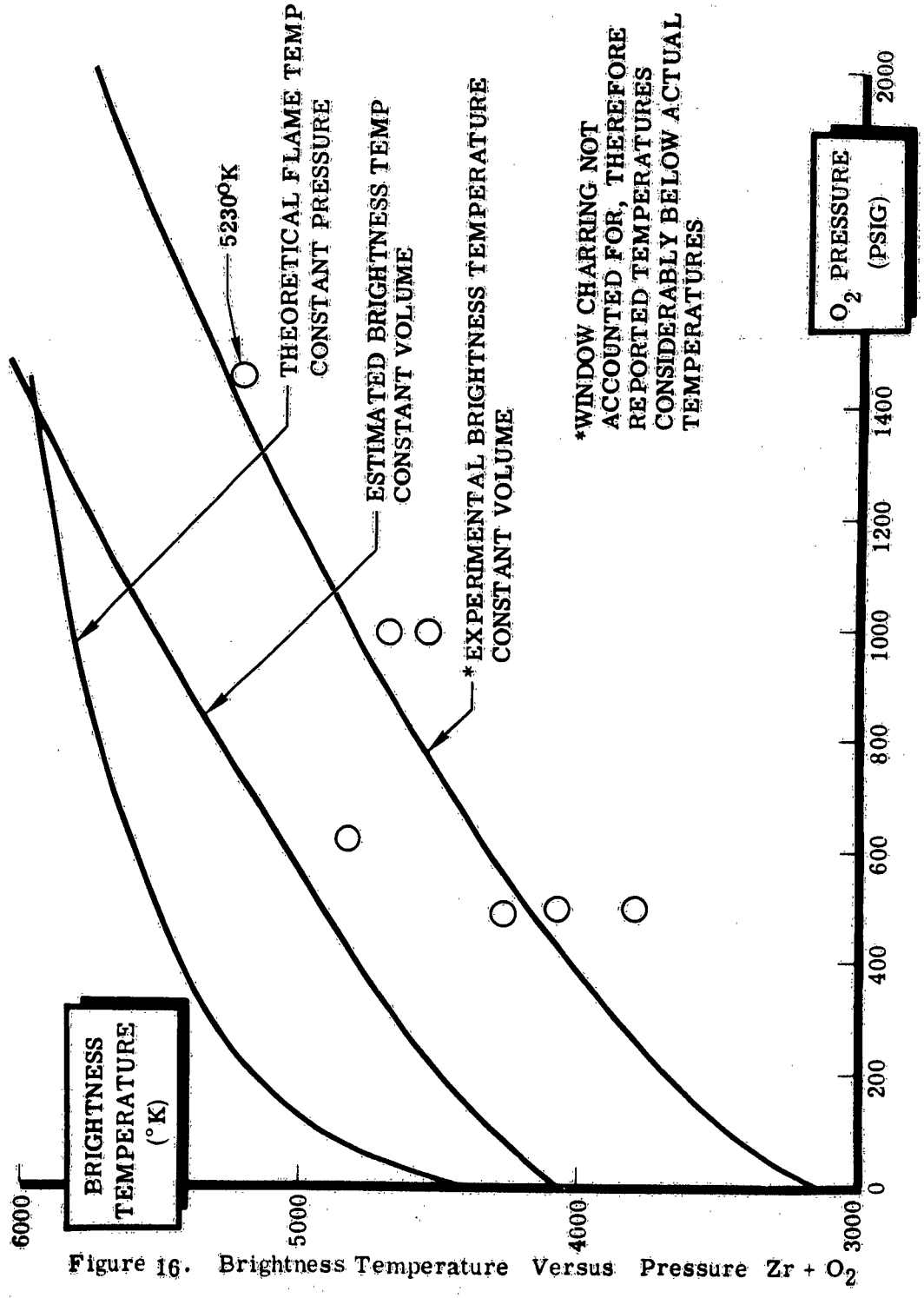

Figure 16. Brightness Temperature Versus Pressure Zr + O_2

High Pressure Chemical Reaction Experiments

To explore the very high pressure region, measurements were taken with solid oxidizer-metal mixtures in the dynamic pressurization chamber. Pressures up to 10^5 psi could be handled in the chamber. Extreme difficulty was experienced in conducting these high pressure tests for several reasons. First, conditions could by no means be duplicated between successive shots. Second, the window sometimes ruptured, nullifying data received. Third, flying fragments from the ruptured window required elaborate protective screens. Fourth, the short duration pulses were hard to record because of large variations in the induction period between the ignition pulse and the combustion pulse. Nevertheless, significant data was obtained on many shots and are summarized in Table III. The pressures reported are very approximate and were found by calculating the pressure necessary to rupture the window.

To alleviate some of the difficulties encountered with the dynamic chamber mentioned above, several modifications were made, as indicated in Appendix I. This modified chamber was equipped with a Kistler gauge piezoelectric pressure transducer which allowed pressure measurements up to 10^5 psi. With this chamber, pressure and temperature could be measured simultaneously.

A typical pressure temperature-time pulse is shown in Figure 17 The pressure trace indicates clearly the detonation wave followed by the smoothly rising then falling chamber pressure. The light emission is seen to start immediately after the detonation wave passes, increase to a maximum corresponding to the point of maximum chamber pressure, then decay at a rate considerably faster than the pressure decay. Before firing, the window transparency is 90%. After the shot, window transparency was approximately 10% because of charring. Because the reaction products

Table III

DYNAMIC CHAMBER TEST RESULTS

Material	KIP/In.^{2}	* Temp °K
Al + Mg + $KClO_4$	20	4150
Hf + $KClO_4$	20	4635
Hf + Mn + $KClO_4$	20	5270

* TEMPERATURES NOT CORRECTED FOR WINDOW CHARRING

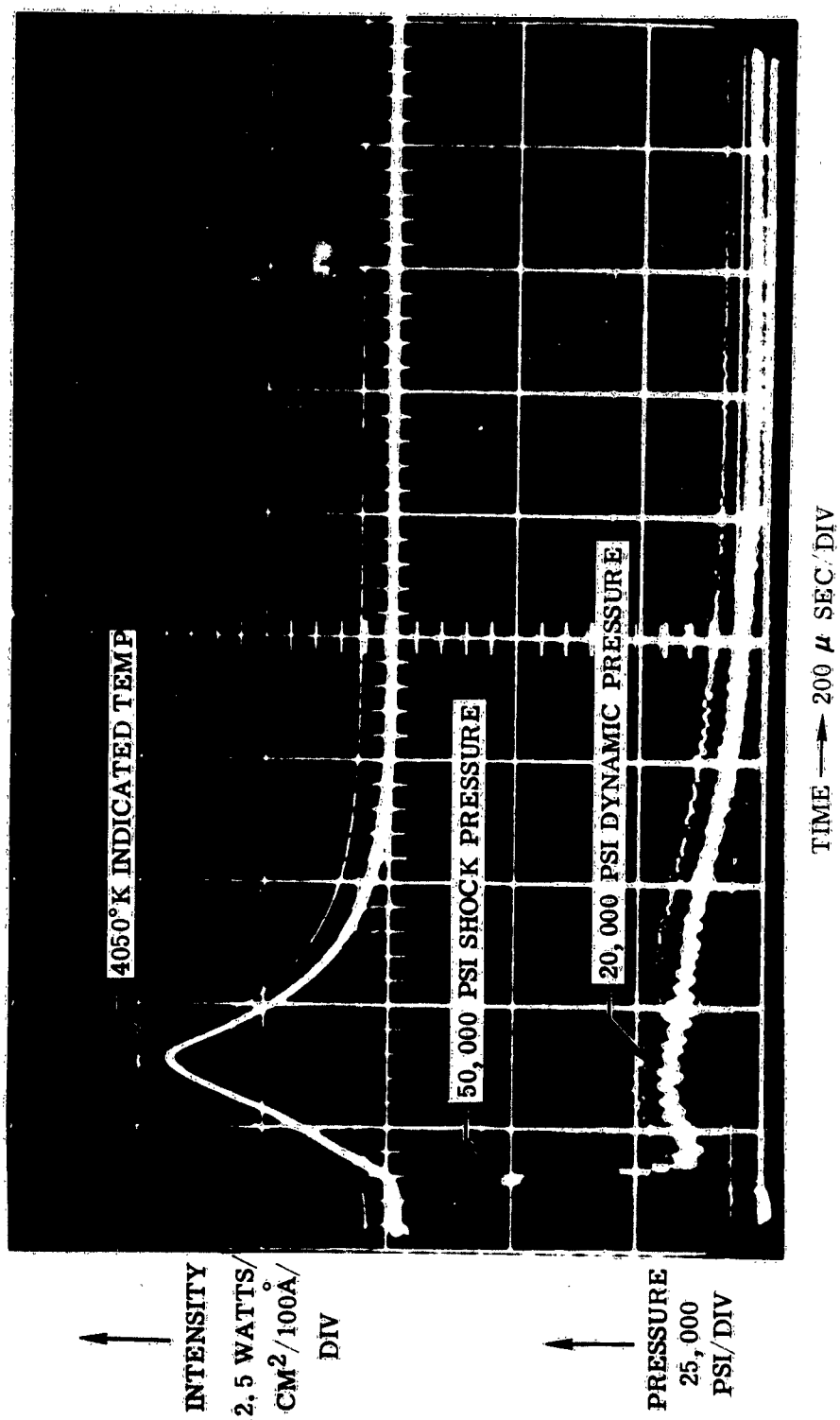

Figure 17. Dynamic Pressurization Chamber Typical Pressure - Intensity Pulse at 5500Å

must be at an extremely high temperature (>3000°K) to exhibit the high pressure, it is evident that the window is considerably charred even before the maximum temperature is recorded. Table IV lists the maximum pressures and temperatures obtained with this chamber.

Several spectra of dynamically pressurized shots are shown in Appendix II. The most prominent feature of those spectra is a complete lack of any emission or absorption lines except for the manganese triplet in absorption at 4033A as indicated in two of the spectra. The sharp spikes present on these spectra are due entirely to mercury emission from the fluorescent lights in the laboratory.

Exploding Wire Chemical Reaction Experiments

An effective way to increase the flame temperature of a reaction is to add extra energy to the reaction mixture. To accomplish this goal, it was decided to test an exploding wire in oxygen. Two types of wires were used, aluminum and zirconium. The wire was exploded in a pyrex capillary tube under sufficient oxygen pressure to effect complete combustion. Just enough electrical energy was used to vaporize the wire. The results are shown in Figure 18 with a sketch of the tube used. The brightness temperatures observed were higher than the temperatures measured with the metal wool burning in oxygen. The saddles observed are probably caused by the condensation of metal oxide. From the observed brightness temperature and the calculated boiling point of the oxide, the emissivity may be roughly measured. The aluminum emissivity is approximately 0.26 and the zirconium emissivity is approximately 0.08. Therefore, the emissivities assumed in the pressurized oxygen studies are further substantiated.

TABLE IV

DYNAMIC PRESSURIZATION SHOTS

PRESSURE MONITORED

MIXTURE	T_B (°K)*	MAXIMUM CHAMBER PRESSURE (psi)
Zr + $KClO_4$	4510	15000
" "	4020	18000
" "	3770	25000
" "	4210	30000
Zr " Mn + $KClO_4$	3720	20000
" " "	4150	35000
" " "	3180	35000
" " "	3600	40000
Hf + $KClO_4$	4510	40000
" "	4370	40000
" "	4600	50000
" "	4000	50000
" "	3180	60000

PRESSURE NOT MONITORED

MIXTURE	T_B (°K)*	
Zr + $KClO_4$	4700	
" "	3700	
Zr + Mn + $KClO_4$	5220	6300°K estimated temperature
" " "	4150	
" " "	3850	
" " "	3700	
Hf + $KClO_4$	5170	6500°K estimated temperature
" "	4900	
" "	4540	

* Quoted brightness temperatures not corrected for window charring.

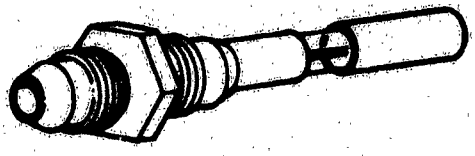

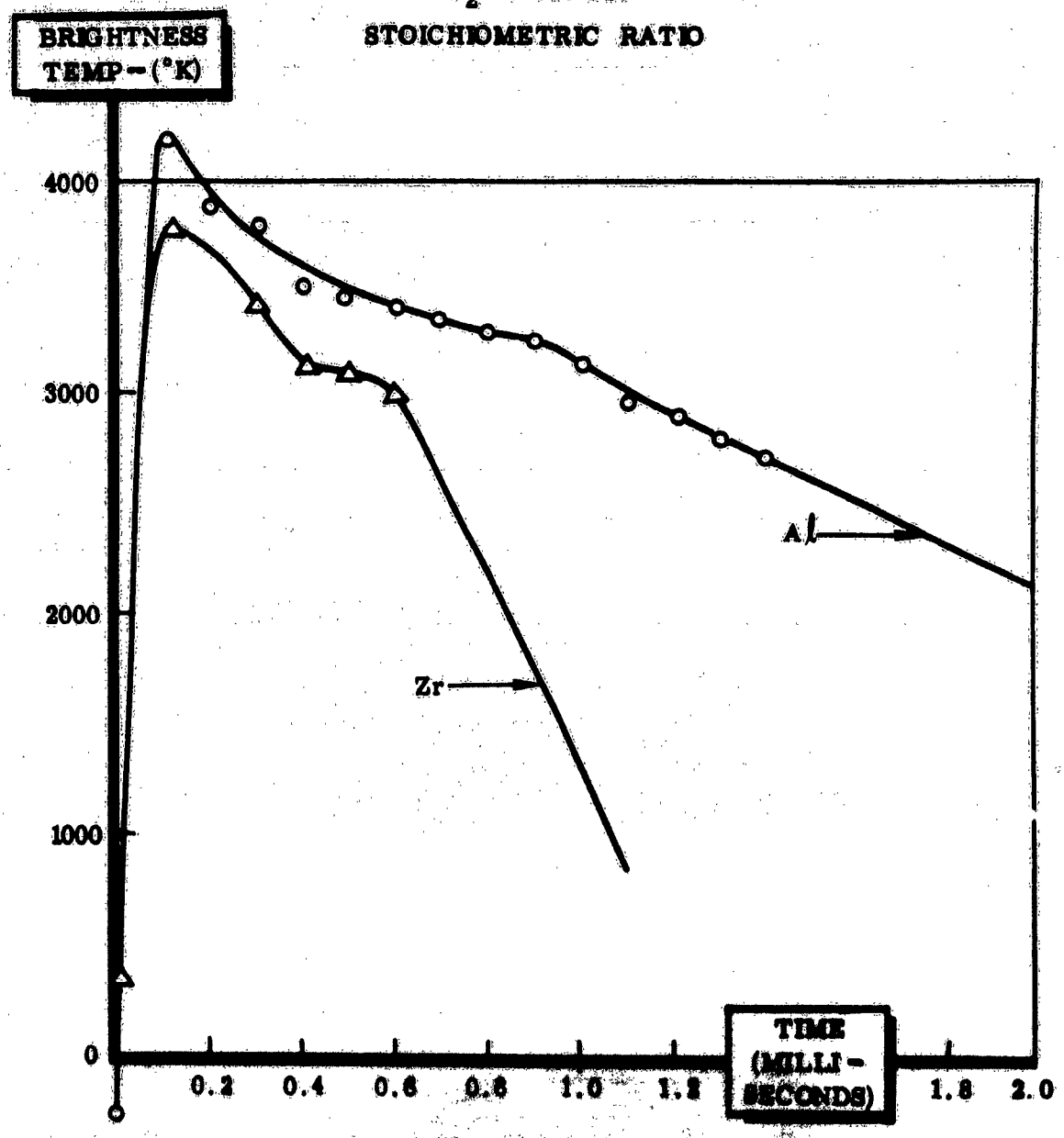

Figure 18 Exploding Wire Chemical Reactions

Measurement of Emissivity and True Temperature

Single-double path measurements: Temperatures determined by phototubes sighted on a radiation source are brightness temperatures, or, the temperature at which a blackbody would be an equivalent radiation source. Measuring the true temperature of a source requires that the emissivity be known. There is evidence from the brightness temperature data taken at both high pressures and at one atmosphere, that the emissivity of the luminous cloud is low. If this is indeed the case, it would indicate that additives to modify the emissivity should be given more consideration.

To measure the true temperature of the flash reaction an apparatus was setup to perform single-double path measurements. The setup is shown in Figure 19. The arrangement is similar to that for measuring brightness temperature except that a spherical mirror and a light chopper have been added behind the flash. The spherical mirror is set at a distance from the chemical reaction equal to its radius of curvature so as to form an image at the focal point of the lens system. The phototube now responds to an alternating signal consisting first of radiation directly from the flash and then, when the chopper opens the optical path to the mirror, radiation directly from the flash plus radiation from the flash that has been attenuated by reflection from the mirror and by traveling through the luminous cloud. The equations for the single-double path process can be set down and easily solved if light scatterings is neglected. (The left hand side of the equations is Wien's approximation to Plank's law).

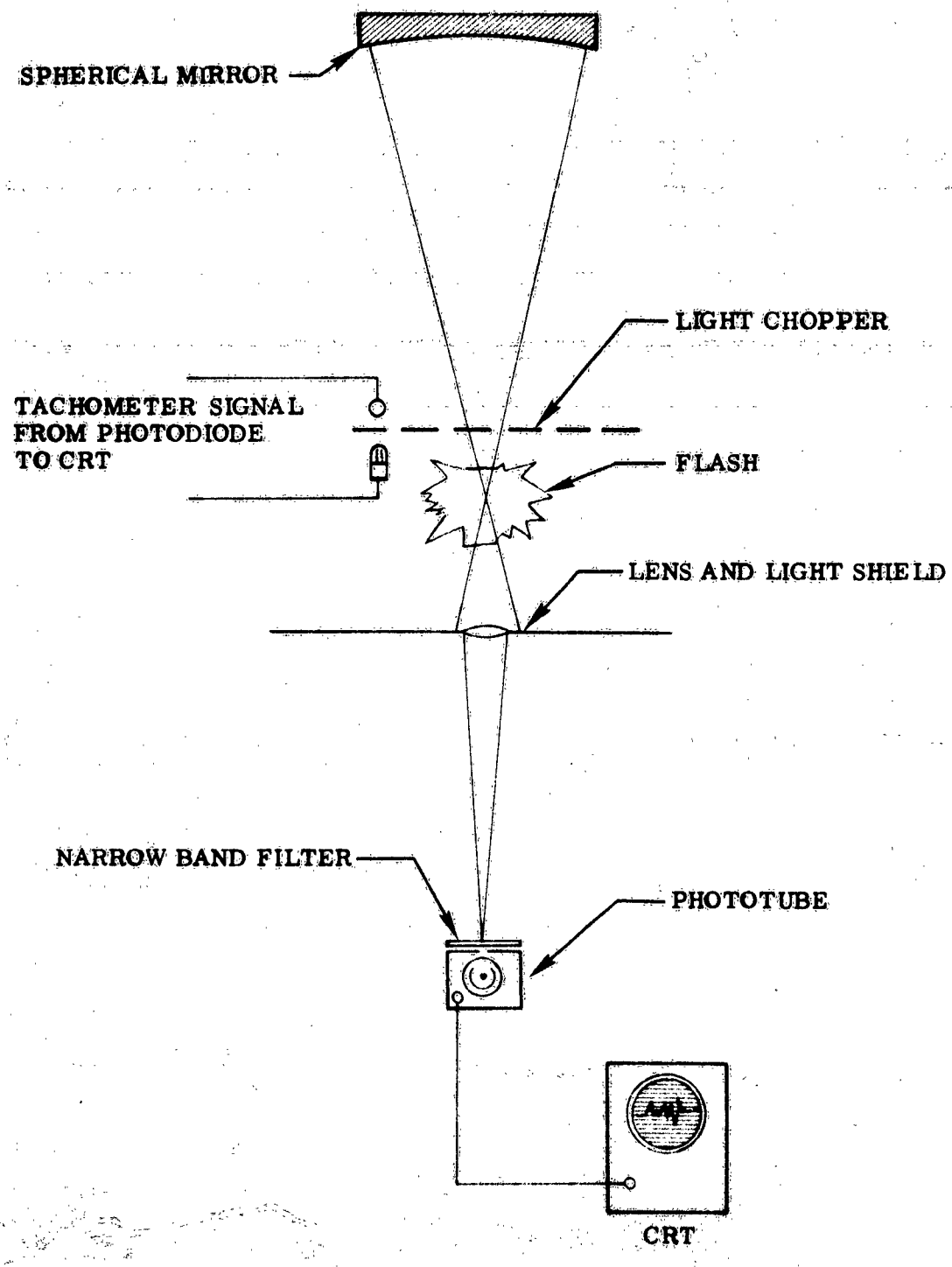

Figure 19 Single-Double Path Apparatus

Single Path

$$\left[\frac{C_2 \lambda^{-5}}{e^{C_1/\lambda T_s}}\right] = \sigma T_F^4 (1 - e^{-\gamma_a L}) \tag{1}$$

Double Path

$$\left[\frac{C_2 \lambda^{-5}}{e^{C_1/\lambda T_s}}\right] = \sigma T_F^4 (1 - e^{-\gamma_a L})(1 + \rho e^{-\gamma_a L}) \tag{2}$$

Solving the two equations for the two unknowns, E_F and T_F, it is found that

$$\varepsilon_F = (1 - e^{-\gamma_a L}) = 1 - \frac{\exp[-C_2/\lambda(1/T_2 - 1/T_1)] - 1}{\rho_m} \tag{3}$$

and

$$T_F = 1/[1/T_1 + (\lambda \ln \varepsilon_F)/C_2] \tag{4}$$

Scattering of light may be of importance to the emissive properties of the cloud and can make the determination of emissivity much more difficult. The simplest analysis that can be made of a situation involving light scattering would be to assume that all scattered radiation leaves the optical path to the sensor and negligible light is scattered into the path. In this case the equations are:

Single Path

$$\left[\frac{C_2 \lambda^{-5}}{e^{C_1/\lambda T_s}}\right] = \sigma T_F^4 \left(\frac{\gamma_a}{\gamma_a + \gamma_s}\right)\left[1 - \exp\{-(\gamma_a + \gamma_s)L\}\right] \tag{5}$$

Double Path

$$\left[\frac{C_2 \lambda^{-5}}{e^{C_1/\lambda T_2}}\right] = \sigma T_F^4 \left(\frac{\gamma_a}{\gamma_a + \gamma_s}\right)\left[1 - \exp\{-(\gamma_a + \gamma_s)L\}\right]\left[1 + \rho \exp\{-(\gamma_a + \gamma_s)L\}\right] \tag{6}$$

These equations cannot be solved rigorously because they contain three unknowns γ_a, γ_s, and T_F. Comparing the equations 1 and 2 and 5 and 6 it can be seen that the solution for E_F from equations 1 and 2 diminished by $\gamma_a/(\gamma_a + \gamma_s)$ when equations 5 and 6 are used (the change

from γ to $\gamma_a + \gamma_s$ in the exponential terms is of no consequence numerically). The equations 5 and 6 are approximations to the rigorous solution of the multiple scattering problem and are valid when $\gamma_a >> \gamma_s$ (36). The relative size of γ_a and γ_s, the absorption and scattering cross sections, can be rigorously calculated for a certain wavelength by use of Mie's theory. One must know, however, the complex refractive index of the material and the particle sizes. Neither of these quantities is known.

Single and double path measurements have been made during flashes of Al, Zr, and Hf with $KClO_4$ at the wavelengths 4500A, 5000A, and 6000A. With a chopper frequency of 1000 to 2000 cycles per second there was no great difficulty in distinguishing the alternating signal output of the phototube from random variations in the light output of the flash process. A typical phototube response during single-double path measurements is shown in Figure 20 as displayed on a CRT. The lower trace is the chopper frequency detected by a phototransistor --- light source combination described in connection with the time resolved spectra.

Since the flashes investigated were set off on a flat plate, the optical path length of the luminous cloud as well as the mass of material in the optical path are unknown. The results of these experiments could not be used for the prediction of emissivity of radiating clouds of similar particles viewed at other optical depths. As stated before, the object was to measure the true flash temperature and estimate flash emissivity.

It was usually observed that the opacity of the luminous cloud increased with time and in some cases the cloud became completely opaque (radiation from the reflecting mirror didn't penetrate the cloud) during the latter portion of the flash.

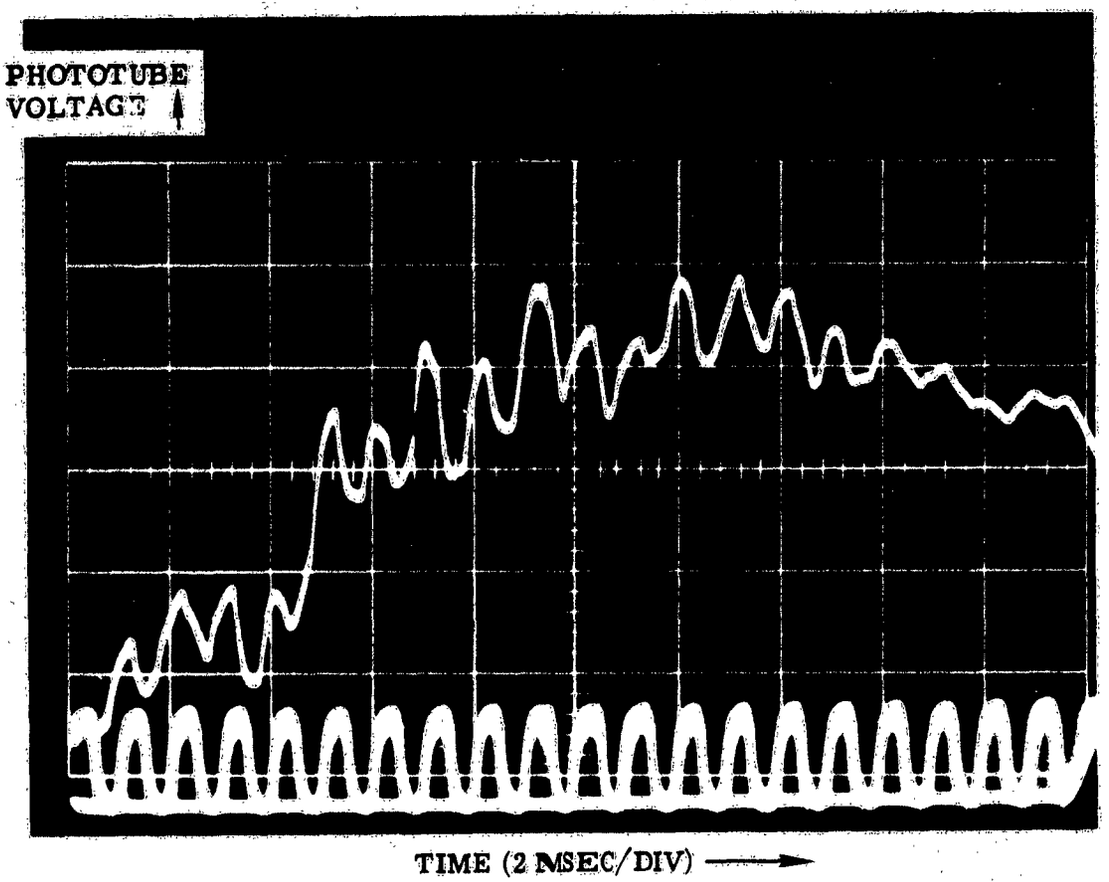

$Zr+KC\ell O_4$ FLASH

$\lambda = 5900 - 6100\text{Å}$

Figure 20. Phototube Output Single-Double Path Measurement

Some experiments were performed in which the phototube and lens was set at a slight angle ($\sim 20^{\circ}$) to the direction of the reflected light from the spherical mirror -- this was done to see if scattered radiation from the background source could be detected. None was detected. The solid angle viewed by the phototube was very small (0.00464 steradians) and scattered radiation would have been difficult to pick up and distinguish from radiation directly from the flash.

Because of the small solid angle viewed by the phototube it appears reasonable to expect that [illegible] of radiation from a source placed behind the flash would obey the Lambert-Beer law: $I_{out} = I_{in} \exp\{-(\gamma_a + \gamma_s)L\}$

The data gathered using the flash-double path technique are compiled in Table V along with the theoretical adiabatic flame temperature of the metals reacting with [illegible] (this was not on the data tapes used in the computations). The [illegible] and temperatures tabulated were calculated using equations I and

Summarized Combustion Results

Before proceeding to the discussion on additives, it is desirable to summarize the major [illegible] with the combustion studies. Table VI presents typical [illegible], pulse durations, and spectral characteristics [illegible] medium pressure, and high pressure reactions studied [illegible]. The $Al+ClO_4$ reaction at one atmosphere pressure was [illegible] additives study. The typical behavior of the reaction should [illegible] the behavior of the other reactions listed in the table [illegible] discussion on additives.

Table V

MEASURED "EMISSIVITY" AND "TRUE TEMPERATURES" FROM SINGLE-DOUBLE PATH EXPERIMENTS

	4500 Å		5000 Å		6000 Å	
	E	T	E	T	E	T
Hf - $KClO_4$	0.86	3640°K	0.628	3655°K	0.9	3590°K
	0.90	3625	0.81	3720		
	0.73	3710	0.83	3720		
Al - $KClO_4$	0.67	3390	0.86	3310	0.80	3307
Zr - $KClO_4$	0.6	3670			0.79	3390
					0.73	3435

TABLE VI

TYPICAL REACTION TEMPERATURES, DURATIONS, AND SPECTRAL CHARACTERISTICS

Reactants	Particle Size	T_b(°K)Obs.	T_b(°K)Est.	(Msec) Pulse Duration	Spectral Characteristics	Max. Pressure
UNPRESSURIZED						
Th + $KClO_4$	-44μ	4200	4200	6-10	Mainly Continuum	1 atm.
Hf + $KClO_4$	-44μ	4200	4200	6-10	"	"
Zr + $KClO_4$	-44μ	3800	3800	6-10	"	"
Zr + $KClO_4$	-105μ, -44μ	4100	4100	20-100	"	"
Zr + O_2	Wool	4000	4000	50-80	"	"
Al " $KClO_4$	-3μ, -44μ	3800	3800	2-10	"	"
Al + O_2	Wool	3800	3800	30-60	"	"
Al + Mg + $KClO_4$	-3μ, -44μ, -44μ	3700	3700	5-10	"	"
Al + Mg + $NaClO_3$	-3μ, -44μ, -44μ	3500	3500	5-10	"	"
Al + Mg + $Ba(ClO_3)_2$	-3μ, -44μ, -44μ	3500	3500	1-8	"	"
MEDIUM PRESSURE (4000 psi)						
Th + $KClO_4$	-44μ	4200	4200	2-10	"	400 psig
Hf + $KClO_4$	-44μ	4500	4500	2-10	"	400
Zr " $KClO_4$	-44μ	4500	4500	2-10	"	1000
Zr + O_2	Wool	5300	6000*	15-200	"	4000
Al + $KClO_4$	-3μ, -44μ	4000	4000	1-2	"	400
Al + O_2	Wool	4200	5000*	2-50	"	1000
HIGH PRESSURE (60000 psi)						
Hf + $KClO_4$	-44μ	5500	6500*	0.5-1	"	60000
Zr + $KClO_4$	-3μ	5000	6000*	0.1-0.5	"	---
Zr + $KClO_4$	-44μ	5000	6000*	0.5-1	"	30000
Zr + $KClO_4$	-105μ, -44μ	5000	6000*	0.5-2	"	30000
Zr + Mn + $KClO_4$	-44μ	5300	6200*	0.5-1	"	40000
Al + $KClO_4$	-3μ, -44μ	4800	5700*	0.1-0.5	"	40000

* Corrected for estimated window darkening.

EFFECTS OF ADDITIVES

Theoretical Selection of Additives

Equilibrium is defined as the condition for which no potential exists for changing the energy distribution. All other conditions are nonequilibrium conditions.

By this definition, it is seen that many different energy modes may be in nonequilibrium. Radiation is generally not in equilibrium; it is usually deficient in energy. Chemical equilibrium generally does not exist unless the system is at high temperature; the chemical system usually has an excess of energy. Electronic, vibrational, rotational, and kinetic energy modes are generally in equilibrium except under low pressure conditions. The problem of interest here is to take the chemical nonequilibrium and convert the excess energy to radiation of a specified frequency range.

To convert chemical energy to radiation, many different techniques are available. These techniques take the energy of the chemical system and transform it one or more times to finally obtain radiation. Each energy transformation is limited by the laws of radiation and thermodynamics, which allows us to put limits on the efficiency of transformation of the proposed techniques.

The occurrence of nonequilibrium and techniques of use are analyzed for guidance in the pumping program.

Theoretical Bases

The bases for an analysis of the radiation and thermodynamic laws, in particular the considerations of interest here are: blackbody radiation (37), emissivity (37), theoretical flame temperatures (38), entropy (39), and

equilibrium energy distribution (40). Since these topics are covered adequately in the literature, only the final equations are given.

Blackbody radiation is described by Planck's equation

$$\rho_\nu^\circ(T) = 8\pi h \nu^3 / [\exp(hc\nu/kT) - 1]$$

where ρ_ν is energy density at the frequency ν (frequency in wave numbers per cm.). The superscript zero indicates blackbody. Defining the radiancy

$$R_\nu^\circ = c^2 \nu^2 \rho_\nu^\circ / 4$$

Integrating over the frequency gives

$$R^\circ = \sigma T^4$$

for the total radiation energy for all wave lengths.

The emissivity is defined as

$$R = \epsilon R^\circ$$

or

$$R_\nu = \epsilon_\nu R_\nu^\circ$$

for the total emissivity ϵ or the spectral emissivity ϵ_ν. The emissivity, ϵ, reflectivity, r, and scattering coefficient, s, are related

$$1 = \epsilon + r + s$$

or

$$1 = \epsilon_\nu + r_\nu + s_\nu$$

Often $s \approx s_\nu \approx 0$ and the scattering is ignored.

Theoretical flame temperatures are calculated by (1) mass balance equations, (2) enthalpy balance equation, (3) pressure balance equation, and (4) equilibrium constants. These equations are all that are needed to specify the system. Since equilibrium is assumed, complete combustion is assumed. Since an enthalpy balance is assumed, an adiabatic system is assumed. (While not used, the flame temperature at constant volume can be calculated by replacing the enthalpy by the internal energy and pressure by density.)

The entropy is important for determining the limits on energy conversion is an isentropic process occurs, the equilibrium conditions hold. Thus, in an isentropic radiation process, the blackbody limit is imposed. The entropy is defined

$$dS = dS_r + dSi$$

$$= \frac{dQ_r}{T} + \frac{dQ_i}{T}$$

where r indicates reversible and i irreversible, Q is an artificial variable to make both terms formally the same. The definition of dQ is

$$-dQ = dU\Big|_{s,\,r}$$

In other words, an irreversible change is accompanied by a decrease in internal energy. The implications of this statement are simplified during the discussion on tapping.

The Boltzman energy distribution is given as

$$n_i = N\omega_i \exp\left(-\epsilon_i/kT\right) \Big/ P.F.$$

where n_i is the population of state i, ω_i is the statistical weight of state i, and E_i is its energy level. Ignoring negligible quantum effects, this gives the equilibrium distribution. Conversely given n_i a temperature for the state is defined. The energy levels are for any mode--kinetic, rotational, vibrational, or electronic.

Nonequilibrium Studies

In a nonequilibrium condition, there is a driving force or potential that will tend to equilibrate the systems. To use the nonequilibrium potential for laser pumping, potential must be converted to radiation in a spectral band. This is the objective of this study.

Nonequilibrium exists as frozen composition (as mixing zirconium and $KClO_4$ at room temperature), radiative nonequilibrium, excess excitation of energy levels (often occurs because of chemi-excitation,) hot spots, and underexcitation are characteristic of low pressure systems (and hence poor radiative systems), these modes of nonequilibrium are not discussed further. In addition, frozen composition is the typical for chemical reactions. The only phase of interest to this study is the energy output and combustion efficiency. Thus, the nonequilibrium aspect is not discussed.

Radiation

There are a number of problems associated with radiation. The ones of interest in this study are emissivity, optical depth, and chemiluminescence. While important, emissivity and optical depth are not discussed in this section. Chemiluminescence is the basis for tailoring and tapping energy of chemical reactions. In a chemical reaction, the energy released goes into kinetic, rotational, vibrational, and electronic energy. Generally, the energy goes to exciting the molecule rather than kinetic energy as:

$$O + H + M \longrightarrow OH^* + M^*$$

Thus, easily excited species are much more effective third bodies than monatomic species. Since excitation is the primary path of a reaction, our problem is to tap this energy before it converts to kinetic energy.

The temperature of the excited state can be calculated from the distribution

* excited states

$$\epsilon_i/kT = \ln (N/n_i)$$

This temperature (which is not the kinetic temperature) controls the radiation equilibrium--assuming no absorption in the surrounding gas. As such, it appears that the blackbody radiation limit for the radiating gas is unimportant. A more serious problem can occur from a mantle of nonexcited gas surrounding the radiating gas.

Overexcitation

Excitation can occur by thermal excitation, excitation transfer, and chemical reaction. In thermal excitation, the excitation is in equilibrium with the kinetic temperature. This produces the normal excitation for comparison. It becomes overexcitation only when the kinetic temperature decreases rapidly--which does not occur in our system. In excitation transfer, the excitation energy is transferred from one species to another. This is the mechanism for tailoring radiation, but overexcitation is not produced this way, only transferred. Chemical excitation is the only method for production of overexcitation in our system. In a chemical reaction, the chemical energy is converted into excitation energy and kinetic energy. The usual conservation laws (mass, momentum, angular momentum, spin, and energy) hold for collision in which a chemical reaction occurs (41). Since momentum is a vector quantity, it is possible that all the energy can be converted to kinetic energy by a superelastic collision. The cross section for the various collisions, must be obtained to give the ratio of excitation to kinetic energy. However, in almost every reaction studied for excitation, it has been found. This is the source of nonequilibrium excitation in our system.

Techniques

In tapping or tailoring radiation, a high emissivity material is used as a dopant. In tailoring the radiation, the emission is raised toward the blackbody limit for the kinetic temperature. In tapping, the energy of excitation is converted to radiation. If the excitation is at an effective temperature higher than the kinetic temperature, the radiation can be above the blackbody limit for kinetic temperature. The limiting temperature in all cases is the effective temperature of the pertinent process. (Unfortunately, this is many times the cool outer portions of the combustion).

As dopants, metals, salts (with strong dipoles), and fluorescent solids are considered. If the fluorescent solid will work, it appears to be the best choice. The energy of condensation should be easily tapped. The emitted radiation is less likely to be reabsorbed, and most fluorescents are radiators. Possibly it will not be able to take the conditions of the combustion. Since the total combustion time is short, there is a chance that the fluorescent solid can survive.

If the fluorescent solid will not work, metals and salts will be tried as dopants. Both are strong gaseous radiators. There is a possibility that, since the condensation is the energetic reaction, gaseous species will not be able to tap the system. Thus, an experimental program is essential for testing the systems.

Candidate Systems

Calculations were run for aluminum and potassium perchlorate, and for zirconium and potassium perchlorate. Adiabatic flame temperatures for the two systems are about 5000°K and 7500°K respectively at 68 atmospheres

pressure. This gives a radiation intensity of $2.31 \times 10^{-2} \epsilon/\rho$ and $3.59 \times 10^{-2} \epsilon/\rho$ kcal/gm in the visible. (The density converts to mass from the area radiation to make the units comparable to the excess energy at lower temperatures.)

If we allow the systems to combust at one atmosphere at a temperature sufficiently high for good combustion (2700°K for Al and 3000 for Zr), there is considerable excess energy. It amounts to 5.4 kcal/gm for the aluminum and 0.99 kcal/gm for zirconium.

Looking at the thermochemical data, only beryllium, boron, and lithium appear to be comparable to aluminum. This easiest system to handle is one of the best.

Most metals are good radiators as are fluorescent materials. Thus, the main interest is to select the correct radiation bands. Examples of metals are Ti, Y, Ag, Cu, Ba, Tl, and Hg. Since we are interested in the metal and not a compound, the metal should be relatively inactive. All except barium in the above list are less active than aluminum.

Typical phosphors that radiate in the correct spectral region are Zn_2SiO_4: Mn, ZnS: Ag: Cu, Zn_3 $BeSi_5$ O_{19}: Mn, and MgSi Sb. In addition, a short persistence and high saturation density are desired. Of the listed fluorescent materials, ZnS: Ag: Cu has a long persistence.

Salts that have large dipole moments are usually good radiators. Since transition probabilities are hard to come by, initial screening is by dipole moments. In general, large dipole moments occur in polyatomic molecules--which have only a limited spectral analysis. Thus, the screening on

molecules will be the heavy metal chlorides and fluorides. It was hoped that augmentation would occur with these salts.

Experimental Selection of Additives

A number of experiments were performed in which salts, metals, or phosphors were added to a stiochiometric mixture of 3μ dia. Al particles with 20μ dia. $KClO_4$ particles. These additives or dopants were used in an attempt to modify the radiant energy output by producing nonequilibrium radiation.

Time resolved spectra were taken of the chemical flashes with Kodak 103-F film that had been calibrated for brightness temperature when using 2 millisecond time exposures. The additives used are listed in Table VII A complete microphotometer trace was taken of at least one exposure on each film. Actually, this was all that was usually necessary since any spectral regions of intense radiation could be spotted by scanning the film by eye.

None of the spectra taken indicated the presence of nonequilibrium radiation anywhere in the region from 3660A° to about 6700A° covered by the 103-F film in conjunction with the Bausch and Lomb spectroscope. Many emission lines stand out from the continuum, or, particle radiation, but have never indicated inordinately large brightness temperatures, i.e. greater than the computed adiabetic flame temperature, (at least when integrated over a 2 millisecond time interval).

TABLE VII

CHEMICALS ADDED TO STIOCHIOMETRIC $Al/KClO_4$ FLASH POWDER

A. Additives Producing Noticeable Band or Line Emission from 3660 to 6700°A.

Additive	Brightness Temperature of Na Emission
$Ba(ClO_4)_2$ Anhydrous	3500°K
$Ba\ F_2$	3600
$Ba\ (NO_3)_2$	3750
$Ba\ (NO_3)_2 + MnO_2$	3600
$Ca\ (ClO)_2$	3400
Cr_2O_3	3600
Cu_2O	3500
$LiNO_2 + MnO_2$	3200
$Mn(ClO_4)_2 \cdot 6H_2O$	3800
$Na\ NO_3$	3550
$Tl\ NO_3$	3450

B. Additives Producing No Change in Spectral Energy Distribution from 3660 to 6700°A.

Additive	Brightness Temperature of Na Emission	
$CdCl_2 \cdot 2\text{-}1/2H_2O$	3400°K	(Max. from Phototube at 6000A = 4680°K
CdS	3530	
$CoCl_2$	3600	(Chance of double exposure on film)
$Cu/KClO_4$	3600	
H_6Cl	3350	
$Ni/KClO_4$	3320	
$Ni\ (ClO_4)_2 \cdot 6H_2O$	3140	
NiF_2	3800	
PbF_2	3450	
$SnCl_4 \cdot 5H_2O$	3375	
$Zn\ (ClO_4)_2 \cdot 6H_2O$	3500	
ZnS	3450	

The list of additives can be broken into two gross and rather obvious groups; group A consists of those that can be seen to have modified the spectral energy distribution by producing pronounced band or line emission, and group B, those additives which have not. TableVII is divided into these two categories. This is a somewhat arbitrary breakdown since for the most part it is based only on one or two flashes. It is seen, for instance, that the additives Cu_2O and Cu are in different groups; this is so because the Cu_2O additives produced evidence of CuCl and CuO band radiation or absorption while the 150 mesh Cu metal powder did not. Perhaps if more finely divided metal had been used or if different ratios of Cu to Al had been used the result would have been different.

It had originally been planned to add many of the metals in the form of perchlorates so as to lessen the heat load, since then the additive would also serve as an oxidizing agent and thus replace some $KClO_4$. Many of the perchlorates proved unsatisfactory however, because of their tendency to rapidly absorb moisture from the air and turn a flash powder mixture into a paste or slurry. Preparation of the mixtures in a dry box and flashing in a closed container such as the modified bomb calorimeter could have set aside some of this trouble, but because of lack of time it was decided to use less deliquescent metal salts. A list of the perchlorates and their replacements is given below.

Perchlorate	Replacement
$Cr(ClO_4)_3 \cdot 6H_2O$	Cr_2O_3
$Pb(ClO_4)_2 \cdot 3H_2O$	PbF_2
$Ce(ClO_4)_3$ - hydrated	$Ce(HSO_4)_4$
$Cu(ClO_4)_2 \cdot 6H_2O$	Cu_2O
$Ca(ClO_4)_2 \cdot 6H_2O$	$Ca(ClO)_2$

While it was possible to ignite a mix containing $Ni(ClO_4)_2 \cdot 6H_2O$, the flash barely registered a voltage output on the phototubes. Perhaps $Ni(ClO_4)_2 \cdot 6H_2O$ could be added to the above list with NiF_2 as the replacement.

The mixture containing $SnCl_4 \cdot 5H_2O$ was extremely difficult to ignite. It was found later that the salt rapidly reacted with the solid aluminum upon mixing the two (probably aided by some absorbed moisture or the water of hydration) to produce metallic tin and $AlCl_3$.

Other compounds which, for unknown reasons, made ignition difficult were $LiClO_4$, $BaCl_2$, and $Ca(NO_3)_3$. $LiClO_4$ was not used as an additive, it was to replace $KClO_4$. A small amount of $Hf/KClO_4$ was used as an ignitor in a last attempt to flash the $Al/LiClO_4$ powder. The attempt did not succeed and

use of $LiClO_4$ was abandoned. Mixtures of $Al/KClO_4$ containing small amounts of $BaCl_2$ burnt slowly and incompletely as did mixtures containing $Gd(NO_3)_3$.

In TableVIIthe brightness temperature in the immediate vicinity of the Na-D lines, as determined from microphotometer traces of the film spectra, is also recorded. The average Na-D line temperature for group A and group B is 3500K and 3460K respectively. It should be kept in mind that the Na-D lines were almost always self absorbed at the peak, thus the temperatures listed are likely to be on the low side. Temperatures recorded by phototubes would be lower still. The phototubes used for this phase of the program were equipped with filters having a 200Å half width. Brightness temperatures measured in this way will correspond more or less to the energy in the continuum and thus the temperature of the particles.

Some of the emission or absorption lines are common to all of the spectra taken in group A or B. These will be discussed first.

Potassium, which was always present in these experiments by virtue of the oxidizer used ($KClO_4$), has a resonance line corresponding to the Na-D line, in the infrared at 7664.98Å. This is beyond the range of the equipment used. More normally only radiation due to doubly excited states of K have been noted on the film. These K lines are located near the Na-D line and appear at 5782.77, 5807.16, 5812.71 and 5832.31 Å. Self absorption of these lines has never been noted in the time resolved spectra taken. In some spectra taken early in the program with another film emulsion batch No. the K doublet at 6938.96 and 6911.30 could be discerned even though the film sensitivity in this spectral region was quite small. Other K lines can be seen at 4044.14 and 4047.20Å.usually in absorption because the lower energy

level is the ground state and thus highly populated.

The Na-D lines always appear in spectra taken of these chemical flashes; this is because trace amounts of sodium are usually present as an impurity. When a sodium compound ($NaNO_3$) was purposely added to an Al/$KClO_4$ flash the result was a surprising broadening of the D lines to at least a 50 Å to 100 Å half width. The peak intensity, however, is in line with normal equilibrium radiation. Addition of $NaNO_3$ also brought out other sodium lines representing transitions from doubly excited states (4^2D and $5^2S\frac{1}{2}$) to the singly excited quantum state (33). Radiation from these more highly excited states have the advantage of not being readily self absorbed because of the small population of the lower energy state. Neither of the doublets at 5682.67, 5688.22 and 6154.27, 6160.73Å had a high peak brightness temperature.

There is also, of course, the band radiation of the $B^2\Sigma \longrightarrow {}^2\Sigma$ electronic transition of the AlO molecule (32). The band heads of all the transitions listed below are plainly visible in the spectra taken.

vibrational transition	wavelength
V ⟶ V-2	4470.5Å
V ⟶ V-1	4648.2
V ⟶ V	4842.1
V ⟶ V + 1	5079.3
V ⟶ V + 2	5336.9

AlO emission structure is most prominent early in the flash and usually fades into the continuum near or soon after the peak light output. The AlO bands are never observed in absorption and so must exist at the highest temperature of the system. Film spectra have shown the Na-D lines

and other emission lines to be more intense than AlO. This is probably because the emissivity of AlO is lower. Al lines appear at 3944 and 3961Å almost always in emission, but has been observed to go into absorption.

Many of the spectra taken show Hg lines, seemingly very intense. These lines are due to stray light from the overhead fluorescent lamps and the fact that there is no shutter on the spectrometer slit.

Barium Salts

Three of the additives tried were barium compounds, Ba $(ClO_4)_2$, BaF_2, and Ba $(NO_3)_2$. (There is a fourth containing $Ba(NO_3)_2$ and MnO_2). Ba $(ClO_4)_2$ and Ba $(NO_3)_2$ produce similar spectra consisting of BaCl bands and a strong Ba line at 5535.53Å, while BaF_2 addition results in these bands plus the band structure of BaF at 5000.6, 4992.1 and 4950.8Å. The BaO bands have not been detected in the flashes. Of the three, the best additive is $Ba(NO_3)_2$ since it produced the highest temperatures (both phototube and Na-D line from the film). BaF_2 as an additive produced a 60 millisecond time delay from spark ignition to the beginning of light emission (15 milliseconds would be average) and a rather long flash. The comparison of these additives might not be a rigorous one since BaF_2 and Ba $(ClO_4)_2$ were present in 1 to 2% quantities, while the $Ba(NO_3)_2$ mixture was 40% Al, 30% $KClO_4$ and 30% $Ba(NO_3)_2$. Ba $(ClO_4)_2$ might have worked as well as the nitrate. The Ba $(NO_3)_2$ is itself an oxidizer and has been reported to be an effective catalyst for $KClO_4$ decomposition to KCl (34). Addition of $Ba(NO_3)_2$ does shorten the flash reaction time, thus bringing about less conduction heat losses from the radiating cloud. Microphotometer traces of time resolved spectra of Al/$KClO_4$/$Ba(NO_3)_2$ flashes in Figure 46

show strong BaCl emission bands at 5136, 5240 and 5321A that appear early in the flash then fade into the continuum as the brightness temperature of the continuum rises and finally show up in absorption as the radiating cloud cools. These bands would increase the light output in the green if the emissivity of the continuum was low or if this green light output was needed very early in the chemical flash.

The Ba line at 5535.53Å is a strong radiator that is not as easily self reversed as the Na-D line. The microphotometer traces show this Ba line to be a good indicator of the gas temperature.

Calcium Compounds

As has already been mentioned, at first the perchlorate $Ca(ClO_4)_2 \cdot 6H_2O$ was tested but rapid water absorption lead to its replacement by $Ca(ClO)_2$. Calcium chloride is known to color flames red because of CaCl band emission. Addition of calcium hypochlorite brought out the CaCl $^2\Pi \rightarrow {}^2\Sigma$ bands lying between 5934Å and 6400Å (32) and a resonance line of Ca at 4226.73Å. No acceleration of the $Al/KClO_4$ reaction was noted and the measured flash temperatures are average.

Chromic Oxide

From time resolved spectra taken of an $Al/KClO_4$ flash containing a few per cent Cr_2O_3 the band structure of CrO at 6451.5, 6394.3, 6051.6, 5794.4, 5623.3 and 5564.1Å (32) as well as five Cr lines at 4254.34, 4274.80, 4289.73, 5204.54 and 5206.04Å could be identified.

It has been reported that additives, such as Cr_2O_3, MnO_2 and other metal oxides will increase the rate of perchlorate decomposition (e.g. 35). Limited data taken on Cr_2O_3 addition are inconclusive.

Cuprous Oxide

Spectra taken of flashes containing Cu_2O indicate CuCl bands in absorption from about 4250A to 4500A ($D\,^1\Pi \rightarrow {}^1\Sigma$ and $E\,^1\Sigma \rightarrow {}^1\Sigma$, (32). Other CuCl bands might be present, but difficult to distinguish from the AlO band structure. From 6059A to 6294A, CuO bands are visible in emission.

Lithium Nitrate

The addition of $LiNO_3$ resulted in Li lines at 4132.8, 4602, 4603, 4971.?, 6103.6A, and a strong broadened resonance line at 6707.85A (2P→1S). The Li line at 6103.6A appears quite intense, having a peak brightness temperature of about 3300K while the self absorbed Na-D lines yield 3200K.

Manganese Compounds

Two manganese compounds were tried, MnO_2 and $Mn(ClO_4)_2 \cdot 6H_2O$. There is no doubt that MnO_2 will accelerate the Al + $KClO_4$ reaction. It has also been postulated that MnO_2 would increase the emissivity of the radiating solid or liquid particles. Time resolved spectra of flashes that contained either MnO_2 or $Mn(ClO_4)_2$ show the MnO emission bands at 5586.4, 5609.5, 5859.6, 5880.3, 6175.9, and 6203.2Å. There is also a Mn triplet at 4030.8, 4033.0 and 4034.5A usually appearing in absorption.

Thallium Salts

The thallium salt additive, $TlNO_3$, produced two Tl lines, one usually in absorption in the continuum at 3775.73A and one very strong line in emission at 5350.47A. The strong Tl line is comparable in intensity to the NA-D lines and could be used for measuring vapor phase temperatures.

Phosphors

Among the series of additives tested were two phosphors, ZnS and CdS. They were tried in the hope that the solid phosphor would survive, for a time at least, the high temperatures produced. Neither additive appears to have altered the basic spectrum of an Al + $KClO_4$ flash and they have been listed in group B of Table VII.

Emission Spectra

In addition to the major additive program, emission spectra have been taken of the reaction of stiochimetric mixtures of $KClO_4$ and aluminum, zirconium, hafnium, lanthanum and neodymium powder. The spectra were taken using the Bausch and Lomb 1.5 meter spectrometer with Kodak 103-F film and covered the region from 3660Å to about 7000Å. Most of the band structures observed have been identified as being due to metal oxides (AlO, ZrO, HfO, LaO) using the tabulation of Pearse and Gaydon (32). The microphotometer traces of the film are shown in Figures 49 and 50 with the metal oxide bands labeled. The band structure of HfO has not been analyzed and only the location of prominent band heads listed by Pearse and Gaydon (32) are pointed out in that figure. These particular spectra, with the exception of Hf, are not time resolved and thus isotherms have not been drawn on them.

Neodymium was included in a list of possible reactants primarily because it was expected that the rare earths might emit in the region where rare earth dopants in the lattices of lasers would have absorption bands. Hopefully, rare earth additives would modify or tailor the spectral emission characteristics of the chemical flash. Spectra of the Nd-$KClO_4$ flash reaction were taken and found to contain only continuum radiation from solid particles and a number of fine lines attributable to Nd vapor or impurities (see Figure 49). None of the NdO emission bands listed by Pearse and Gaydon could be identified. There was no evidence of higher emission in spectral regions where Nd in glass lasers can be pumped.

Neodymium addition was tried in zirconium and aluminum powder flashes to see if the emissive characteristics of the flash reactions could be tailored. The spectra taken appear in Figure 50. It was found that small amounts of Nd in Zr resulted in a large reduction or disappearance of the band structure of ZrO; the emission is mostly continuum and resembles that of the Nd-$KClO_4$ flash in its lack of band structure. Also shown in Figure 50 is the spectrum of Al $KClO_4$ with and without Nd addition. Addition of about 20 per cent by weight of Nd-$KClO_4$ to Al-$KClO_4$ did not obscure the AlO band structure and produced some identifiable band structure of NdO extending from 6585.2 to 6620.6 Å. There also appeared to be a slight enhancement of continuum radiation in the red; this enhancement however, is not in the Nd glass laser pumping bands.

Probably the boiling point of ZrO_2 is high enough so that additivies resulting in a lowering of the flame temperature greatly reduce the amount of ZrO vapor present. This colder burning mixture will then exhibit a much reduced oxide band structure. The aluminum burns mostly in the vapor phase and the flame temperature of Al-$KClO_4$ mixture is closer to the maximum temperature of Nd-$KClO_4$ so that the cooling effect of Nd is less. The NdO bands are not visible in the zirconium metal flashes because the continuum radiation is intense enough to obscure them.

Section IV

LASER SYSTEM STUDIES

As has been pointed out before, chemical reactions can release large amounts of energy per pound and this energy can be efficiently converted into light. However, to be a useful laser pump the light must be emitted at an intensity above that required to reach lasing threshold. The lowest threshold laser is Dy^{+2} in CaF_2. This material has been pumped with a tungsten light indicating that it requires a brightness temperature less than 3000°K. Neodymium has no specific threshold temperature requirement since its characteristics are so greatly influenced by its host material. The fluorescent lifetime can vary from 8.1 μ sec. to 637 μ sec.[1], depending on the type of glass used for the host. Similar variations exist for the fluorescent line width and absorption coefficients. Neodymium, therefore, has a range of threshold temperatures from approximately 3500°K to 5000°K. Ruby is more amenable to analysis and the threshold brightness has been determined to be about 5250°K[2]. It is possible to analyze the efficiency of a light source of a particular spectral distribution if it were used to pump a laser amplifier which was continually being swept out by a driver beam. In other words, we determine the efficiency of the production of excited Nd^{+3} atoms. For neodymium, this was determined by using the data available

1. Eastman Kodak Co.
   Laser Material Study
   Contract Nonr 3834(00)

2. T. H. Maiman et al
   Stimulated Optical Emission in Fluorescent Solids
   Physical Review, Aug. 15, 1961

for American Optical's AOLUX 3669 Neodymium Laser Glass. From a plot of the transmission of a 1/4 inch piece of glass, the area under each of the absorption bands was determined and evaluated for energy efficiency and quantium efficiency. These plots were made for black body spectral distributions from 2000°K to 10,000°K.

In the case of ruby, a ruby amplifier being pumped by a black body radiating cavity was analytically examined to determine its efficiency as a function of pumping temperature.

The model consisted of a 1/4 inch diameter ruby which was only being pumped by the green absorption band. The violet band was not used for two reasons: It is not as efficient as the green absorption band; and Maiman[2] has shown that appropriate violet radiation can stimulate transitions from the 2E level to the charge transfer band, producing a net depopulation of 2E when the laser is being pumped. There is also a 50% reduction in efficiency for ruby because of line splitting of the 2E level.

Figure 21 shows the results of this laser study. The ruby amplifier shows a sharp rise in efficiency at 5250°K because this is the temperature where amplification begins. With neodymium there is no true minimum pumping temperature because absorption at the lasing frequency can be decreased as laser glass technology improves.

Present day lasers are not perfect, so they will not reach the efficiencies shown on this graph. Neodymium glass rods in production have an absorption of 0.6%/cm at 1.06μ with experimental glasses as low as 0.1%/cm at this wavelength. The lasing output of ruby rods suffers from the defects of scattering centers and nonhomogeneous crystals. The defects

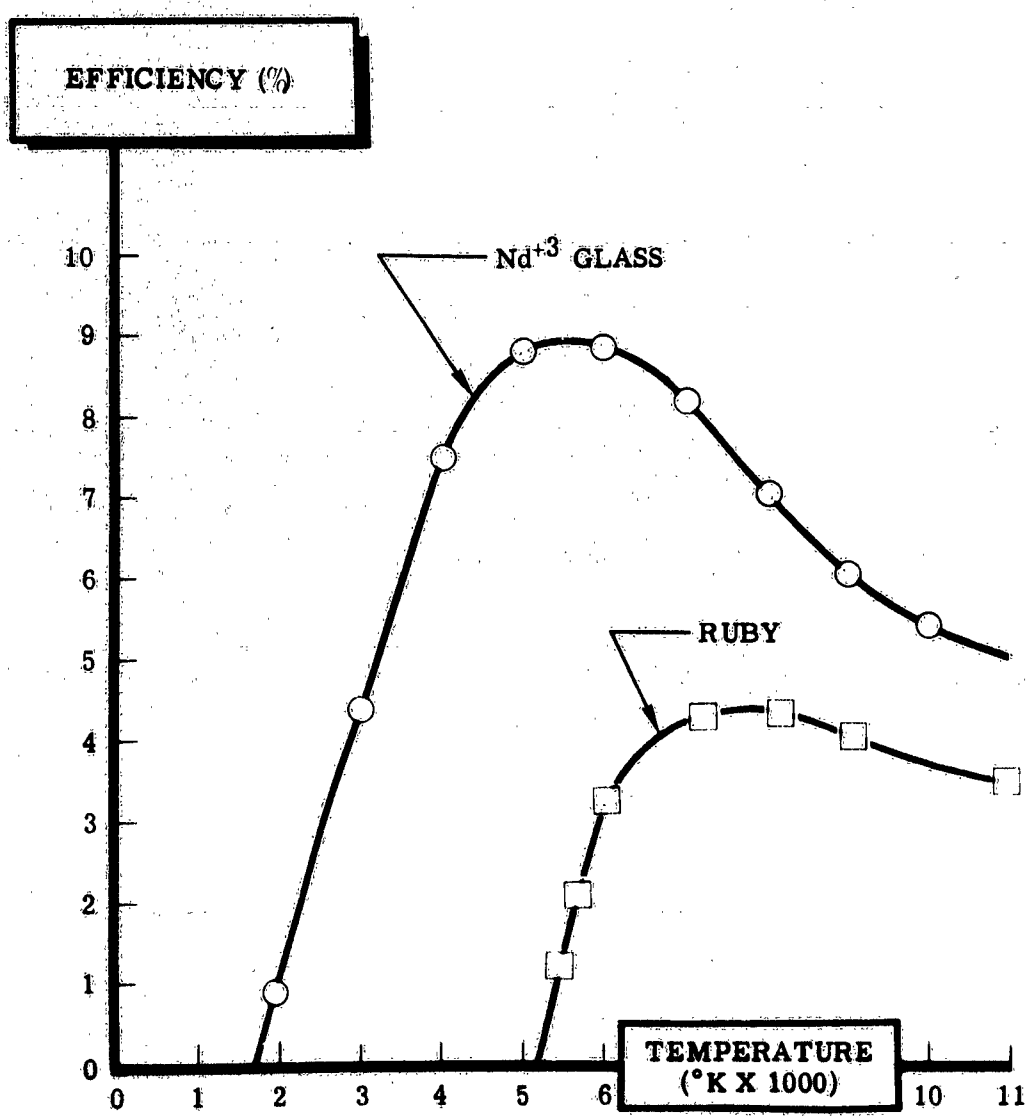

Figure 21. Efficiency of Conversion of Black Body Radiation to Laser Output for Idealized Laser Materials

decrease the efficiency further, but have not been included because they vary from rod to rod. From Figure 21 it is obvious that both ruby and neodymium can be pumped by 5500°K chemical reactions. However, the output from ruby would not be very far above its threshold and would not be very efficient. On the other hand, a neodymium amplifier could be efficiently operated even at a much lower temperature.

In chemical reactions suitable for laser pumping there are three increasingly difficult levels in obtaining high temperatures. The easiest is using a metal and solid or gaseous oxidizer at one or two atmospheres pressure. With this technique there is no need for a high pressure chamber because no attempt to pressurize the reaction is made. With this type of system it is possible to obtain 4400°K with hafnium and potassium perchlorate or 4000°K with zirconium and gaseous oxygen. The unpressurized gaseous oxidizer reactions can be contained in a replaceable glass cylinder and convert approximately 40% of the available chemical energy to radiation. The radiated energy can then be converted into laser output with an efficiency approaching 7.5%.

The next level of difficulty is to use a metal chamber to contain a reaction of zirconium wool and 1500 psi oxygen. This achieves about 5300°K brightness temperature at an undetermined efficiency suspected to be between 2 and 15%. The highest level of difficulty is to use a very strong chamber which can withstand a shock wave of 100,000 psi and a pressure pulse of 40,000 psi. Protecting a laser rod against such pressures and keeping any window area clean becomes a very serious problem. The temperatures generated are in the 6500°K region, however, the window fogging problem lowers the useful brightness temperature. The measured efficiency of this

reaction was about 2.5%, however, no compensation was made for incomplete burning, venting, and window charring. The efficiency would be 10 to 15% if these factors were controlled.

In a practical device a neodymium glass oscillator-amplifier combination appears to hold the most potential. Present neodymium glass amplifiers can be swept out when a driver beam of 10 joules/cm^2 is passed through it. Experimental rods are being fabricated which can be swept out with even lower energy densities. Pumping with the easiest to handle chemical reactions - the nonpressurized reactions in the 4000°K to 4400°K range - would permit between .25 and .35 joules/cm^3 to be swept out of a 1/4 inch diameter amplifier. This amounts to approximately 50 joules per pound of laser rod. In terms of laser rods a 50 joule system could be built using 17 rods 1/4 inch in diameter by one foot long, or five rectangular rods 1/5" x 1" x 12". These rods need not be placed end to end but could be optically folded using prisms. A driver beam produced from a laser oscillator pumped by the chemical reaction or by a small capacitor-flashtube system is required to sweep out these amplifier rods. The driver could have an output of 1 or 2 joules if it is to be amplified first in smaller diameter rods. The resulting oscillator-amplifier combination could be designed to weight between 10 and 15 pounds at an output rating of 50 joules.

A higher brightness temperature is desirable because it permits more energy to be obtained from each laser rod. However, the weight of the pressure vessel and protection of the laser become problems. To determine the problems encountered in pumping a laser in a high pressure chamber NAA/LAD designed and constructed such a chamber on internal funds. The

chamber shown in Figure 22 has been designed for constant volume reactions to a peak pressure of 100,000 psi, and will accept laser rods up to 1/2" x 6".

The laser rod is mounted in a quartz tube passing down the axis of the chamber. The chemical charge, which can be either a metal powder-solid oxidizer mixture or a metal wool-pressurized oxygen mixture, is packed around the quartz tube. Ignition is accomplished by explosion of a helix of primacord wrapped around the quartz tube. To facilitate loading of the chamber the head is equipped with a quick-disconnect split ring retainer.

Preliminary firing data has been accumulated on the durability of the quartz tube and on the brightness temperatures available from metal wool oxygen mixtures packed into the chamber.

Initial measurements have shown that the quartz tube is capable of withstanding the high pressures generated by the metal wool-oxygen reactions. Failure of the quartz tube on detonation was eliminated by coating the tube with a transparent silicone rubber. This protective coat seemed to dampen the shock that is transmitted to the quartz tube.

The brightness temperature measurements were performed by putting a 1/4" diameter conical reflector of known reflectance in the quartz tube and measuring the reflected intensity with the wedge interference filter-phototube spectrophotometer described in Appendix I.

Zirconium wool-pressurized oxygen mixtures have been fired at several initial pressures in the range of 0 to 1500 psi. The maximum brightness temperature recorded was 5230°K at 1450 psig. Extrapolation of the brightness temperature - initial pressure data indicates that a brightness temperature of 5500°K can be achieved in the 1700 - 2000 psig range. The

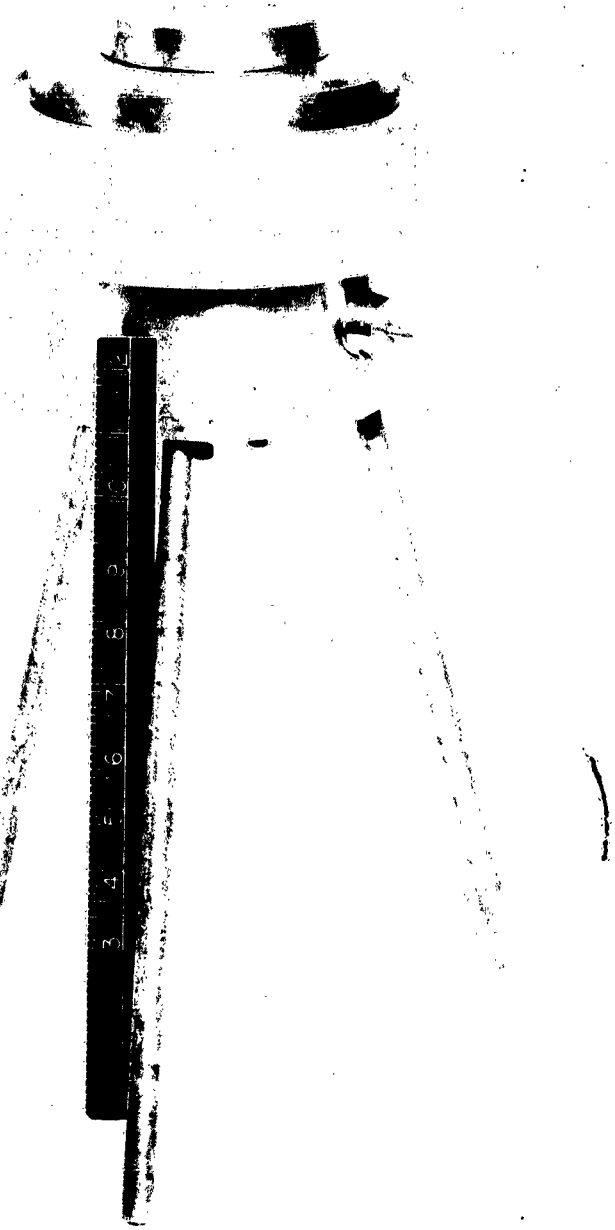

Figure 22. Constant Volume Laser Pump Chamber

chamber is designed to pump both ruby and neodymium lasers, although thus far only safety tests and temperature measurements have been made.

This chamber not only proves the point that higher temperature laser pumps can be built, but also illustrates the fact that some of the weight saving that is gained by going to chemical pumping is lost in the weight of the chamber.

The minimum theoretical weight for a chamber capable of withstanding 100,000 psi pressure would be that of a high strength titanium hollow sphere. This type chamber would weigh approximately 4 grams per cc of internal volume. However, a practical chamber designed to pump lasers would weigh more than 10 grams per cc. In a practical system only about one-fourth of the total volume can be occupied by laser rods. Therefore, the chamber weighs about 40 grams per cc of laser rod. If the pumping temperature were increased to 6000°K this would increase the output of a laser rod by a factor of five over what would be obtained if it was pumped by a reaction in the 4000°K range. However, the weight of the pressurized system would still be greater than a nonpressurized system of similar output. Problems of reloading and protecting the laser also become more acute with the pressurized system. These problems appear as if they can be overcome, but there are other methods for obtaining higher brightness temperatures which have to be evaluated to determine the best area for future work.

External Methods for Increasing Brightness Temperature

From the second law of thermodynamics we know that it is impossible to create an image more intense than the source of the radiation if we are dealing with Lambert law radiators and if the refractive indices of the

object and image space are the same. These last two conditions offer a clue to how the intensity might be increased. First of all, if the refractive indices are different it is possible to achieve a higher brightness temperature. This can be accomplished with a laser rod by the familiar process of cladding the laser rod. In this process the cylindrical laser rod is jacketed by a transparent material which has the same index of refraction as the laser rod(43).

For best results $$n = \frac{D_o}{D_i}$$

where n = the index of refraction of the laser rod

D_o = outer diameter of the cladding

D_i = inner diameter of the cladding, i.e., the diameter of the laser rod.

This produces an increase in intensity equal the index of refraction of the materials. If the shape of the cladding is spherical rather than cylindrical the increase is approximately equal to n^2. Thus, for ruby it is possible to increase the intensity by 1.76 with cylindrical cladding and 3.1 with spherical cladding. With neodymium glass the laser rods have an index of refraction from 1.5 to 1.8 so similar increases are possible with glass laser rods.

With a factor of three increase in intensity it is possible to achieve intensities which correspond to effective temperatures above 5000°K from a blackbody radiating at 4000°K.

Another method for achieving a brightness temperature at specific wavelengths, higher than the source, is to use fluorescent devices which are not in thermal equilibrium and thus fall outside the scope of the

previously discussed law.

A study of fluorescent devices has been conducted at NAA/LAD under internal funding. This study has demonstrated that it is possible to obtain substantial intensification at a specific wavelength. To understand the fluorescent intensification process it is necessary first to briefly review the fluorescent excitation and re-emission process.

Fluorescence is the absorption of light and emission of the energy as light before internal conversion degrades it to heat. Of these fluorescent excitation-emissions, the two level system (an example of which is the Hg 2537A absorption and direct re-emission) is of no use in trying to reach higher brightness temperatures since the emission is blackbody limited to that of the source or less by an equilibrium in the (reversible) process.

The multi-level systems with intermediate (irreversible) vibration level changes of the excited state can and do give rise to non-equilibrium populations in the excited state, and thus can have higher brightness temperatures than the exciting light. Anti-stoke's fluorescence of this type though, is not useful since the thermal energy which causes excitation to higher vibrational levels also helps to cause quenching, and therefore, results in higher energy, low intensity emissions. The more common and useful Stoke's fluorescence occurs when vibrational de-excitation takes the molecule to the ground vibration level where the fluorescing de-excitation is observed. Due to the very fast deactivation rates this type of fluorescence will yield very high brightness temperatures and thus is the one we have studied.

Another possible thermodynamically irreversible path from the excited electronic state is a system crossover to an excited state with a different multiplicity than the ground state giving rise to phosphorescence. This has the potential ability to achieve high temperatures though it has not been investigated as yet. The main problem would to be effectively use one of the known methods such as the Gruden-Pohl effect of shortening the extremely long half life associated with the forbidden transition to ground state, or to find an efficient means of forcing the molecules back into the initial excited state (having the same multiplicity as the ground state) which will then de-excite by fluorescence.

The utility of fluorescent enhancement of pumping sources lies in using materials which emit into a particular laser's pumping band, but absorb at wavelengths outside of this or other pumping bands. This has the double advantage of concentrating more energy into useable wavelengths and preventing useless light from entering the laser where it is degraded to heat. In general, it is desirable to use materials which absorb over a wider wavelength range than in which they emit, thus allowing a greater useable energy concentration. As an example, a suspension which absorbs most of the light of wavelength less than about 5700A and fluoresces between 5700 and 6000A could give about fifteen times the enhancement fluorescein could give and would be good for pumping a neodymium laser.

Our initial experiments were conducted using uranine, the sodium salt of fluorescein ($C_{20}H_{10}O_5$) since it is easy to handle and known to be a strong fluorescent. The aqueous or methanolic solutions of the salt were contained in a small diameter tube with a flat window at one end for measurements. The fluorescein was pumped along a three inch length by

two flash tubes. The fluorescent material emits spherically; however, light emitted within a right angle cone is trapped within the cylinder due to internal reflection. Not until it reaches the flat plate at the end of the tube can it escape. Since the fluorescent material absorbs very little of its emitted light the intensity of the trapped light increases with the length of the tube that is being pumped. Only self-absorption and scattering limits the output intensity which can be achieved with a given pump source. Figure 23 demonstrates the principles of this application of fluorescent pumping. Figure 24 shows a representative spectral distribution of the output of the fluorescein; it indicates the absorption and emission regions and the enhancement of emission. The observed brightness temperature of the fluorescein solution is approximately linear with flash tube pumping temperature in the 5500A region, the highest obtained to date being about 24,400°K, as shown in Figure 25 along with the highest flashtube scan achieved. These data indicate that for a three inch pumping length a general increase in brightness temperature of about a factor of two and an increase of about four times in energy output (at 5500A).

Theoretical calculations have been made for a possible configuration utilizing fluorescent enhancement to pump lasers. This configuration is in the shape of a paddle wheel made of thin vanes of a fluorescent suspension arranged around an axis formed by the laser. Figure 26 shows a vane and the laser rod. The fluorescent material is to be pumped through the sides of the vanes and the fluorescent emission directed by internal reflectance through one edge to the laser. The advantage of this configuration over those tried by other groups (generally some form of annular cladding) is

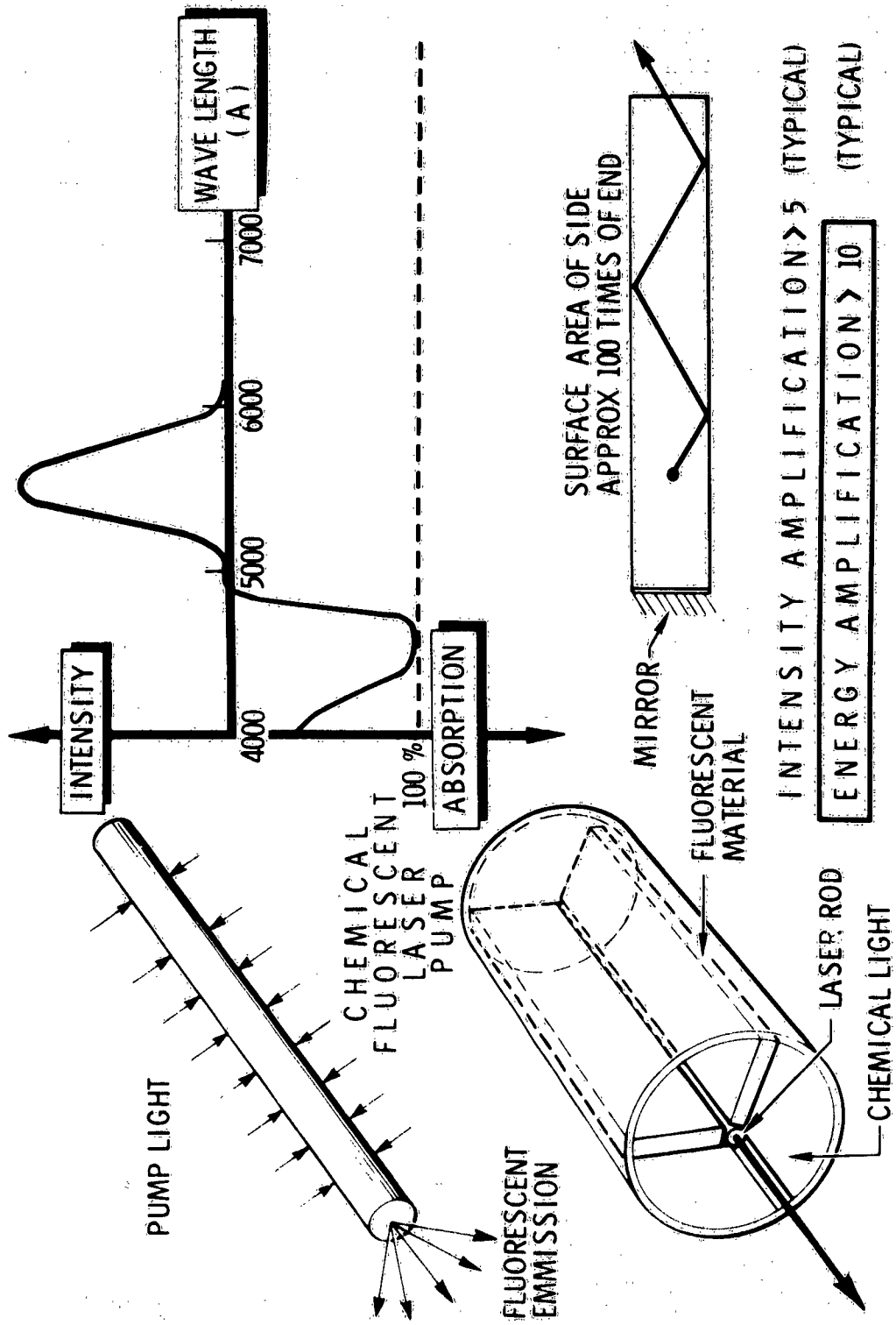

Figure 23. Fluorescent Laser Pump

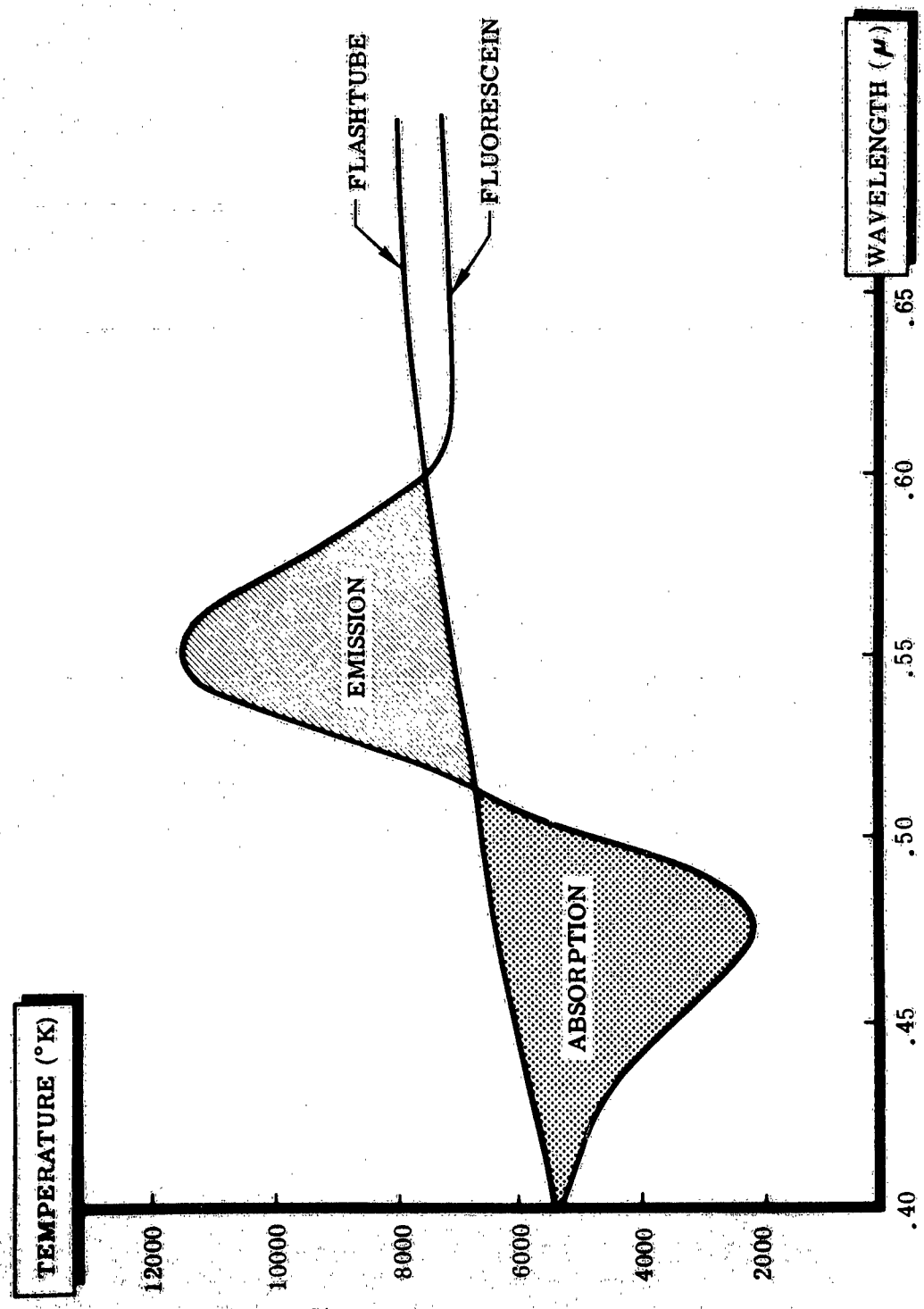

Figure 24 Intensity Increase Fluorescence

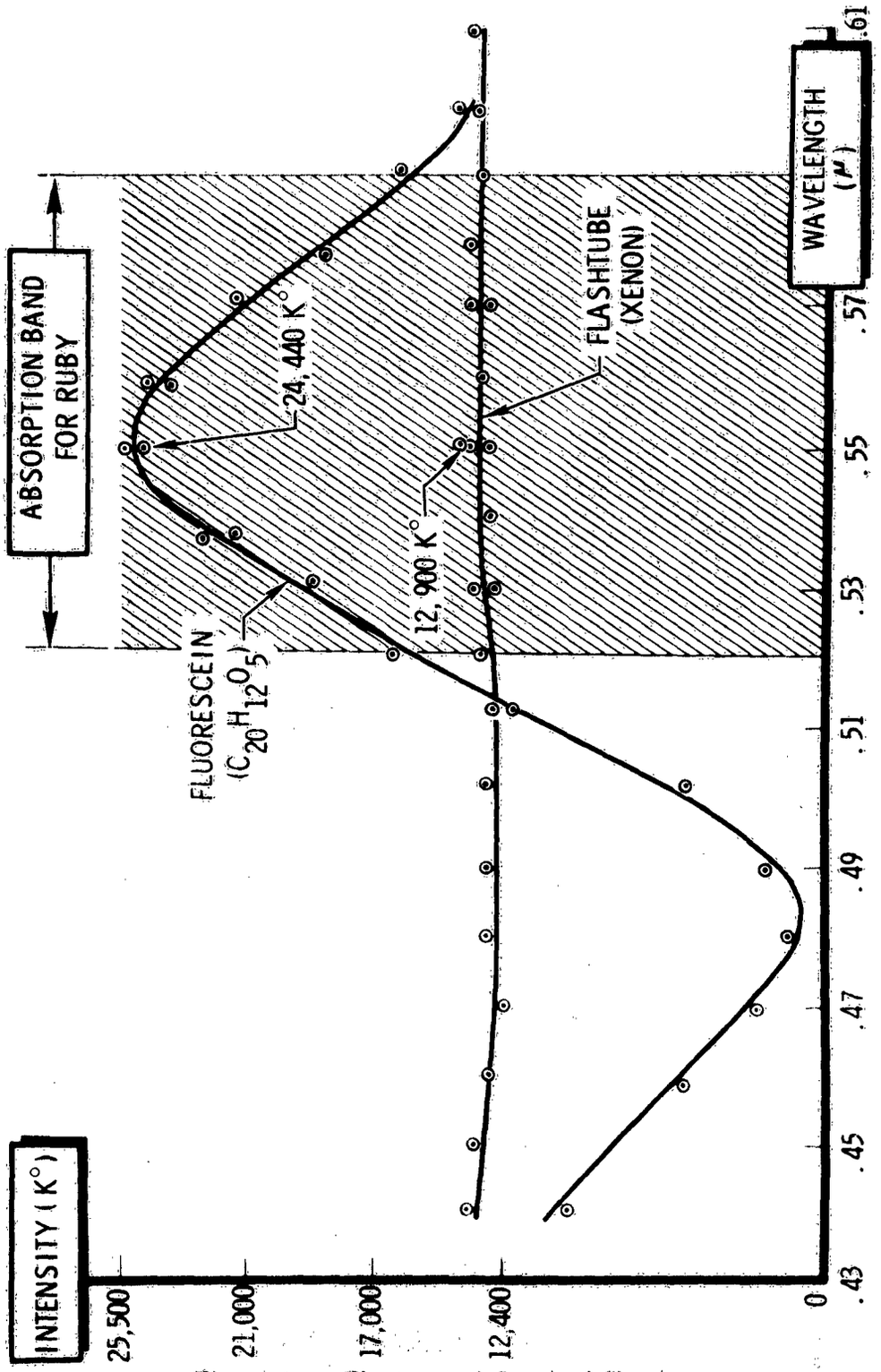

Figure 25. Fluorescent Spectral Shaping

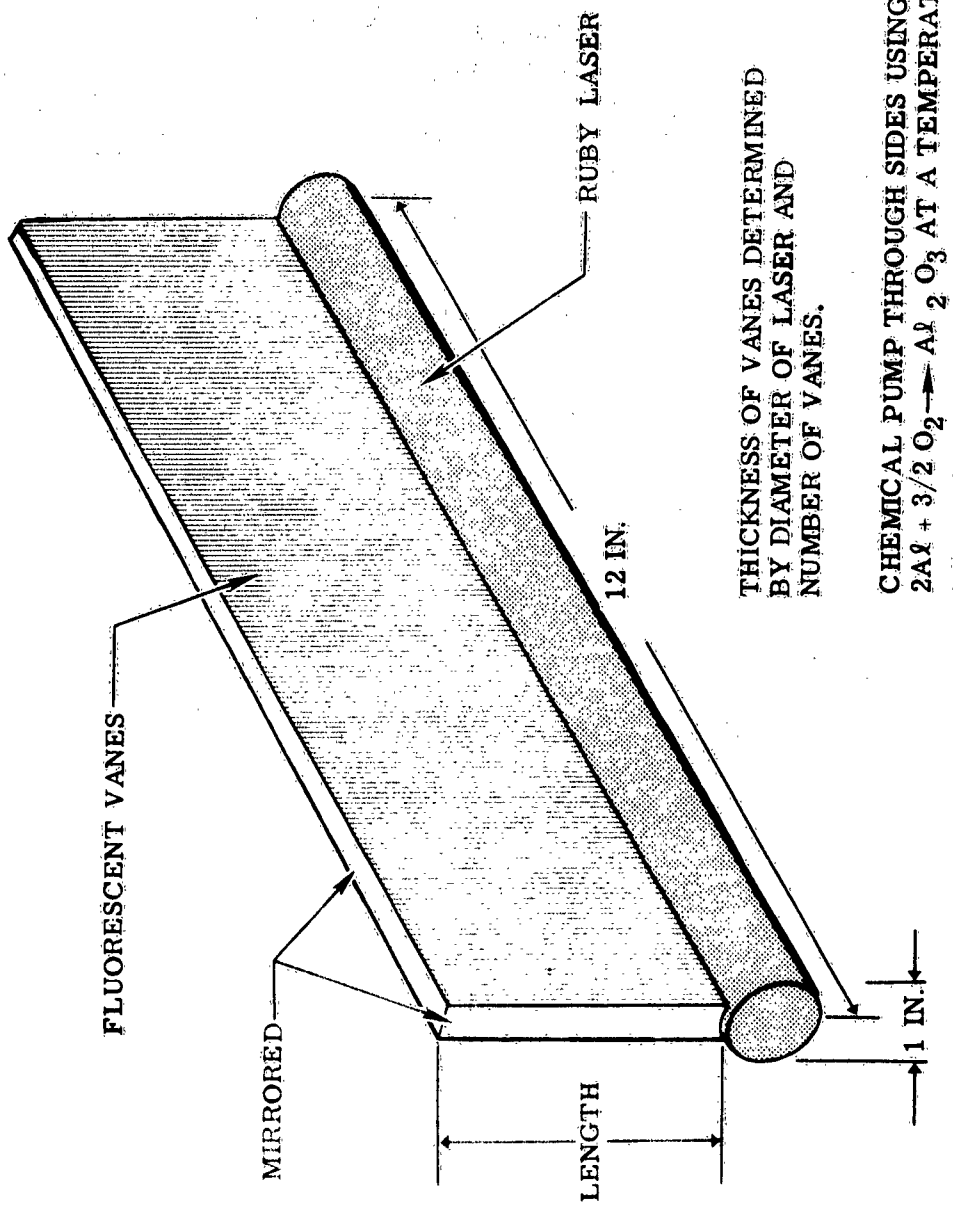

Figure 26. Chemically Excited Laser Pumping Vane Configuration

that the faces of the vanes allow a much larger area to pump the fluorescent material and a large increase in efficiency of pumping a given volume. Also, the trapping efficiency approaches 75 per cent for the vanes as opposed to 25 per cent for the tubes. Using chemicals reacting at 5000°K (which can be readily reached in straight-forward reactions) the calculations as shown in Figure 27 indicates that the device can achieve effective temperature of 7000 to 10,000°K in the pumping bands necessary for high efficiency laser pumping. Figure 28 shows efficiency of output of the green light (0.52-0.60 μ) to the laser. Note that energy per pound relationship of 10^4 or 10^5 joules per pound are evidenced for these unoptimized approaches and does not include any light from the pump, some of which will undoubtedly reach the laser rod.

These are only theoretical predictions based on the data of one fluorescent substance and a rough model, but there is good indication that further research would result in the development of a very useful device with higher efficiencies than shown here. To be found are other fluorescent materials suited to various lasers and the conditions under which they are most efficient (such as solvent, concentration, pH, etc.). The model will also have to be refined through experimentation to find such things as the best size, thickness, and number of vanes and the best angles and mirroring of top and ends.

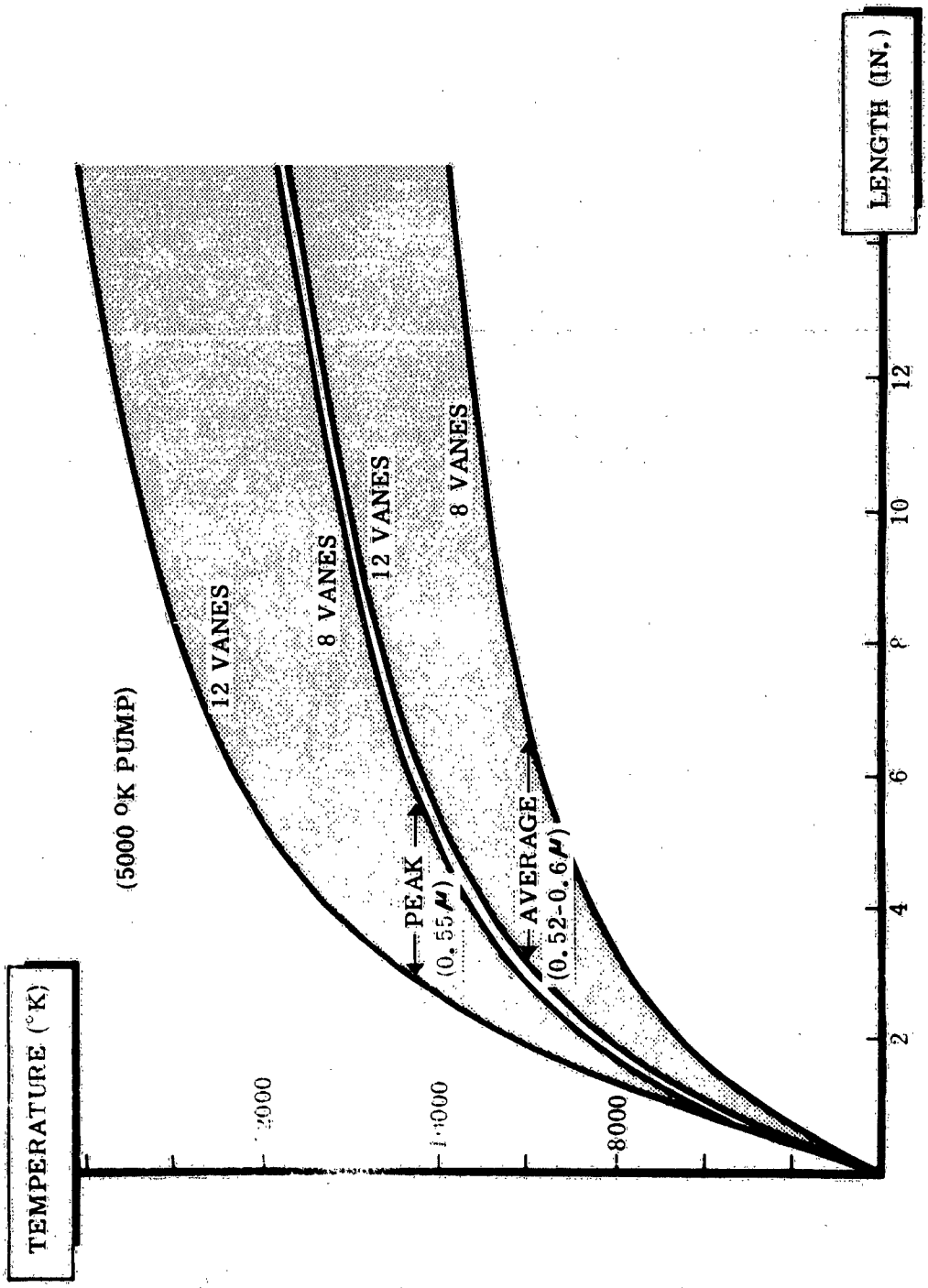

Figure 27. Brightness Temperature of Vanes

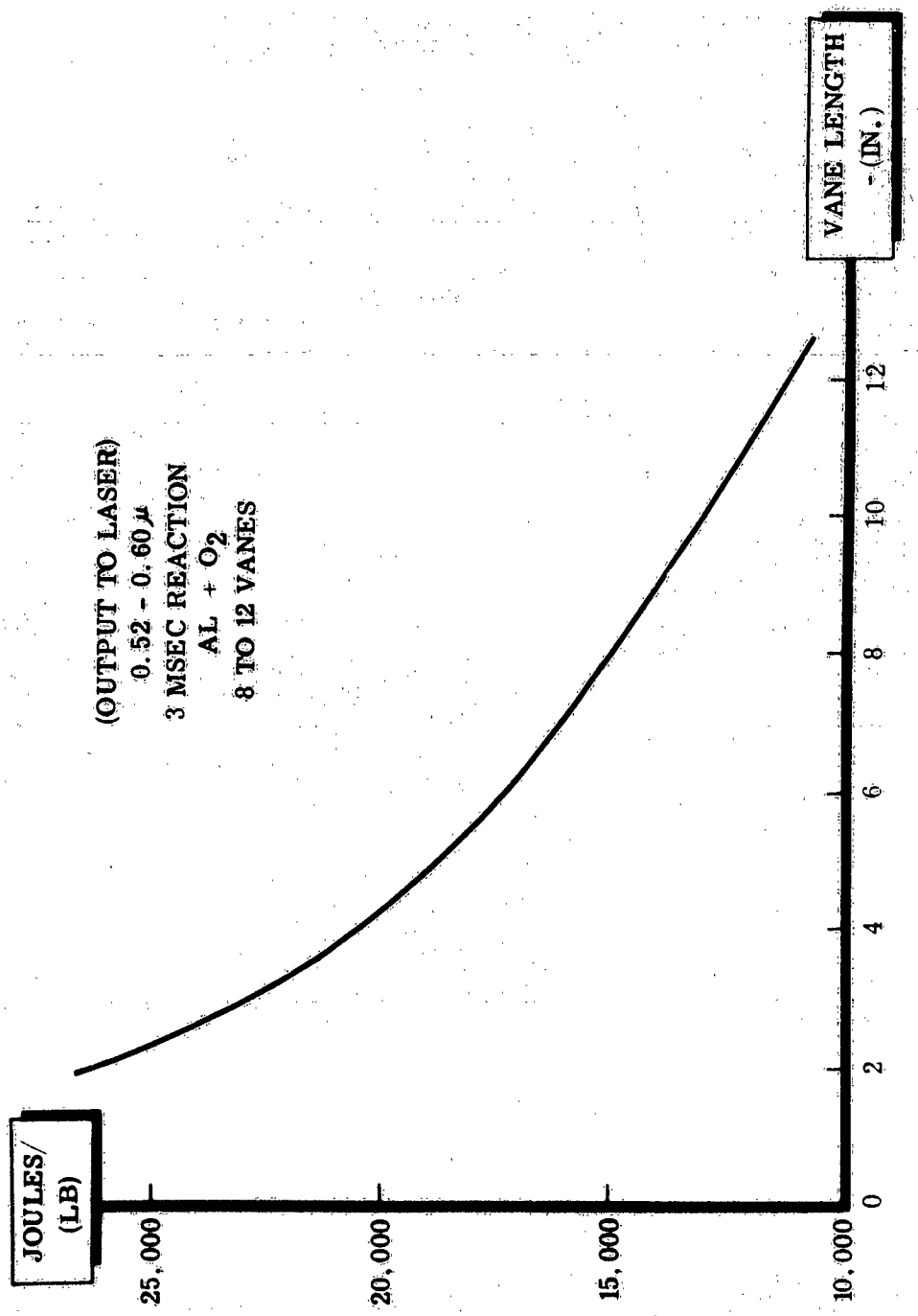

Figure 28. Efficiency of Chemically Pumped Vanes

Section V

CONCLUSIONS AND RECOMMENDATIONS

Theoretical and experimental studies have provided data that support several important conclusions. The most important is that brightness temperatures have been achieved that are adequate to pump neodymium and ruby lasers. It is believed that higher temperatures have been achieved by chemical reactions through this contract than ever before. Records indicate that prior to this contract, the highest brightness temperatures measured were about 4000°K. The highest temperature was achieved with hafnium and potassium perchlorate, about 6500°K, and therefore this would be the best reaction if temperatures must be this high. Zirconium and potassium perchlorate reaction produces temperatures almost as high as hafnium and thorium and since it is more readily available, it would be recommended for most applications where temperatures in this range are required.

It is concluded that the best use of chemical reactions for pumping lasers is to use the low or medium pressure techniques. These techniques produce lower temperatures, but they do not have the penalties associated with the high pressure reactions, namely a heavy high pressure chamber, low efficiencies, laser protection against shock waves, and window charring. One atmosphere reactions are best for application which require temperatures up to 4400°K. For those that require temperature between 4400°K and 5500°K, the pressurized oxygen-metal wool reactions are better. For those applications that require intensities corresponding to brightness temperatures higher than 5500°K, other methods appear more promising than

use of high pressures. Two examples are: 1) cladding of the laser rod and; 2) the use of fluorescent devices to increase the intensity in specific spectral regions.

This study has established the characteristics and the potential of pyrotechnic reactions for pumping lasers. Some of the most important observations are:

a) Radiation from the reactions is essentially a continuum.

b) Emissivity is not constant as a function of wavelength but generally ranges from 0.5 to 0.7.

c) Durations can be varied between 0.1 to 100 milliseconds.

d) Reactions studied showed no non-equilibrium radiation.

e) Efficiency varied between 2% and 40%. Generally, efficiency decreased as pressure increased above about 200 psi.

f) Temperatures ranged from 3000 to 6500°K. Generally, the temperatures measured were about 1000°K lower than those predicted by the computer program.

Although incremental improvements are possible in each of these areas, further study of reactions is not warranted at this time. Sufficient information is available to proceed to the system study.

System studies are recommended that would explore four important areas as follows:

a) Basic laser system performance using a chemically pumped cavity.

b) Oscillator - amplifier system to increase laser output efficiency.

c) Cladding of the laser to increase light intensity at the laser rod.

d) Fluorescent conversion devices to increase intensity in specific spectral regions.

The basic system study would be conducted as follows:

a) Establish laser material, size, and shape.

b) Determine output of the laser versus brightness temperature using a conventional pumping system.

c) Select the reaction elements most likely to give best performance for the laser.

d) Design chamber, including emitter, pre-ionization method, window, laser holder and protection, etc.

e) Perform tests on the pumping system to determine brightness temperature and efficiency versus pressure and select operating pressure.

f) Test laser using the chemical reaction pumping system to determine total system efficiency. Optimize system performance through iteration.

An amplifier system would be designed for chemical reaction pumping. This would be controlled with a laser oscillator which may or may not be pumped with a chemical reaction. This is not important because it would be a low power device. Tests would be conducted to determine system performance, particularly system efficiency. The total energy density for the system would be determined.

Further improvement in efficiency would be attempted by cladding the laser rod with a dielectric that would increase the intensity of the radiant output from the pump as seen by the laser rod. The chamber would be adapted for the clad laser rod and tests conducted to determine efficiency and other performance data.

The chamber and possibly the reaction conditions would then be modified to utilize a fluorescent converter to again attempt to increase the system efficiency.

Section VI

BIBLIOGRAPHY

1. W. M. Fassell, C. A. Papp, D. L. Hildenbrand, and R. P. Sernka, "The Experimental Nature of the Combustion of Metallic Powders," Progress in Astronautics and Rocketry, Vol. I Solid Propellant Rocket Research, pp. 259-269. Academic Press (1960)
2. D. A. Gordon, "Combustion Characteristics of Metal Particles," Ibid pp. 271-78.
3. C. P. Talley, "The Combustion of Elemental Boron," Ibid. pp. 279-85.
4. W. A. Wood, "Metal Combustion in a Deflagrating Propellant," Ibid, pp. 287-91.
5. T. A. Brzustowski and I. Glassman, "Spectroscopic Investigation of Metal Combustion," Bulletin of the 17th Meeting of the JANAF Solid Propellant Group, SPI - APL, Johns Hopkins University, Silver Spring, Maryland (May 1961).
6. K. P. Coffin, "Some Physical Aspects of the Combustion of Magnesium Ribbons," Fifth Symposium (International) on Combustion, pp. 267-76. Reinhold Publ. Co., New York (1955).
7. G. H. Markstein, "Magnesium - Oxygen Dilute Diffusion Flame," Ninth Symposium (International) on Combustion, pp. 137-47, Academic Press, New York (1963).
8. R. Friedman and A. Macek, Combustion and Flame Vol. 6, P. 9, (1962).

9. R. Friedman and A. Macek, "Combustion Studies of Single Aluminum Particles," Ninth Symposium (International) on Combustion, pp. 703-9, Academic Press, New York (1963).

10. A. Macek, R. Friedman and J. M. Semple, "Techniques for the Study of Combustion of Beryllium Particles," AIAA Heterogeneous Combustion Conference, Palm Beach, Florida, Dec. 11-13, 1963.

11. A. V. Grosse and J. B. Conway, "Combustion of Metals in Oxygen," Ind. Eng. Chem. Vol. 50, pp. 663-72, (1958).

12. W. L. Doyle, J. B. Conway and A. V. Grosse, "Combustion of Zirconium in Oxygen," Inorg, Nucl. Chem. Vol. 6, pp. 138-44 (1958).

13. J. B. Conway and A. V. Grosse, Final Report pp. 2-30, High Temp. Project, Research Institute of Temple University. Contract N9-ONR-87301 (1 July 1954).

14. J. B. Conway and A. V. Grosse, "Powdered Metal Flames" 3rd Technical Report High Temperature Project. Research Institute of Temple University, Contract N9-ONR-87301, (Aug. 1953).

15. A. V. Grosse and C. S. Stokes, "Study of Ultra High Temperatures," (Temple University Research Inst. Philadelphia, Pa.) U.S. Dept. of Commerce Office Tech. Serv. PB Rept. 161-460, 26 pp. (1960).

16. P. L. Harrison, "The Combustion of Titanium and Zirconium," Seventh Symposium (International) on Combustion, pp. 913-18, Butterworths Scientific Publications, London (1959).

17. P. L. Harrison and A. D. Yoffe, "The Burning of Metals," Proc. Roy. Soc. A, Vol. 261, pp. 357-70 (1961).

18. F. G. Brockman, "The Nature of the Light Emitter in Photoflash Lamps," J. Optical Soc. Am., Vol. 37, pp. 652-59 (Aug. 1947).

19. T. H. Rautenberg, Jr. and P. D. Johnson, "Light Production in the Aluminum - Oxygen Reaction," J. Optical Soc. Am., Vol. 50, pp. 602-6 (June 1960).

20. T. A. Brzustowski, "The Peaking Process in Metal Filled Photoflash Lamps," General Elect. Res. Lab Memo Report P-243 (Sept. 1960).

21. J. F. Tyroler, "Development of a High Speed Brightness Pyrometer," Picatinny Arsenal Technical Report 2042, July 1954.

22. H. J. Eppig and D. Hart, "Bomb, Photoflash, T9 Series," Picatinny Arsenal Report 1757, Feb. 1950.

23. S. F. Sarner, "Tolerances Permissible in the Percentage Composition of Type III Class A Photoflash Powder," Picatinny Arsenal Technical Report 2074, Oct. 1954.

24. S. Resnick, "Simulated High Altitude Tests of Illuminating Compositions," Picatinny Arsenal Report 2166, April 1955.

25. D. J. Edelman and S. M. Kaye, "Progress in High Altitude Flash Composition," Picatinny Arsenal Technical Notes FRL-TN-117, May 1962.

26. S. M. Kaye and J. Harris, "Effect of Fuel and Oxidant Particle Size on The Performance Characteristics of 60/40 Potassium Perchlorate/Aluminum Flash Composition," Picatinny Arsenal Technical Report, FRL-TR-44, Nov. 1961.

27. I. M. Baumel, "Burning Characteristics of New and Improved Green Pyrotechnics Compositions," Picatinny Arsenal, Research and Development Lecture No. 42, May 1956.

28. J. Hershkowitz, F. Schwartz and J. V. R. Kaufman, "Combustion in Loose Granular Mixtures of $KClO_4$ and Aluminum, "Eighth Symposium (International) on Combustion, pp. 720-727, The Williams and Wilkins Co., Baltimore Maryland. (1962).

29. J. B. Conway, W. F. R. Smith, W. J. Liddell, and A. V. Grosse, "The Production of a Flame Temperature of 5000°K, J. Am. Chem. Soc., Vol. 77, p. 2026 (1955)

30. R. Edse, K. Narahari Rao, W. A. Strauss, and M. E. Mickelson, "Emission Spectra Excited in Metal Powder - Oxygen Flame," J. Optical Soc. Am., vol. 53, pp. 436-38 (1963).

31. A. V. Grosse, "High Temperature Research," Science, Vol. 140. pp. 781-89 (17 May 1963).

32. Pearse, R. W. B. and Gaydon, A. G., "The Identification of Molecular Spectra," - 2nd Ed. Revised, John Wiley and Sons, Inc., New York (1950).

33. Mitchell, A. C. G. and Zemansky, M. W., "Resonance Radiation and Excited Atoms," Cambridge University Press, (1934).

34. Hogan, V. D. and Gordon, S. J., Phys. Chem., 62, 1433-5 (1958).

35. Hermoni (Makovky) A. and Salmon, A., Eighth Symposium (International) on Combust on, p. 656, Williams and Wilkins, Baltimore (1962).

36. R. V. Stull, and G. N. Plass, J. Am. Opt. Soc., 50, pp. 121-129 (1960).

37. S. S. Penner, "Quantitative Molecular Spectroscopy and Gas Emissivities," Chapter 1, Addison - Wesley, Reading, Mass., (1959).

38. R. J. Thompson, "High Temperature Thermodynamics and Theoretical Performance Evaluation of Rocket Propellant," Rocketdyne Report, June 1959.

39. I. Prigogine and R. Defay, "Chemical Thermodynamics," Chapter 1, John Wiley, New York (1954).

40. R. Fowler, and E. A. Guggenheim, "Statistical Thermodynamics," Chapter 5, Cambridge University Press, Cambridge, England (1939).

41. J. Hirshfelder, C. F. Curtiss, and R. B. Bird, "Molecular Theory of Gases and Liquids," Chapter 7.6, John Wiley, New York (1954).

42. "Kodak Plates and Films for Science and Industry," Eastman Kodak Co. (1962).

43. B. Lengyel, "Lasers," Chapter 11, John Wiley, New York (1962).

APPENDIX I

EXPERIMENTAL EQUIPMENT

The necessary experimental equipment for a study of the light output of chemical flash reactions may be divided into three groups: Sensors, ignitors, and chambers. The sensors must measure light intensity as a function of time and wavelength. Two general types are in use. One type is used for producing time resolved spectra and the other type is used for measuring monochromatic intensities as a function of time. The calibration technique is discussed in detail because all temperatures quoted are accurate only insofar as the calibration is accurate.

The ignitor is used to ignite the reaction mixture at a predetermined time and with a minimum disturbance of the system. Therefore, a brief discussion of the ignitor design is presented.

The chambers in use may be divided into four types: Flat plate, atmospheric solid oxidizer, pressurized oxygen, and dynamic pressurization. Each is designed to provide a specific function for accurate intensity measurement at various specified conditions such as with pressurized oxygen, a solid oxidizer, or under high pressure. Consequently, a knowledge of a chamber design is important for an understanding of the data presented in section three.

TIME RESOLVED SPECTRA

The variation of light intensity from chemical flashes with wavelength and time can be measured by the use of the apparatus shown schematically in Figure 29 . A Bausch and Lomb 1.5 meter grating spectrometer

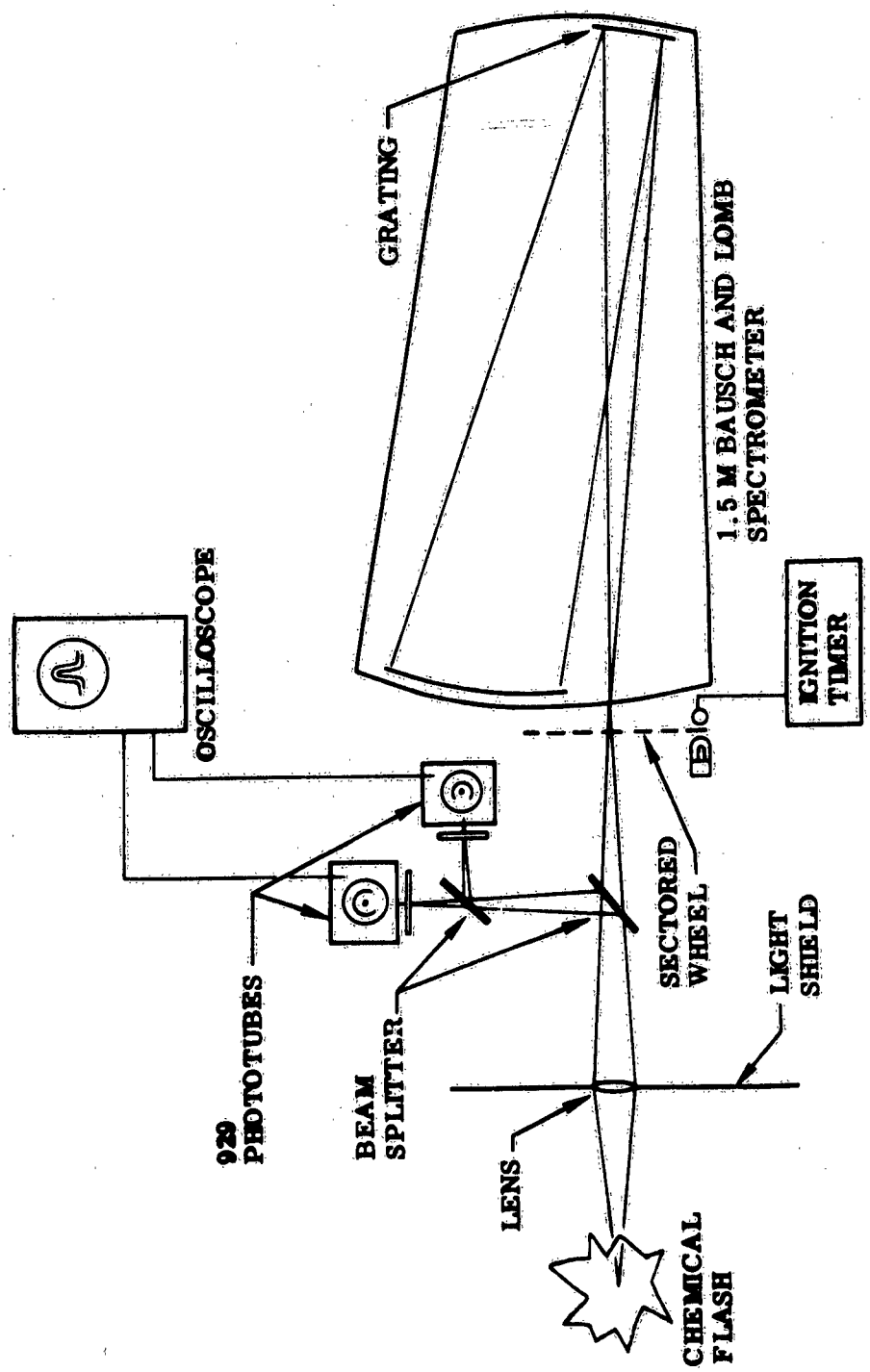

Figure 29. Radiant Energy Analyzer System

serves to record on film the light intensity incident on the entrance slit as a function of wavelength. Time resolution is accomplished by a sectored wheel revolving in front of the slit. At any particular time during the flash only a certain portion of the slit height is exposed to incident radiation by the sectored wheel. A sample sectored wheel is shown in Figure 2C; this wheel has ten sectors each cut at a different radius. Each of the sectors shown occupies 18 degrees of arc of the wheel. Thus, for example, a wheel turning at one revolution in 40 milliseconds would allow a series of two millisecond exposures to be taken. Since the spectrometer is stigmatic, light from various portions of the slit height will be recorded at various corresponding heights on the film. To avoid the possibility of light being gathered from different portions of the radiating cloud leading to a confusion of spectral distribution of the light with a time distribution, the optics have been arranged so that the object image at the spectrometer slit is enlarged about three and one-half times.

A DC light source-phototransistor combination is used to measure the time per revolution as well as acting as a timing trigger for ignition of the chemicals-when the firing switch is flipped the ignition spark will be thrown the next time the phototransistor senses the light source through a slot in the sectored disk. Some of the light focused on the spectrometer entrance slit is deflected by beam dividers to two calibrated phototubes equipped with narrow band filters. The output of the phototubes versus time is displayed on a C.R.T. and photographed. Using the phototube output to measure light intensity and a microphotometer to measure spectral film darkening versus time and wavelength, it is possible to calibrate the

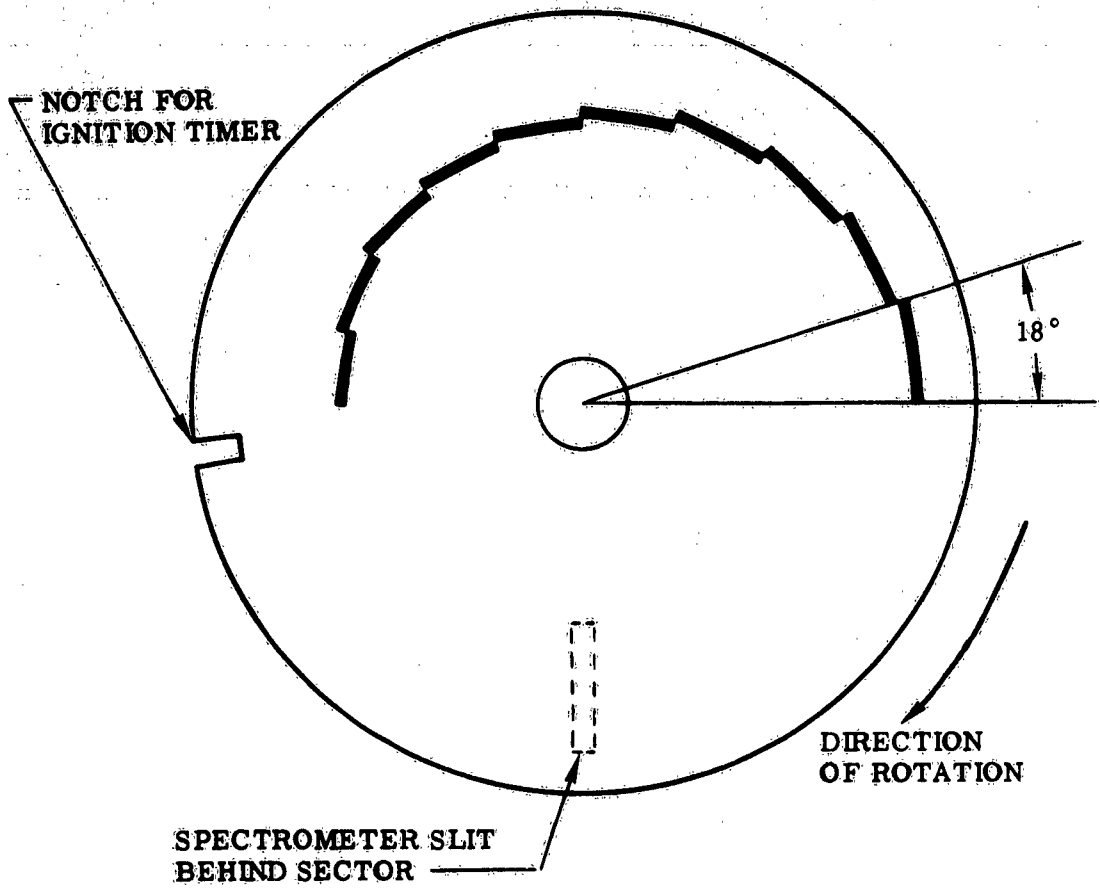

Figure 30. Sectored Wheel

film darkening with radiant intensity and hence brightness temperature. By careful duplication of the exposure time and developing technique, and use of the same film emulsion batch number, the film can be similarly calibrated at enough wavelengths to allow one to plot isotherms directly on any microphotometer trace of spectra taken in the same fashion. This seemingly complicated system for calibrating film darkening versus radiant intensity is necessary because of the reciprocity effect (42). The film must be calibrated using identical exposure times as the exposure to be measured and available calibration standards do not have a high enough radiant intensity to do the job.

Time resolved spectra should allow the rapid determination of brightness temperature as a function of wavelength and time. This would be very helpful in determining the effect of various additives on brightness or on the light output in any narrow spectral region in the wavelength range of the instrument. If nonequilibrium radiation can be produced, it is much more likely to be detected by use of the spectrometer than by phototubes with narrow band filters. It is also possible that the way in which intensity is observed to change with time could reveal something about the combustion process.

MONOCHROMATORS

Measurement of light intensity in a given spectral region requires some form of monochromator for selection of the spectral region. Several types of monochromators have been tried in an effort to find a simple yet sensitive device.

One of the first methods tried was the use of Wratten filters. The Wratten filters chosen were selected for narrow bandwidths and high transmittances in the bandwidth. However, even the best Wratten filters had very wide bandwidths (± 500A) which produced anomalous results if the system under study deviated greatly from a blackbody. Consequently, Wratten filters were scrapped.

After further study it was felt that interference filters would be the best because they offered the advantage of narrow bandwidths (± 50A) and high transmittance. Two types of interference filters are available:

1. The fixed type which is manufactured for a specific transmittance region.
2. The wedge type which transmits a given wavelength at a specific region on the filter.

Each type has found use in the laboratory. The fixed type has been used in conjunction with the Bausch and Lomb spectrograph for calibrating the intensity response of the photographic films. For this purpose it is admirably suited because scanning is not necessary. Figure 29 shows use of these filters on the time resolved spectra apparatus.

The wedge type is quite useful as a quick scanning device for rough plotting of intensity distribution from flash reactions. It is extremely compact, and may be easily calibrated because the dispersion is linear. Furthermore, it may be mounted permanently to a phototube pickup box to construct a very small spectrophotometer. Figure 31 shows the wedge filter mounted on a phototube box.

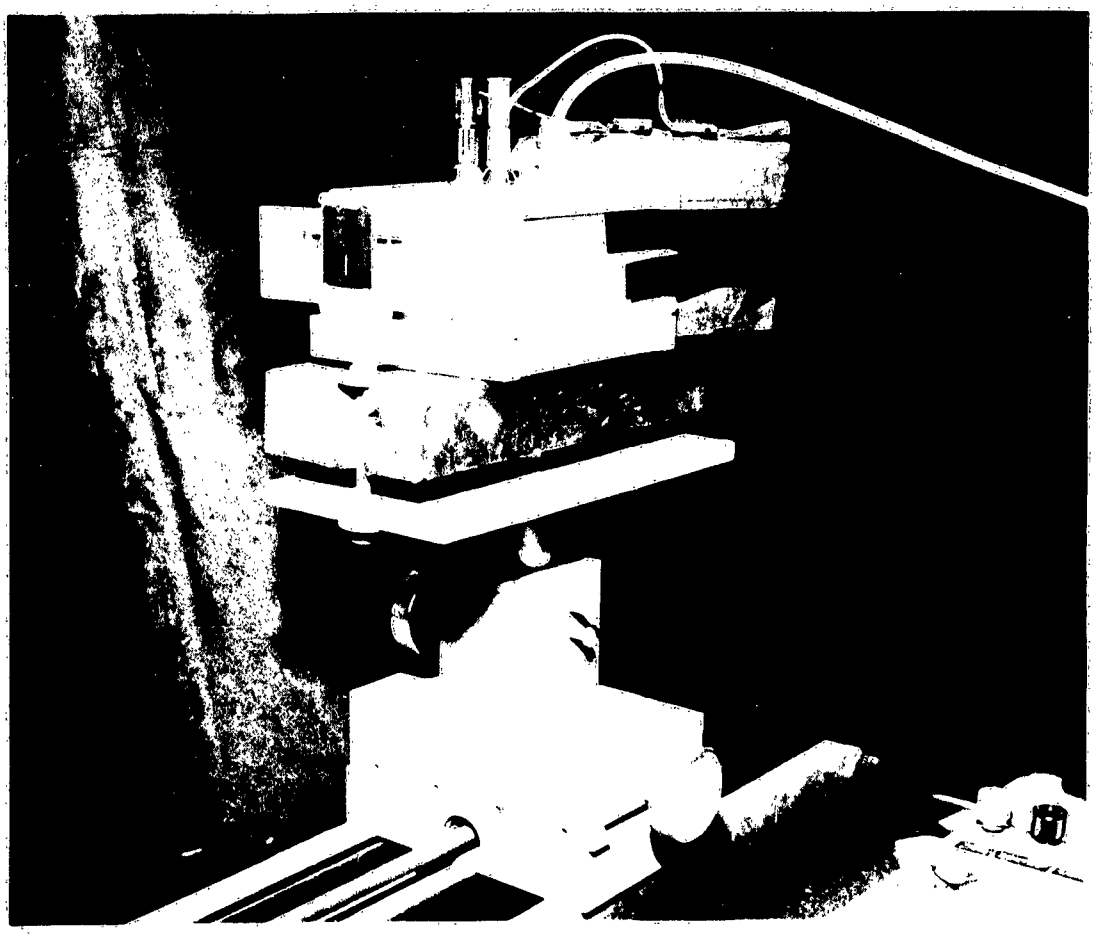

Figure 31. Phototube Spectrophotometer Sensor Unit

DETECTORS

Several types of detectors are currently in use in the laboratory. These may be divided into three categories: Solid state, photodiode tube, and photomultiplier. Each type is being used in its specific area of sensitivity.

The solid state photocells are currently in use in low sensitivity applications such as for pulse counters on the time resolved spectra setup. However, their high sensitivity in the infrared makes them admirably suited for measurements in the infrared. An infrared sensor is currently under construction which will utilize the solid state infrared detectors.

The photodiode tubes have been utilized in the visible range in conjunction with the wedge interference filters. Maximum sensitivity is at 5400A.

The prime disadvantage of the photodiode tubes is that sensitivity is rather low when used with the wedge interference filters. Therefore, the minimum signal detectable above noise level corresponds to a blackbody temperature of approximately 2300°K.

For high sensitivity applications such as measurement of narrow line (± 5A) intensities in conjunction with the grating spectrographs, photomultiplier tubes are used. These tubes offer the advantage of extremely high sensitivity, but are subject to microphonic pickup. For this reason, the photomultiplier tubes are not in more general use in the laboratory.

SYSTEM CALIBRATION

Accurate measurement of absolute light intensities requires an accurate system calibration. Before a system calibration can be undertaken,

suitable intensity standards must be chosen.

As a primary standard, a tungsten ribbon bulb calibrated by the National Bureau of Standards was chosen. Because it was necessary to preserve this standard, several tungsten ribbon bulbs were calibrated against the primary standard to serve as expendible secondary standards. At the time of calibration of these secondary standards, an optical pyrometer was also calibrated for use as a cross check on the decay rates of the secondary standards. Thus, as the secondary standards are used, they may be continuously recalibrated with the optical pyrometer. In actual operation, however, recalibration was not necessary until the filament approached burnout. It was assumed that the pyrometer calibration did not decay because the calibration had remained unchanged during a two year period of use prior to use in the laser laboratory. A second calibration of the pyrometer in the laser laboratory after six months operation has confirmed this assumption.

To eliminate random errors in calibration, the radiant intensity of two secondary standard bulbs was calculated at several operating temperatures by use of the tungsten emissivity tables prepared by the National Bureau of Standards and the blackbody radiation tables. Cross check with the original calibration gave no significant errors, therefore, the tables were assumed correct for the two bulbs in question.

Because random errors could occur during system calibration, the system was calibrated at several bulb temperatures between 2,200°K and 3,000°K to give statistically significant calibration curves. The actual response curves were found to be linear with intensity as was originally

assumed. Figure 32 shows the normalized calibration curves plotted for one of the wedge interference filters and 929 phototubes currently in use in the laboratory. A similar calibration procedure was used on all sensors currently in use.

Calibration of film response as shown in Figures 33, 34, 35, 36, and 37, used in the grating spectrographs is performed during each shot by measuring the radiant intensity at three or four selected spectral regions with interference filters plus 929 phototubes. With this data isotherms may be plotted on the microphotometer readouts to assist in determination of film response.

Brightness temperatures found by use of the present calibration techniques are accurate to ± per cent below 4000°K with the error increasing to ± 2 1/2% at 6000°K. Higher temperatures will require a higher temperature standard source for accurate calibration.

DEVELOPMENT OF IGNITION SYSTEM

The ignition of metal-oxidizer mixtures requires that some of the metal be raised to its boiling point before autocombustion can begin. Because it was desired to measure the temperature of the chemical reaction, and not the ignition temperature, a second requirement was that the ignition energy must be much less than the available reaction energy. Third, sensing and recording equipment to be used required synchronization of the flash with the recording period. Therefore, some form of electrical ignition with a very short delay was necessary.

The first attempts at controlled ignition were performed with Pyrofuze triggered by a battery. Ignition was erratic, often occurring several seconds after the electrical impulse. Furthermore, rapid firing in

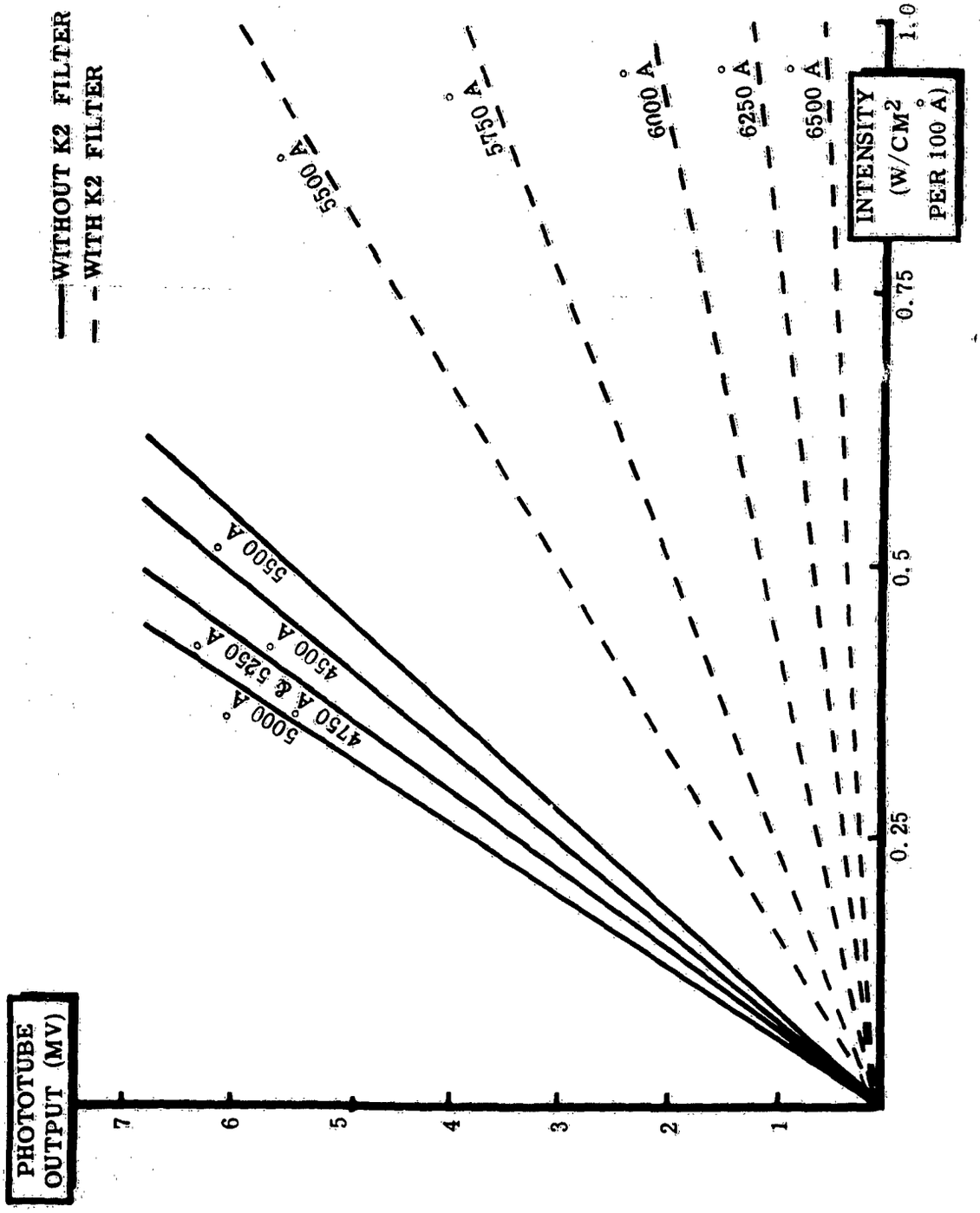

Figure 32. Photocell + Interference Filter Calibration

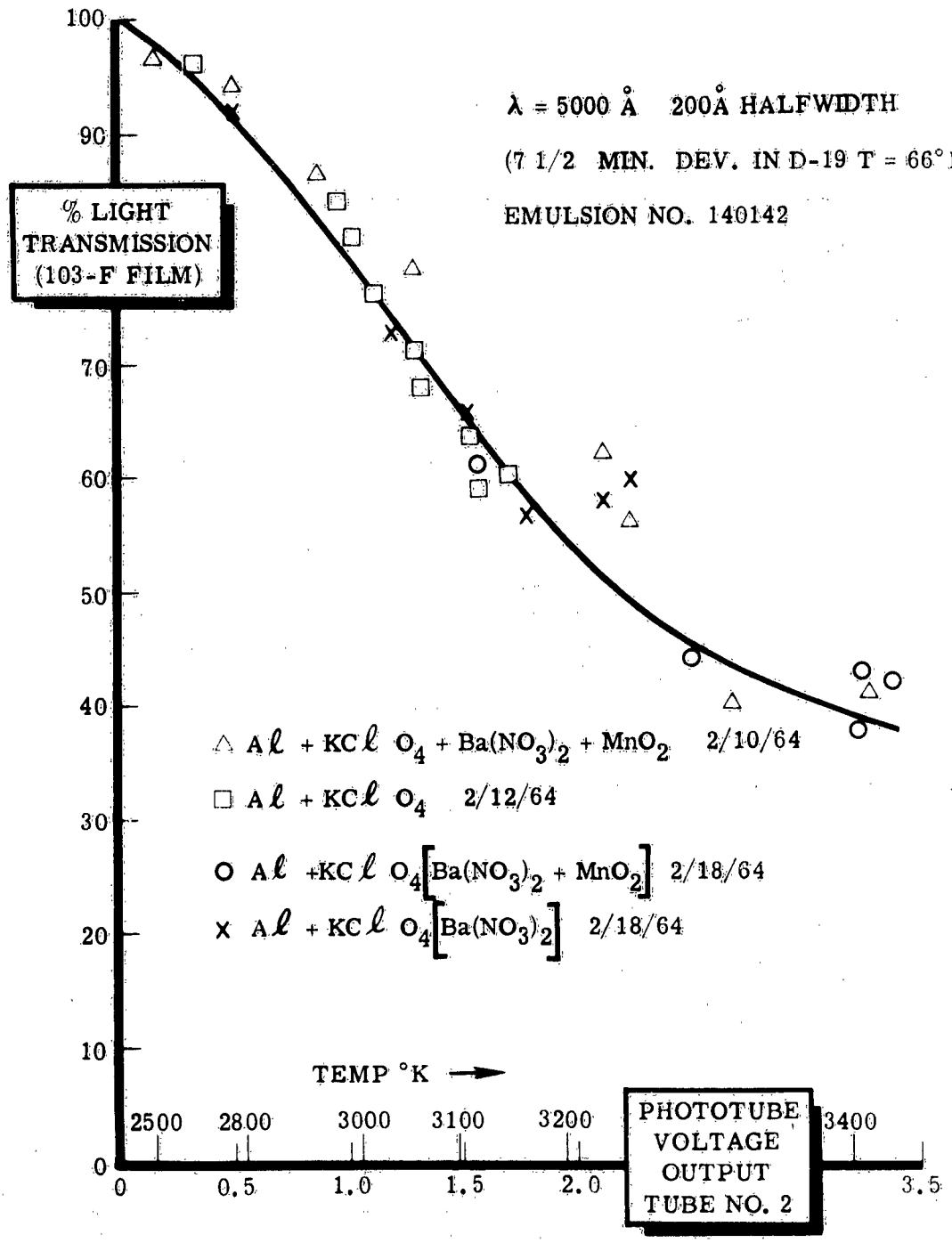

Figure 33. Percent Light Transmission Through 103F Film Versus Phototube No. 2 Output Voltage

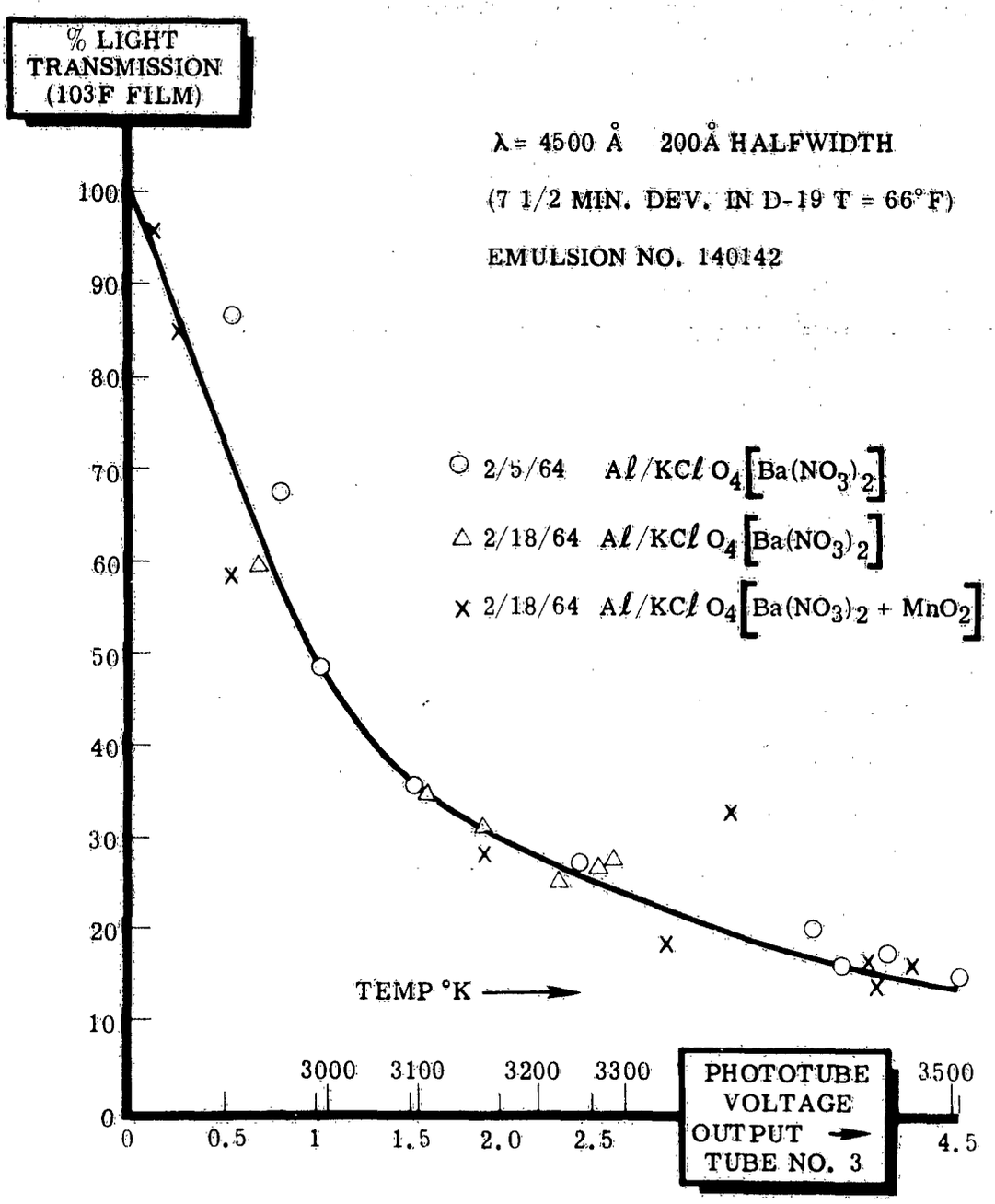

Figure 34. Percent Light Transmission Through 103F Film Versus Phototube No. 3 Output Voltage

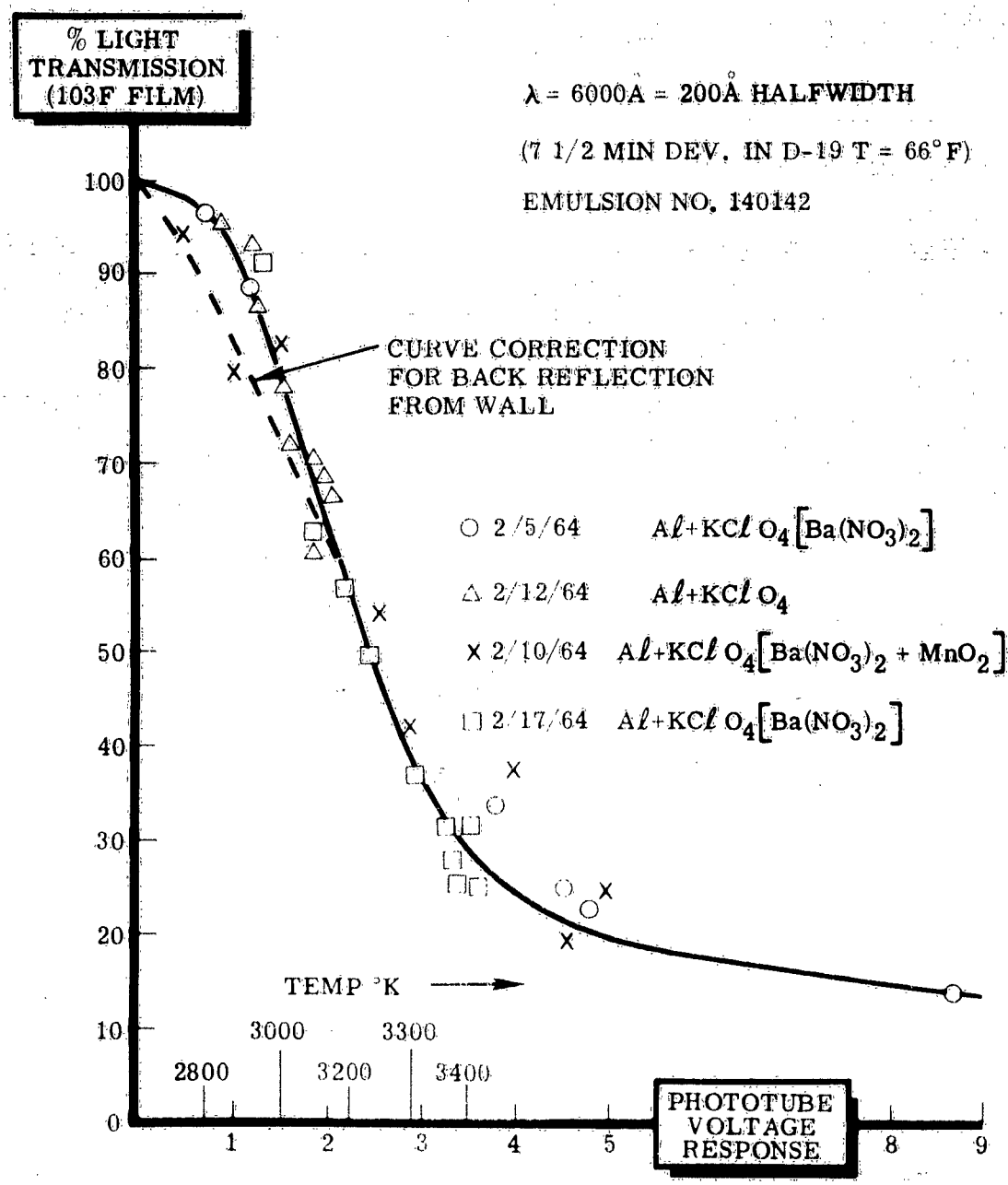

Figure 35. Percent Light Transmission Through 103-F Film Versus Phototube No. 3 Voltage Output

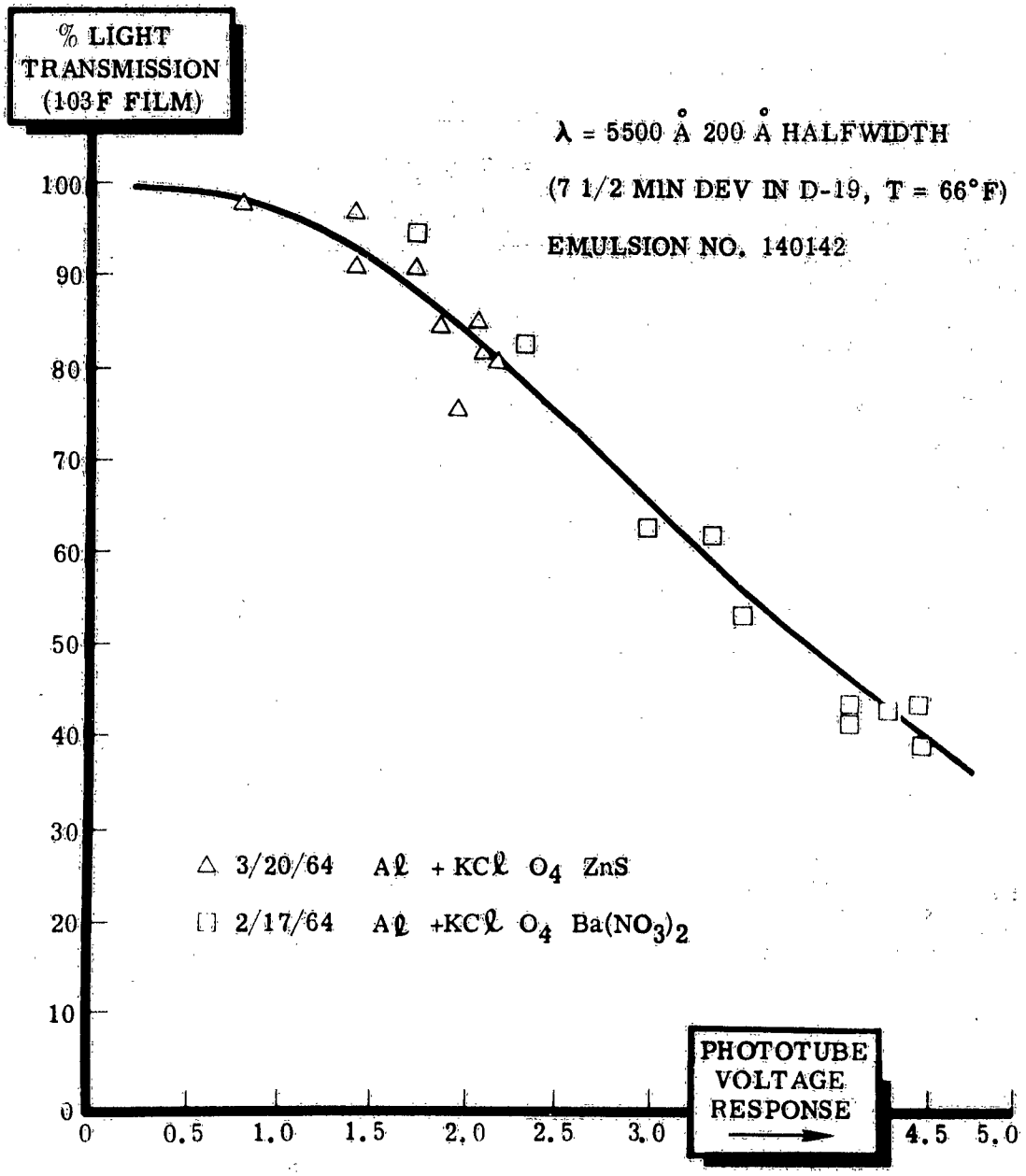

Figure 36. Percent Light Transmission Thru 103-F Film Versus Phototube No. 2 Output Voltage

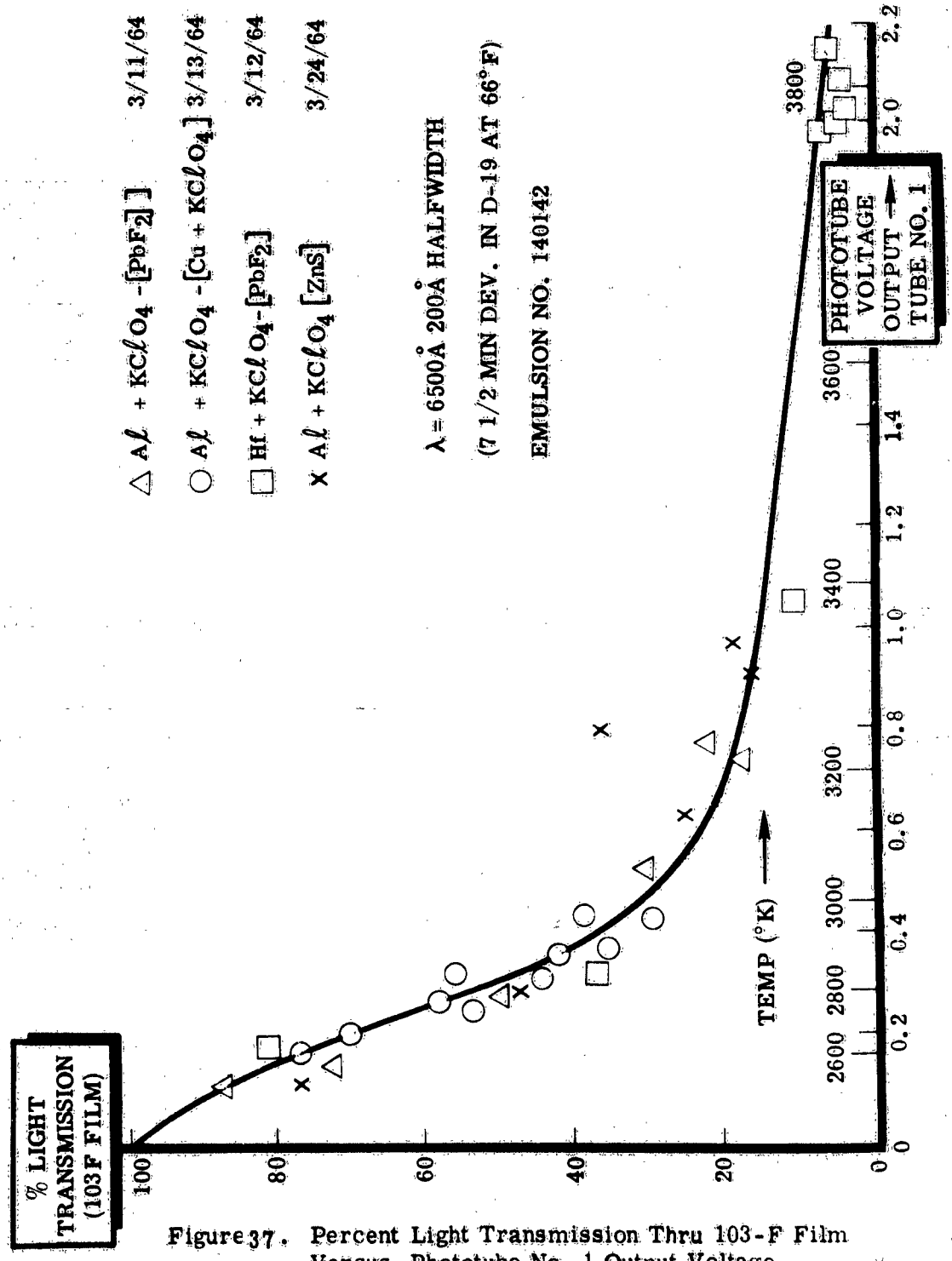

Figure 37. Percent Light Transmission Thru 103-F Film Versus Phototube No. 1 Output Voltage

sequence was almost impossible.

A second approach was to use an exploding wire triggered by a high voltage capacitor discharge. Ignition occurred almost instantaneously, but again rapid firing was almost impossible.

Spark discharges were tried next, but ignition was erratic, apparently because of a low current density. However, rapid firing could be easily accomplished if the erratic behavior could be corrected.

To increase current densities, a capacitor discharge was used. Ignition was uniform and instantaneous in all fixtures tried. The wire electrodes used initially were easily jarred from alignment and were vaporized very quickly. Therefore, only two or three firings could be made before the electrodes had to be replaced.

To solve the electrode problem a search was made for more rigid electrodes. Automobile spark plugs proved suitable. The base of the plug was filled with epoxy resin to provide a flat surface for the pyrotechnic powder.

Control of the capacitor discharge circuit was first tried by using a mercury thyratron. However, a large leakage voltage was always present across the electrodes which could cause premature ignition. The thyratron was replaced with a high voltage, heavy duty, double pole relay which provided complete isolation of the electrodes until actuation.

The final ignition circuit and its operating behavior is shown in Figure 38.

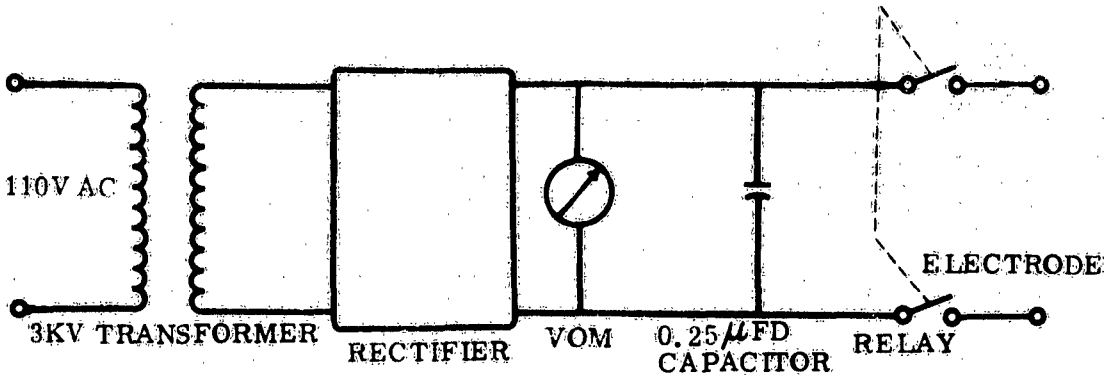

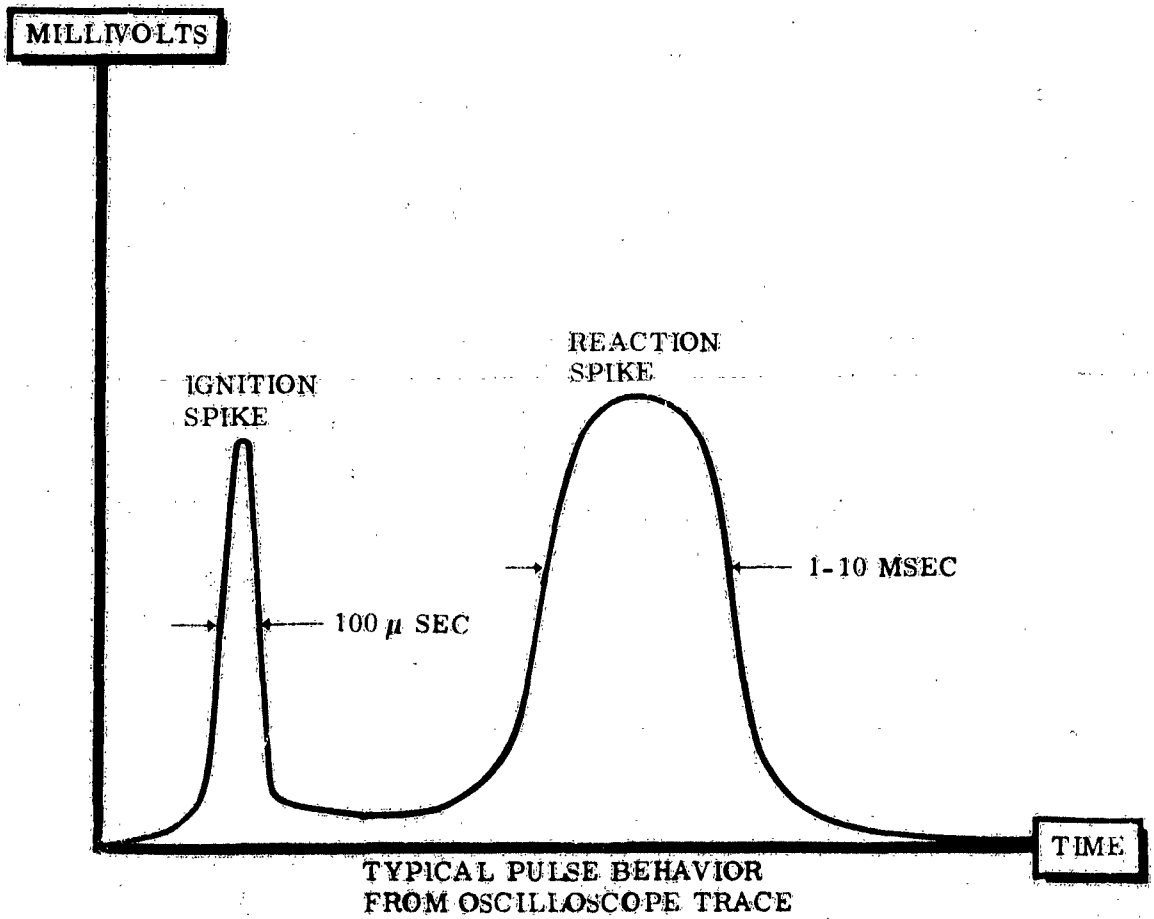

Figure 38. Ignition Circuit

DESIGN OF CHAMBERS

Chamber design is perhaps the most important variable affecting temperature measurement of pyrotechnic flashes. Consequently, very careful thought has been given to the design of special chambers to insure accurate temperature measurement.

One of the first designs tried is the simplest. It consists merely of a flat metal sheet upon which the flash mixture is ignited. In general a hemispherical fireball is formed. The flat sheet design provides for minimal pressure and shock effects while allowing complete access to the flame. The prime disadvantage is that rapid cooling occurs at the outer surface of the fireball which produces a zone of line reversal and scattering, thereby giving optical temperatures somewhat lower than the true temperature. A second disadvantage is that fireball size is uncontrolled and varies greatly between shots.

To alleviate some of the problems associated with the flat sheet, the atmospheric omnidirectional chamber was designed. This design controls the size and shape of the fireball by directing it upward through a short chimney equipped with a 90° window at its base. Measurements are made near the base of the fireball at a point where the size is relatively constant for each shot. The greatest disadvantage is that large eddy currents are set up in the apparatus during firing which circulate a large amount of dust into the field of view. Thus, scattering of emitted light becomes a serious problem.

The final atmospheric chamber design resulted when the omnidirectional chamber was modified to correct the scattering problem. An adapter was

designed to fit the omnidirectional chamber which would highly collimate the flame and send it through an overexpanding nozzle to bring the flame to one atmosphere pressure. Slightly downstream, a 1/2 inch window was placed for a view of the center of the flame. With this adapter, eddy currents developed downstream from the window, thus correcting the smoke [illegible] problem. Pressure variations of approximately five per cent were observed between successive shots, but this could be attributed mainly to variations in powder mixing. See Figure 39 for the final design of the atmospheric solid oxidizer chamber.

Studies with pressurized oxygen placed these stringent requirements on chamber design:

1. Chamber must be completely sealed.
2. Chamber must be inert to high pressure oxygen.
3. Chamber must withstand shock loading.
4. Chamber must have sufficient volume to prevent excessive pressure buildup.
5. Chamber must be equipped with a window capable of withstanding maximum pressure of chamber.
6. Chamber must be equipped with an igniter capable of withstanding maximum chamber pressure and 3,000 volt capacitor discharge.

The final design of the pressurized oxygen chamber based on these requirements is shown in Figure 40. Other moderate pressure studies were performed in a modified oxygen bomb calorimeter previously discussed in Section III.

ASSEMBLED

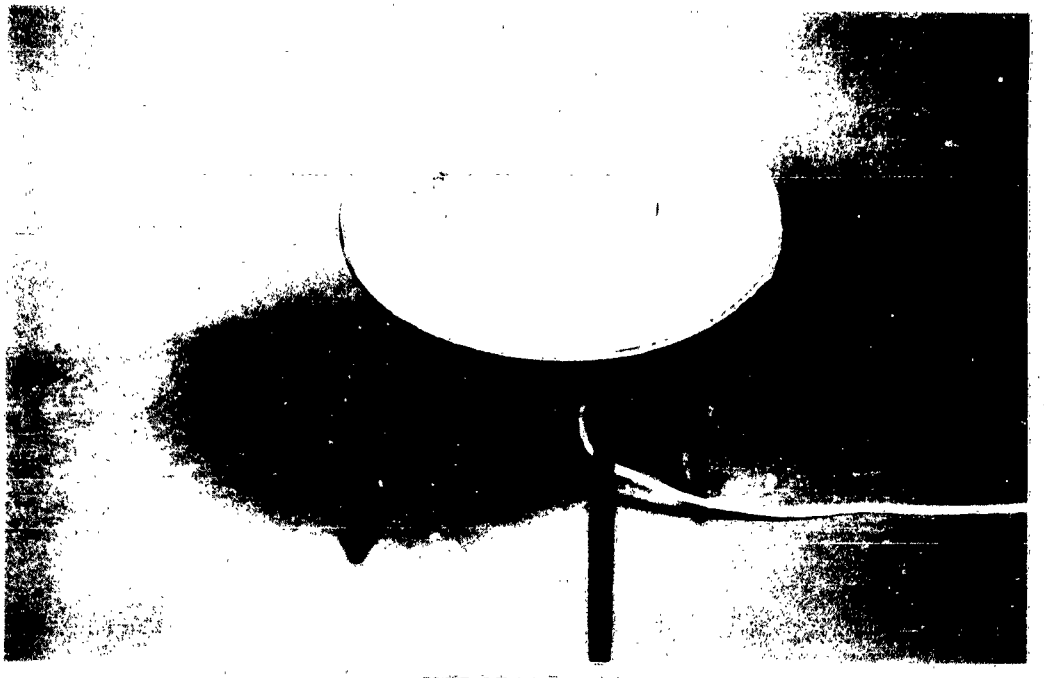

INTERIOR VIEW

Figure 39. Atmospheric Chamber

ASSEMBLED

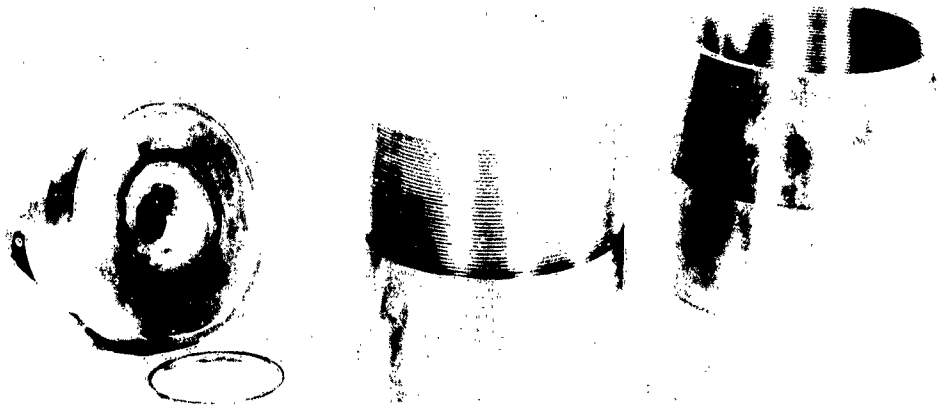

DISASSEMBLED

Figure 40 Static Pressurization Chamber

A dynamic pressurization chamber was designed to allow measurements at extremely high pressures ($> 10^4$ psi). Design criteria were:

1. Provide for containment up to 10^5 psi.
2. Electrical ignition of charge.
3. Transparent window for viewing.

The chamber is shown in Figure 41. Operation of this chamber has presented two major difficulties. First, alignment of the optical system with the view port was almost impossible. Second, the window almost invariably ruptured, and the scattered fragments presented a serious personnel hazard unless adequate shielding was used.

These two defects were corrected in the construction of the modified dynamic pressurization chamber shown in Figure 42

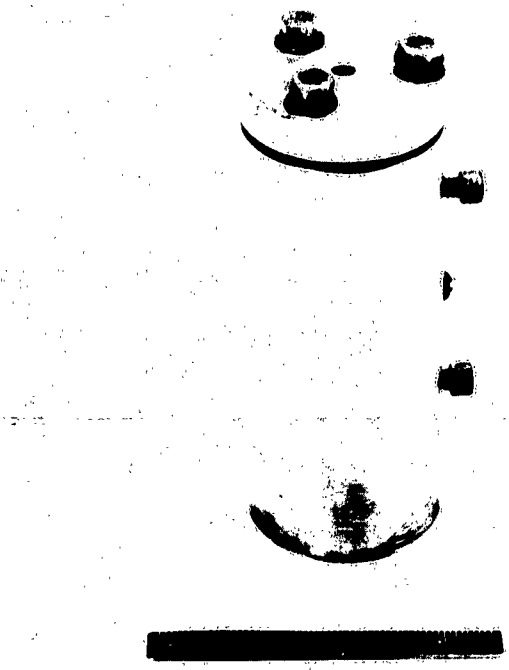

ASSEMBLED

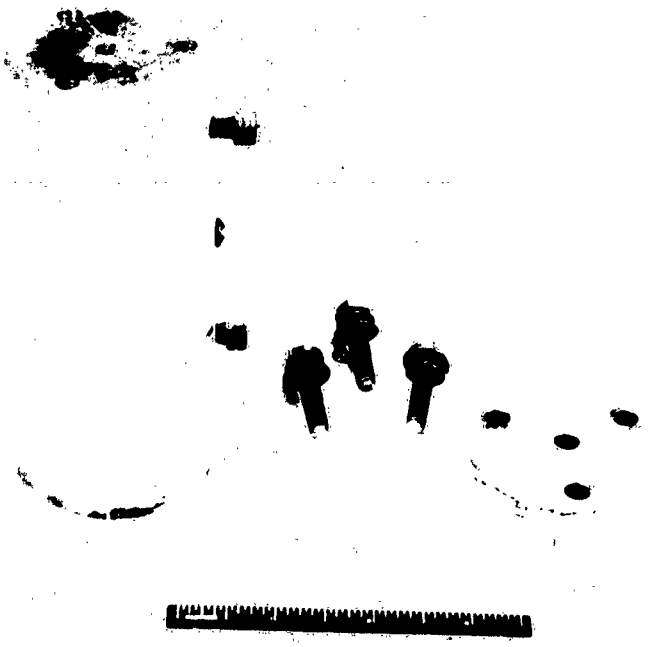

DISASSEMBLED

Figure 41. Dynamic Pressurization Chamber

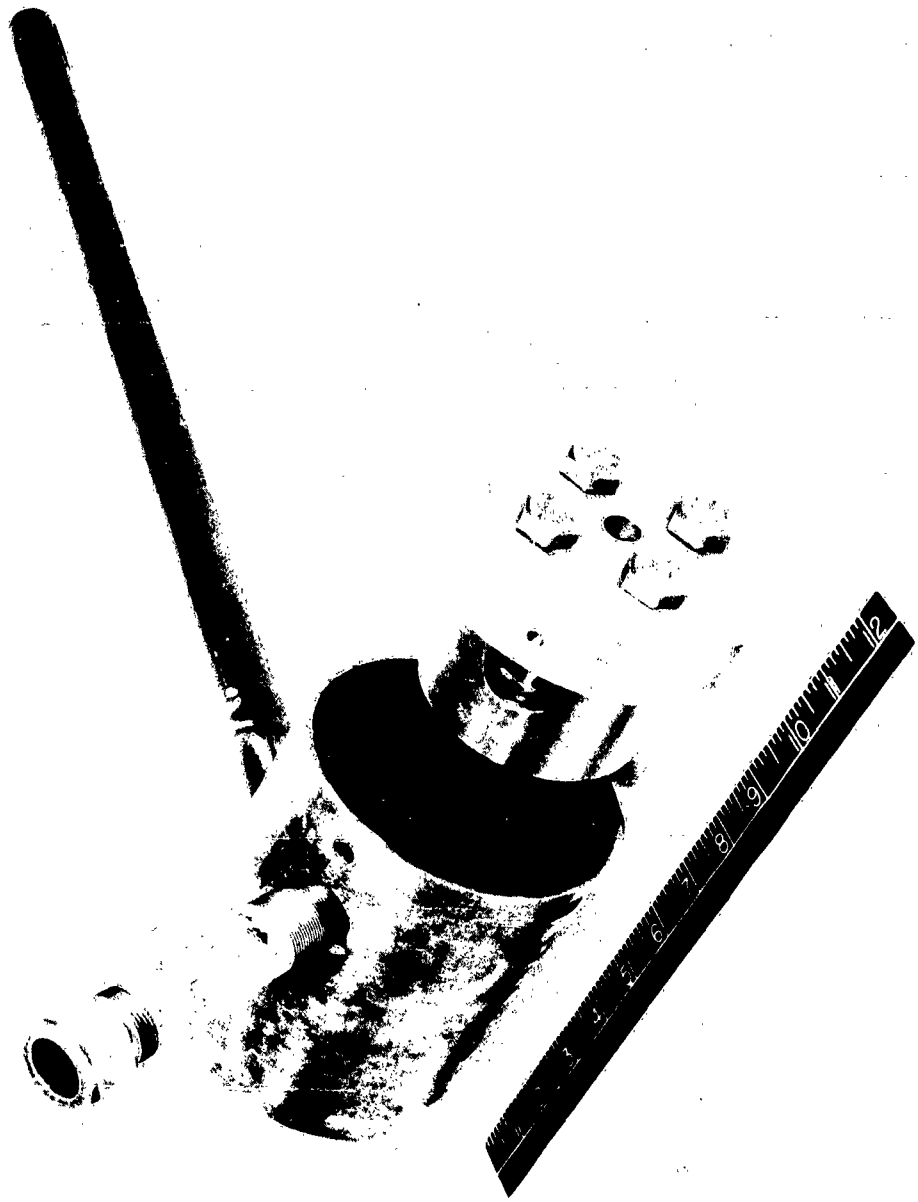

Figure 42. Modified Dynamic Pressurization Chamber

APPENDIX II

SUPPLEMENTARY TEST DATA

The spectra presented on the following pages have been obtained by taking densitometer readouts of the spectrographic films on which the original spectra were recorded. Most of these readouts have isotherms faired in as described in Section III. Three brightness temperatures vs. wavelength plots (Figures 43, 44, and 45) are included for comparison with the densitometer readouts. These plots were obtained by reduction of intensity measurements made with the spectrophotometer device described in Appendix I.

The majority of the spectra consist of aluminum-potassium perchlorate reactions containing various additives. A few spectra of zirconium, thorium, lanthanium, and hafnium powders, reacted with potassium perchlorate, are included here because they contain data of interest to the additives study. The importance of these spectra is discussed in Section III.

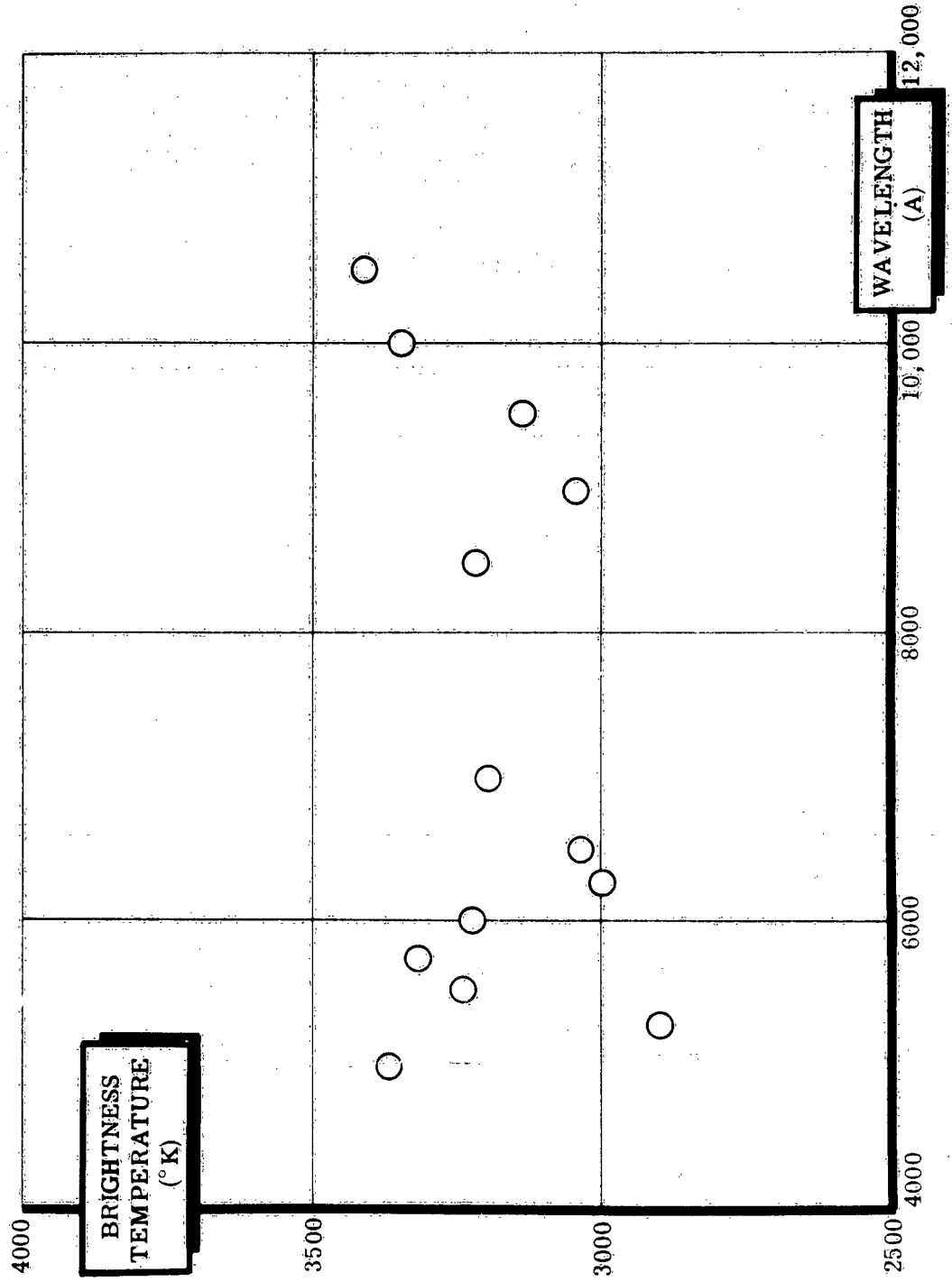

Figure 43. Brightness Temperture Versus Wavelength
Mg + Al + BA(ClO_3)$_2$ (1-2-8)

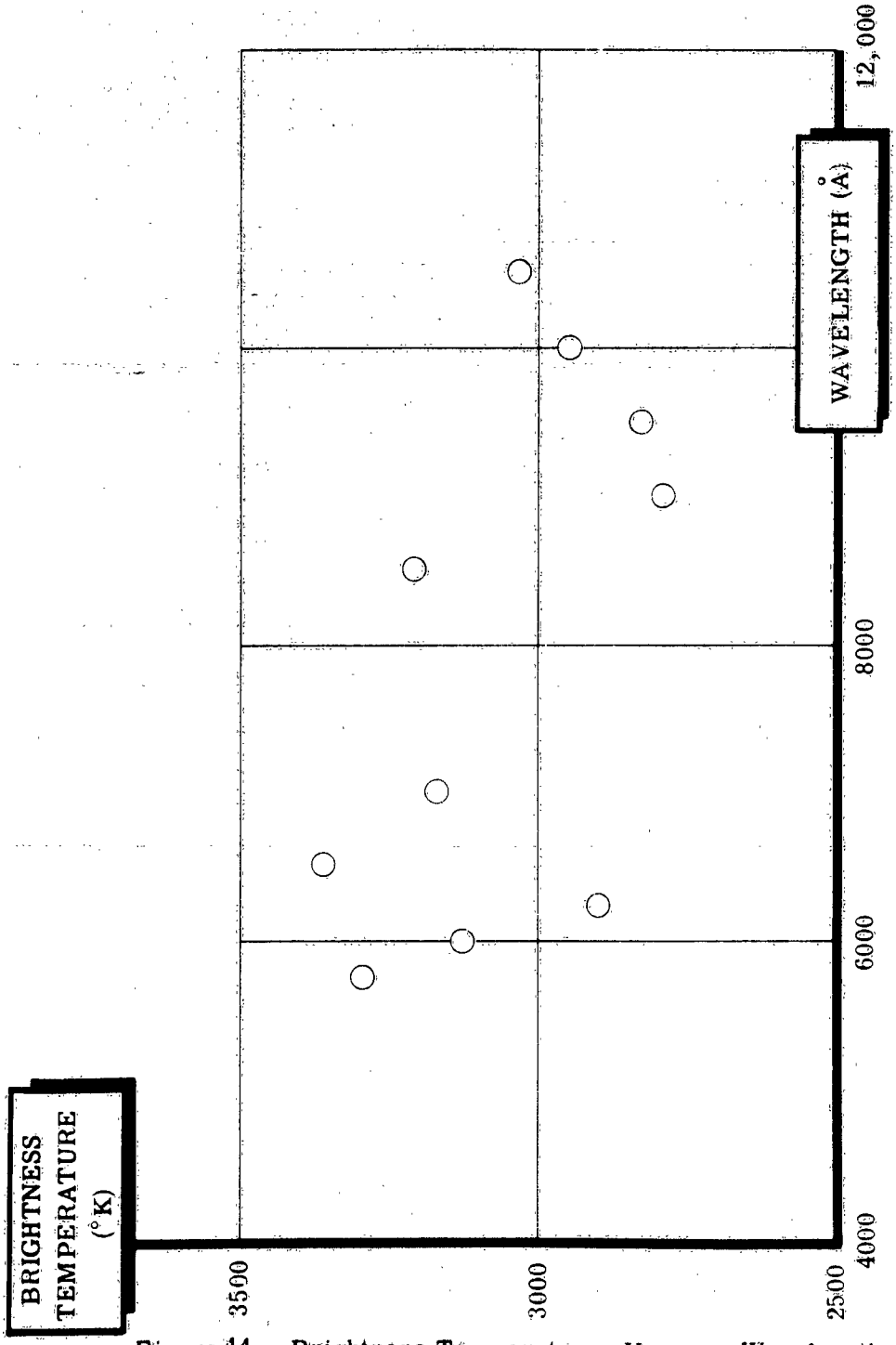

Figure 44. Brightness Temperature Versus Wavelength
$Zr + KClO_4$ (4-3)

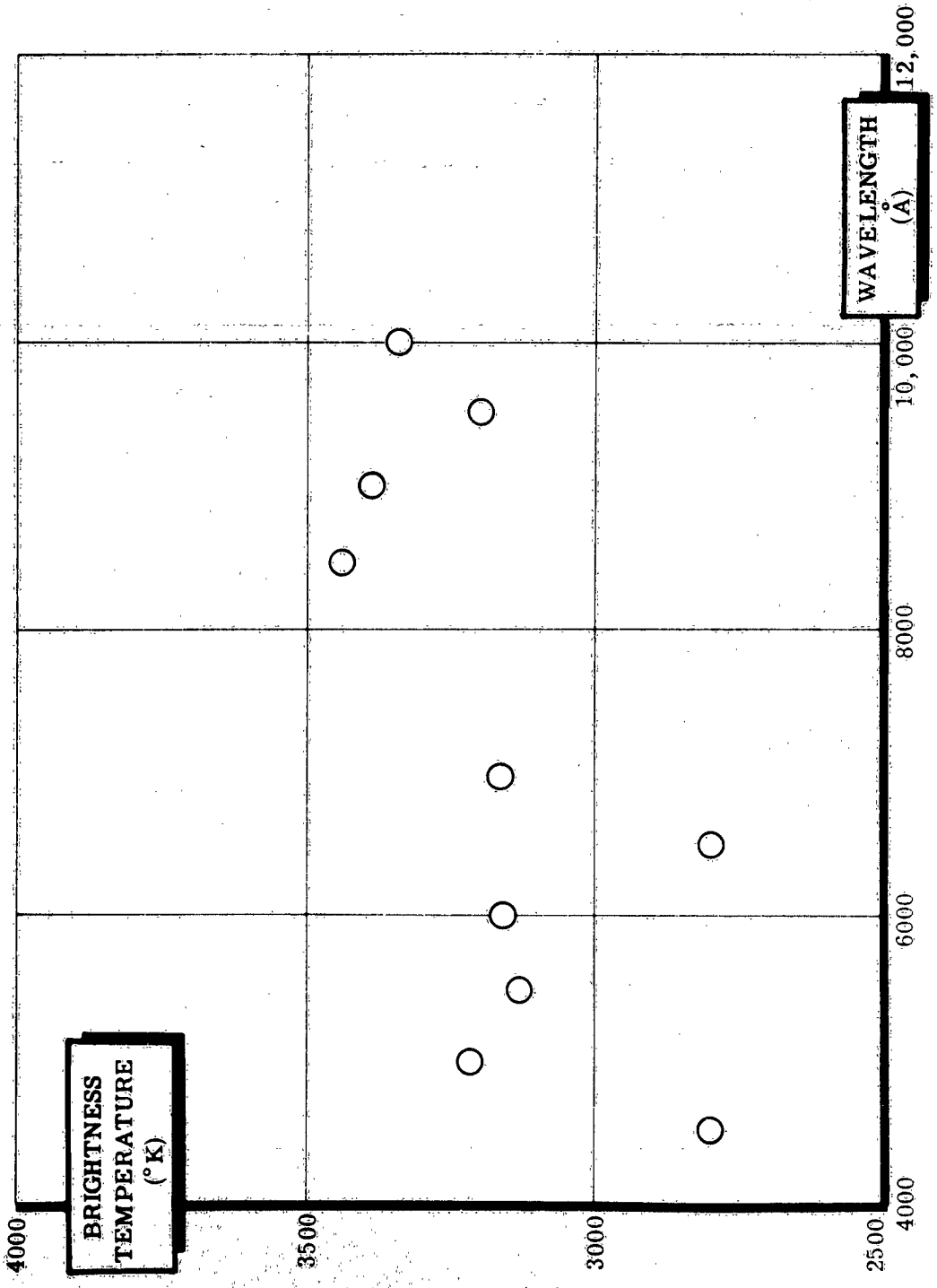

Figure 45 Brightness Temperature Versus Wavelength Hf + $KCl O_4$ (5-2)

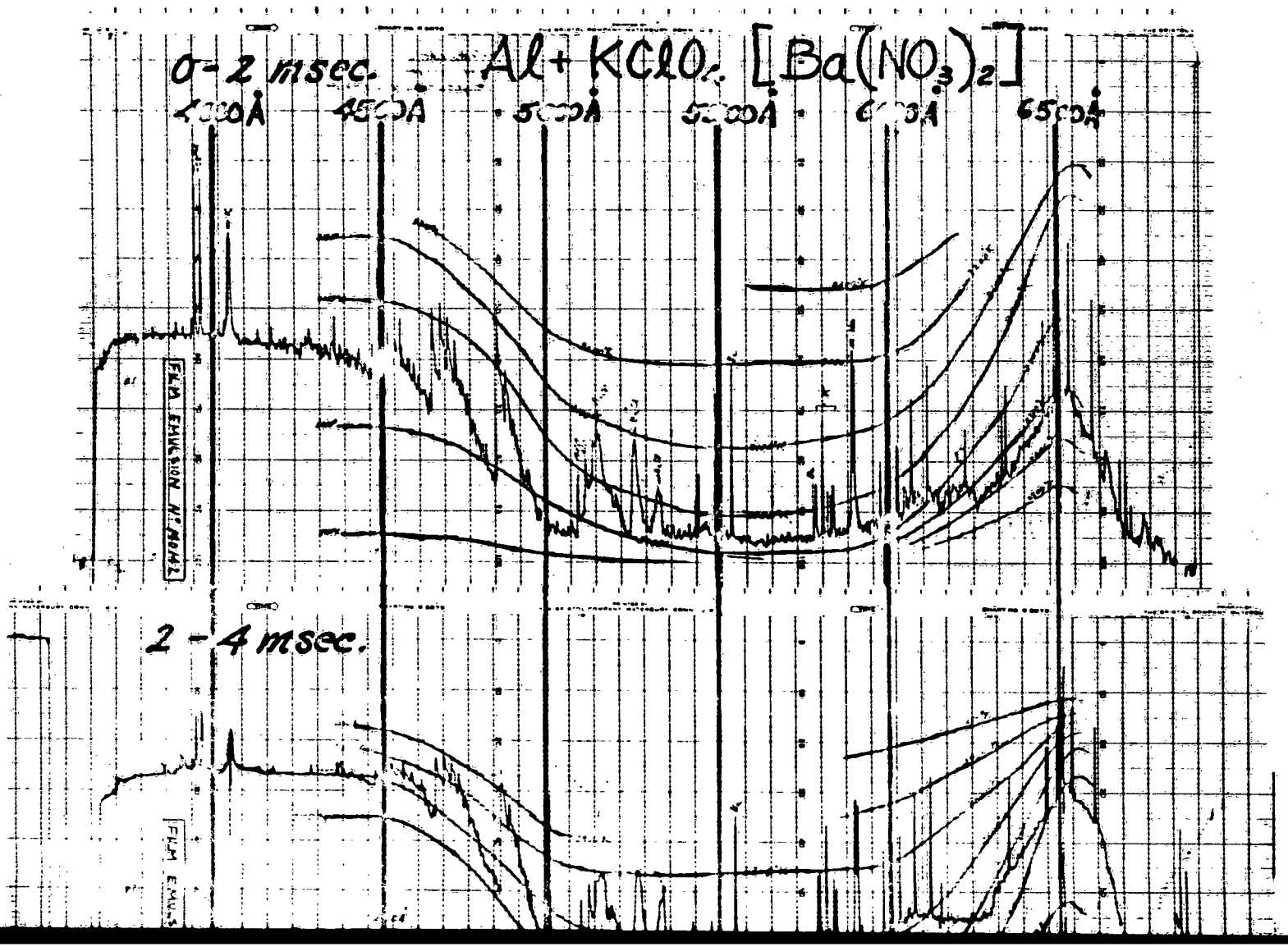
0-2 msec.
Al + KClO4 [Ba(NO3)2]
4000Å
4500Å
5000Å
5500Å
6000Å
6500Å
FILM EMULSION N° 80442
2-4 msec.
FILM EMULSION

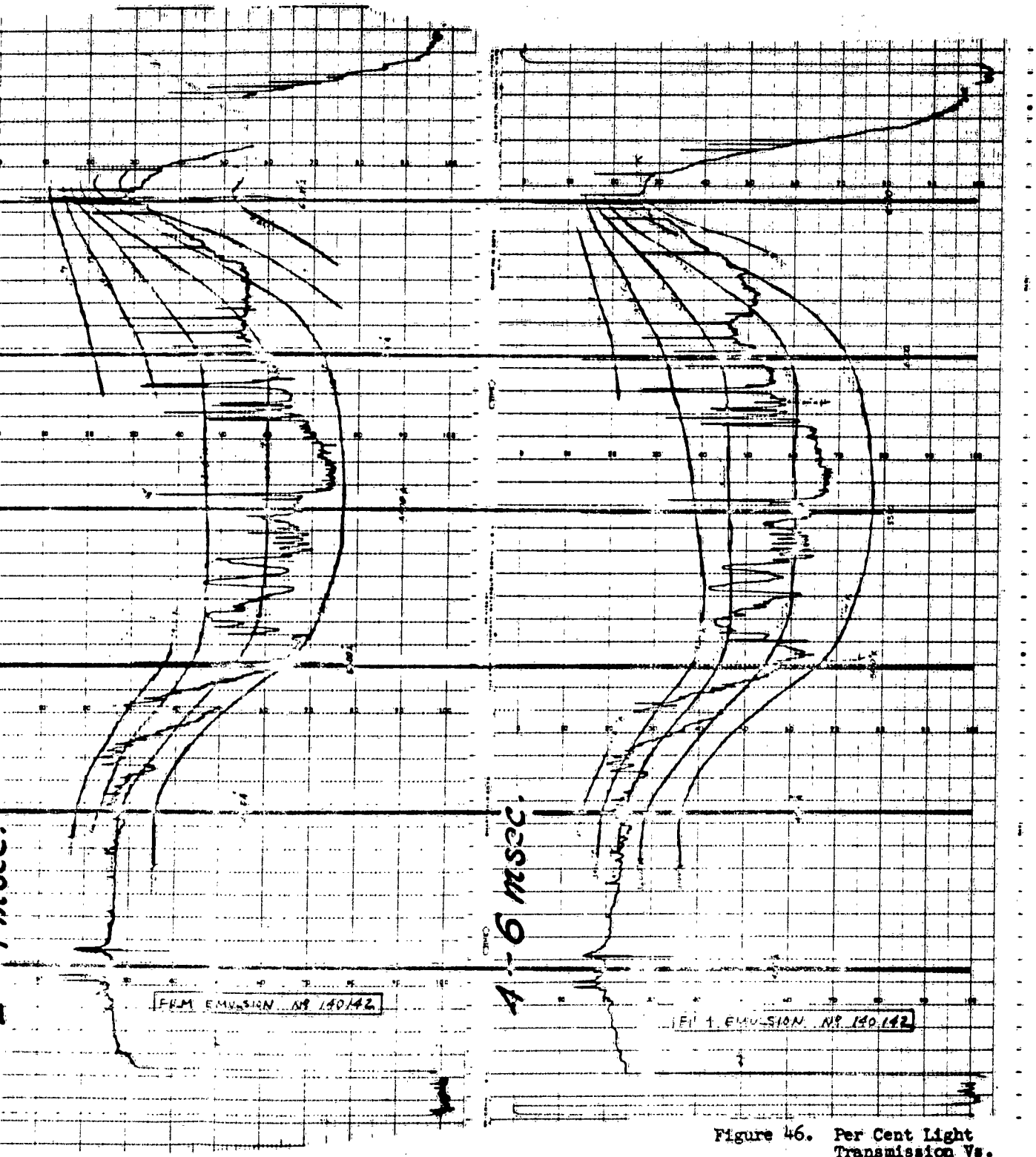

Figure 46. Per Cent Light Transmission Vs. Wavelength

B C

1
6-8 msec.
4612 Å
8-10 msec.
FILM EMULSION No. 140/42
A
B

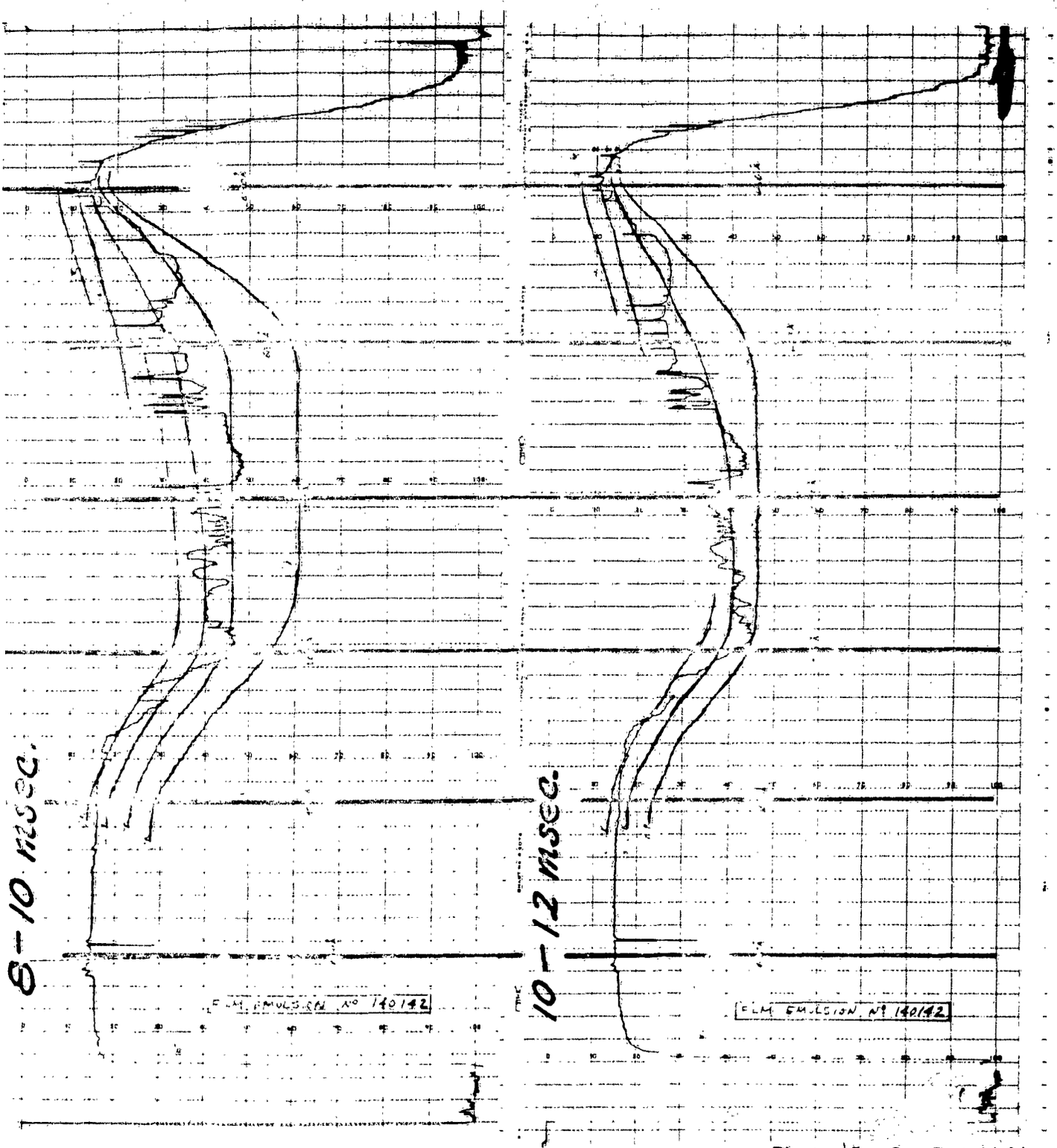

B C

Figure 47. Per Cent Light Transmission Vs. Wavelength

1

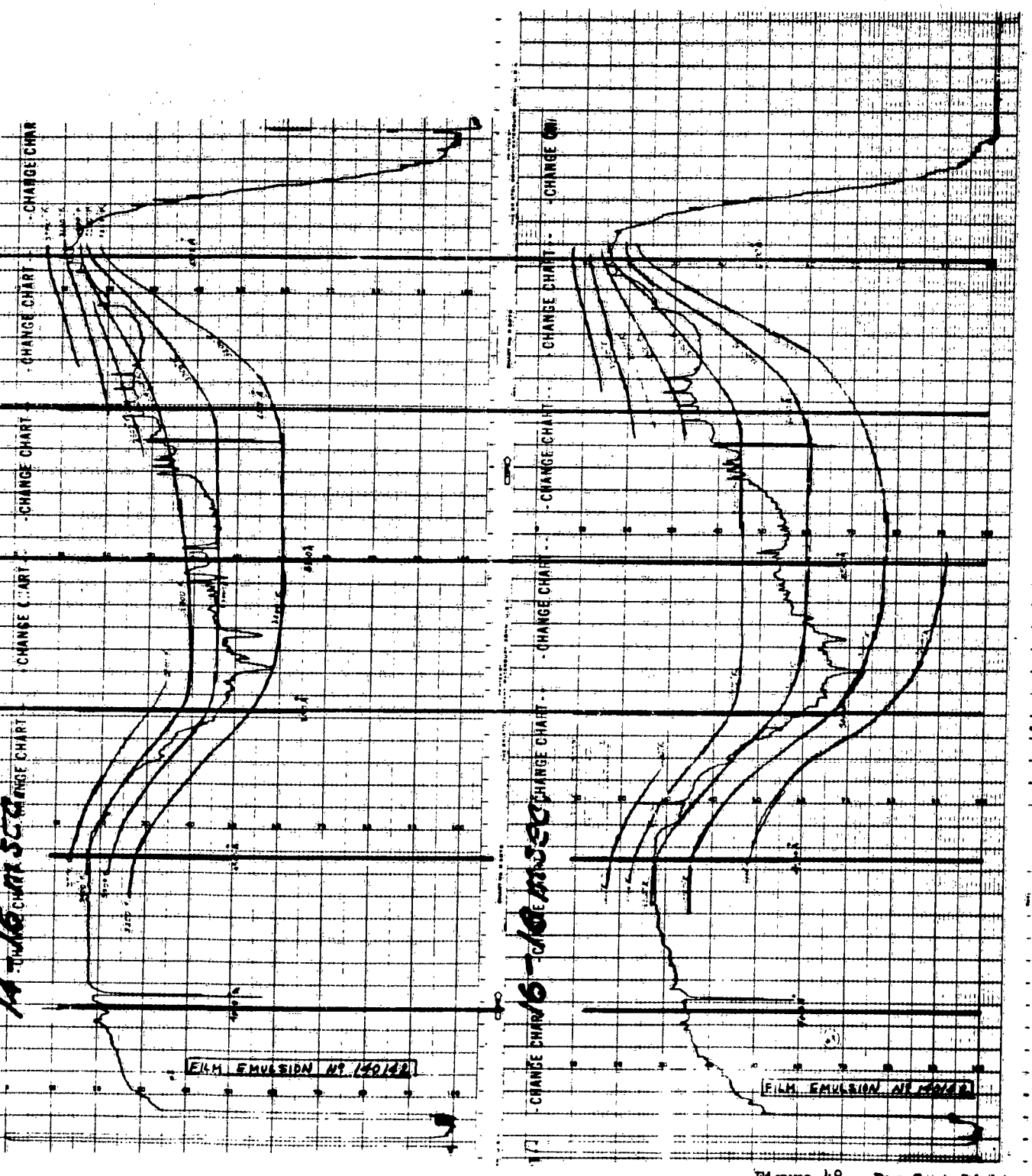

Figure 48. Per Cent Light Transmission vs. Wavelength

B C

1

6500Å
6000Å
5500Å
5000Å
4500Å
4000Å
Zr+KClO4
A
6500Å
6000Å
5500Å
5000Å
4500Å
Nd+KClO4
B

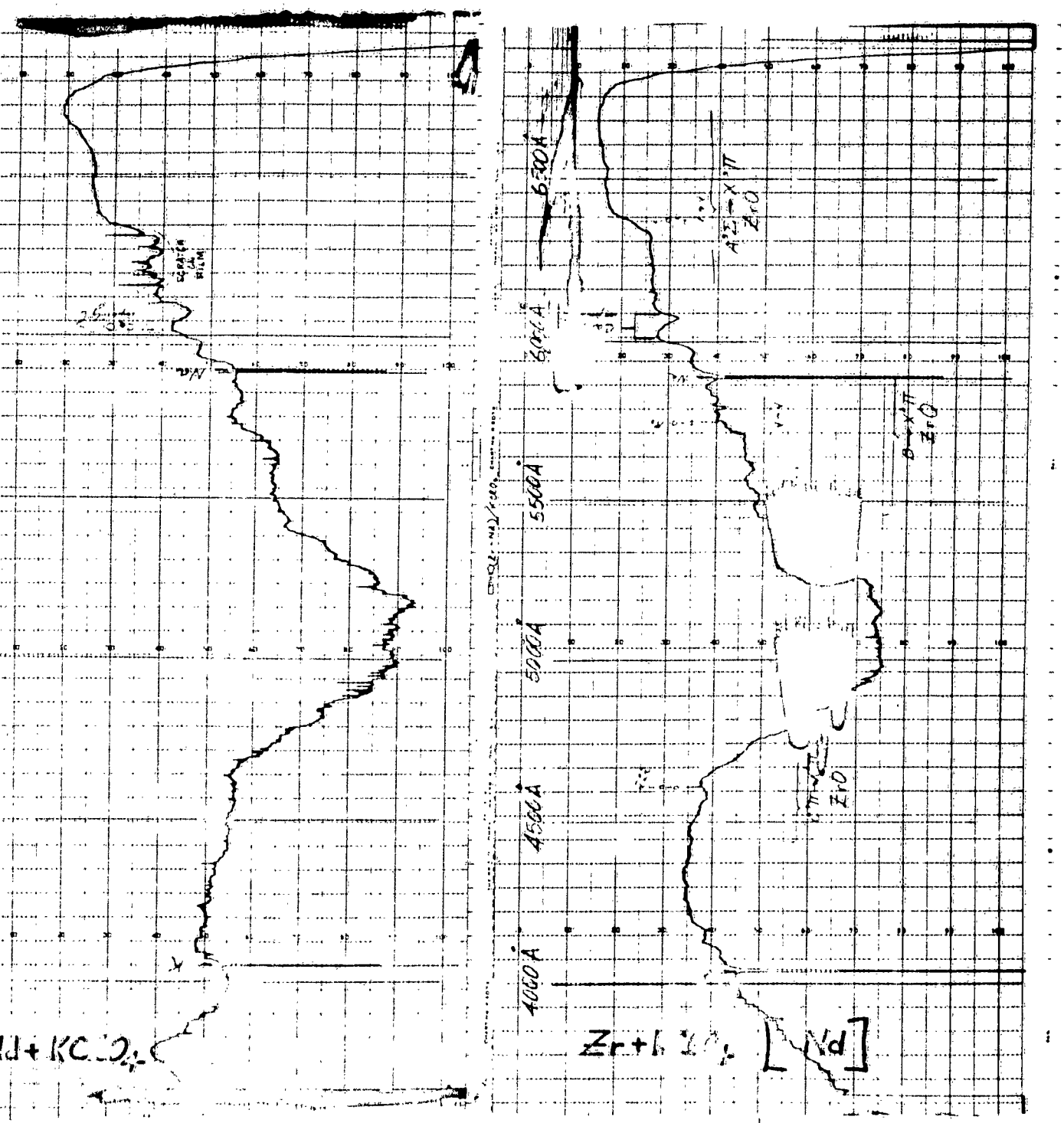

Figure 49. Per Cent Light Transmission vs. Wavelength

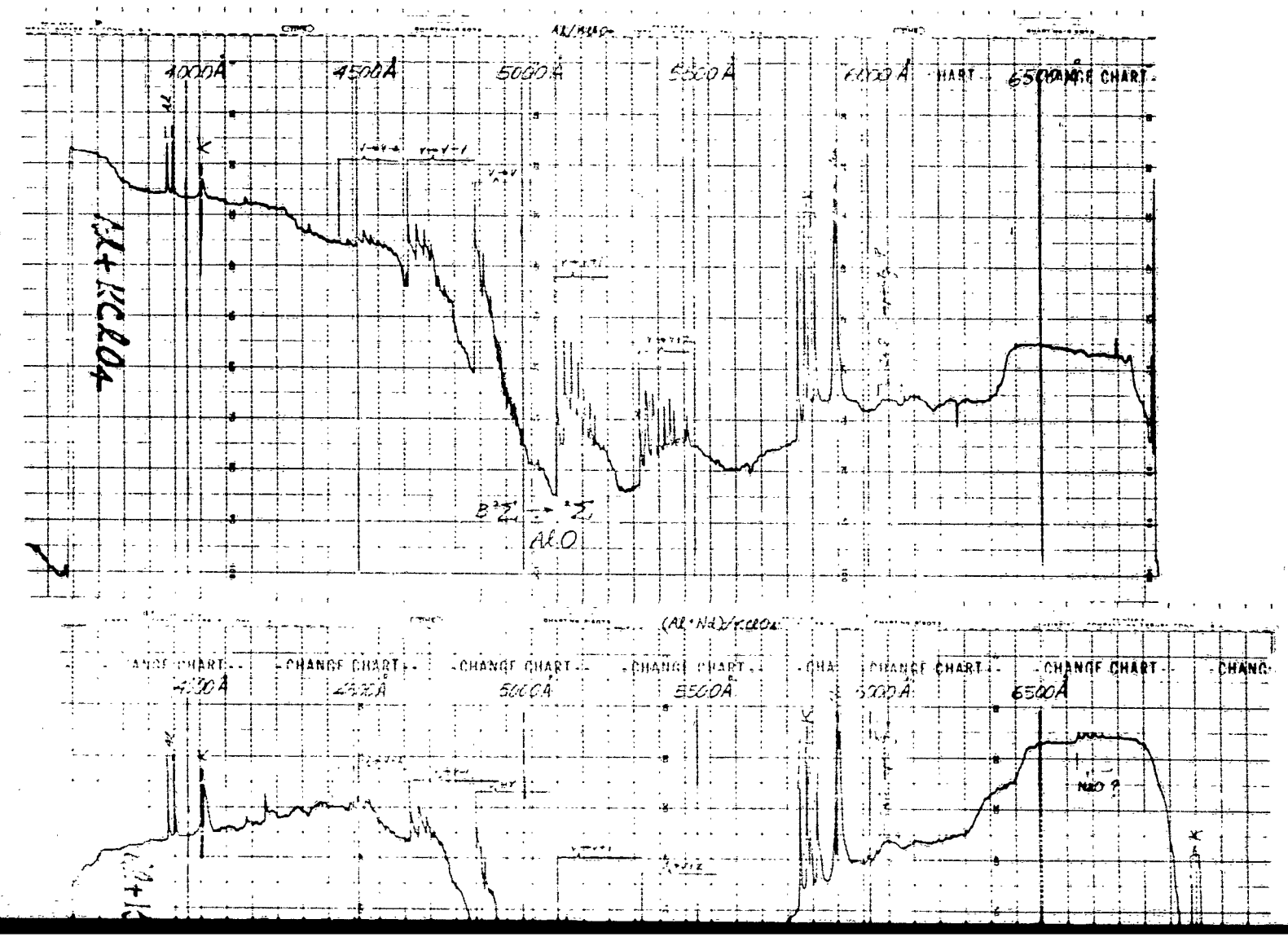
4000Å
4500Å
5000Å
5500Å
6000Å
6500Å
Al+KClO4
Al2O3
(Al+Nd)/KClO4
4500Å
5000Å
5500Å
6500Å
Nd2O3

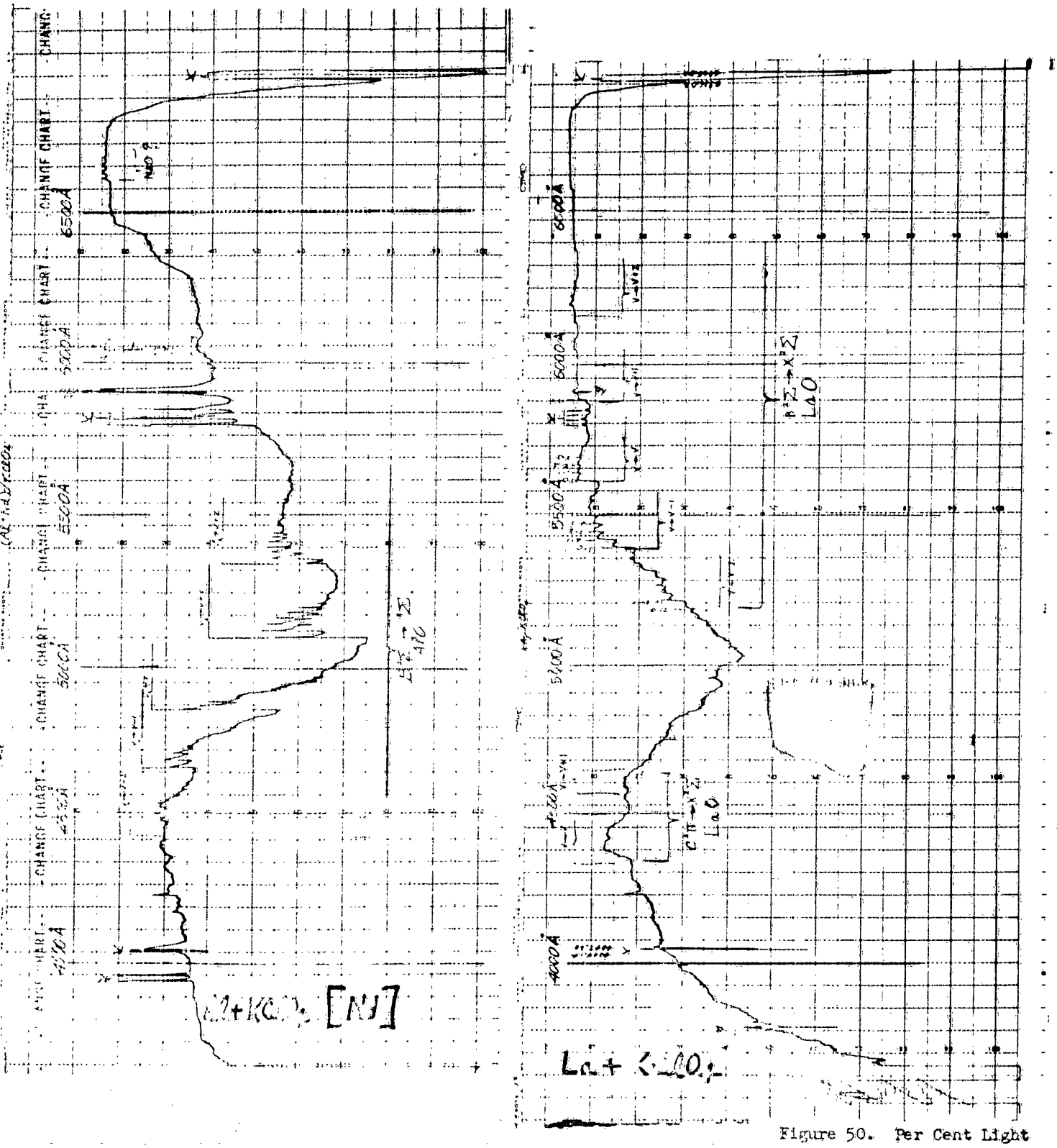

Figure 50. Per Cent Light Transmission vs. Wavelength

B C

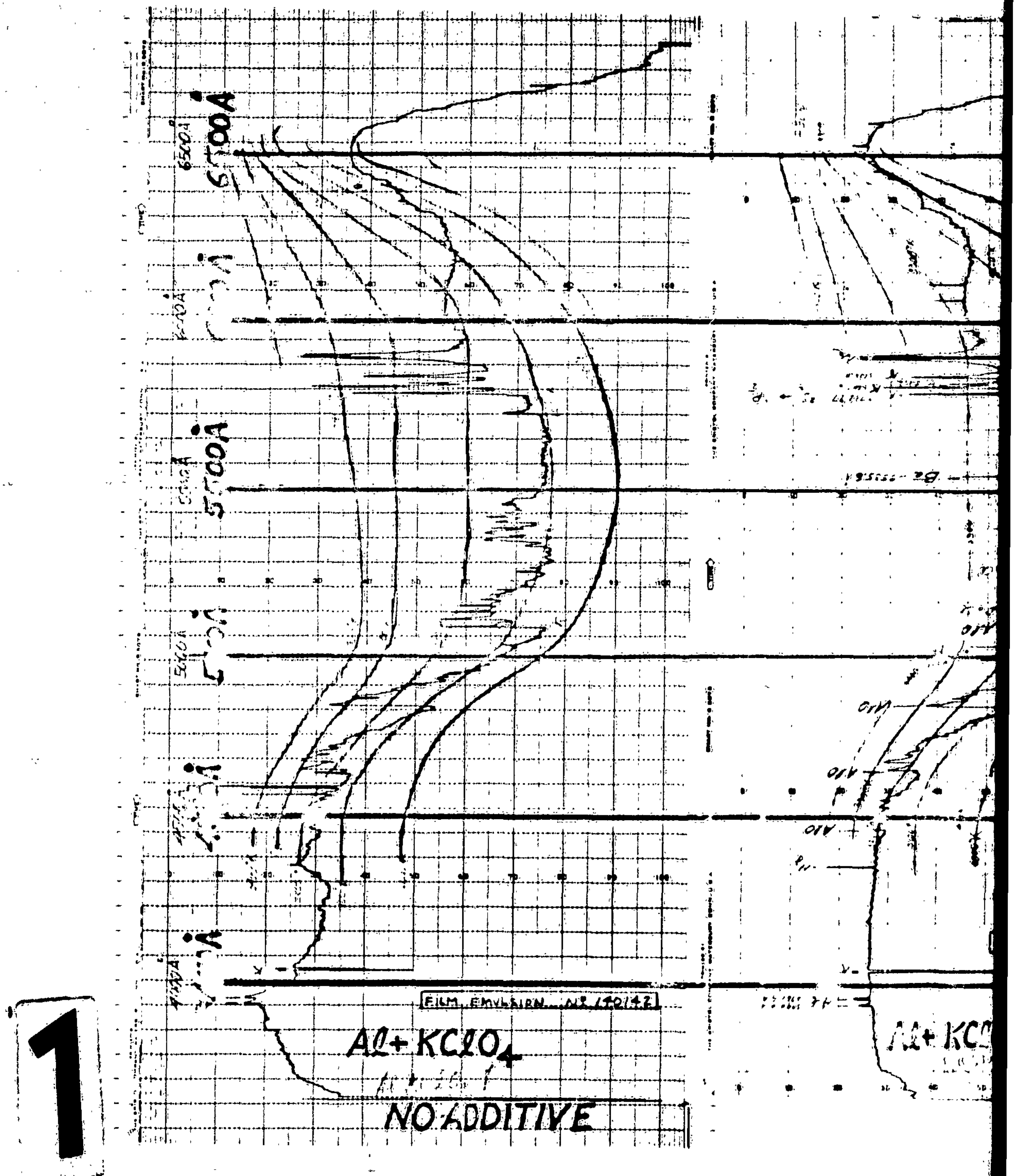
6500Å
6500Å
5500Å
5500Å
5000Å
Film Emulsion No. 140142
Al+KClO4
NO ADDITIVE
1

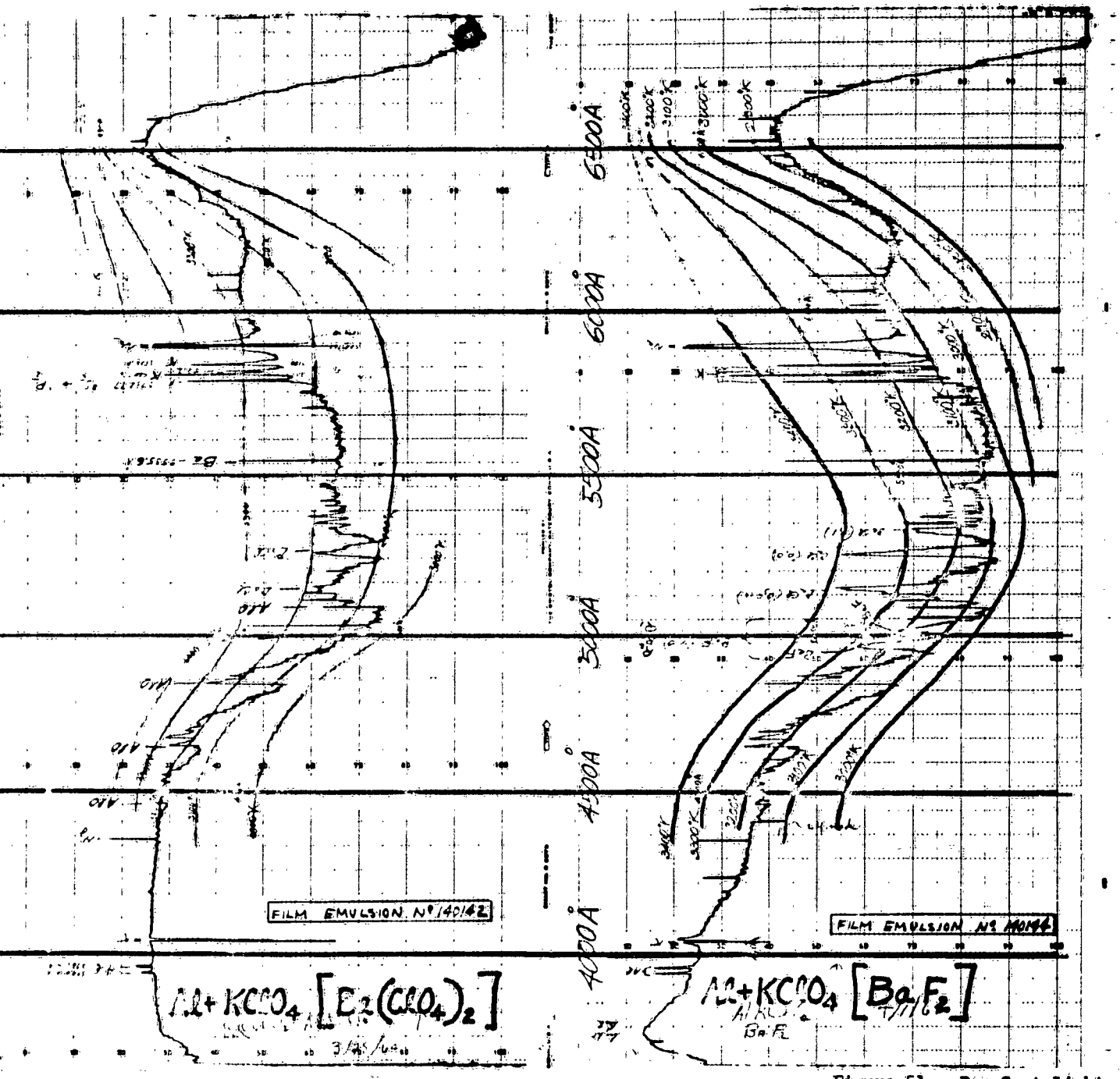

Figure 51. Per Cent Light Transmission vs. Wavelength

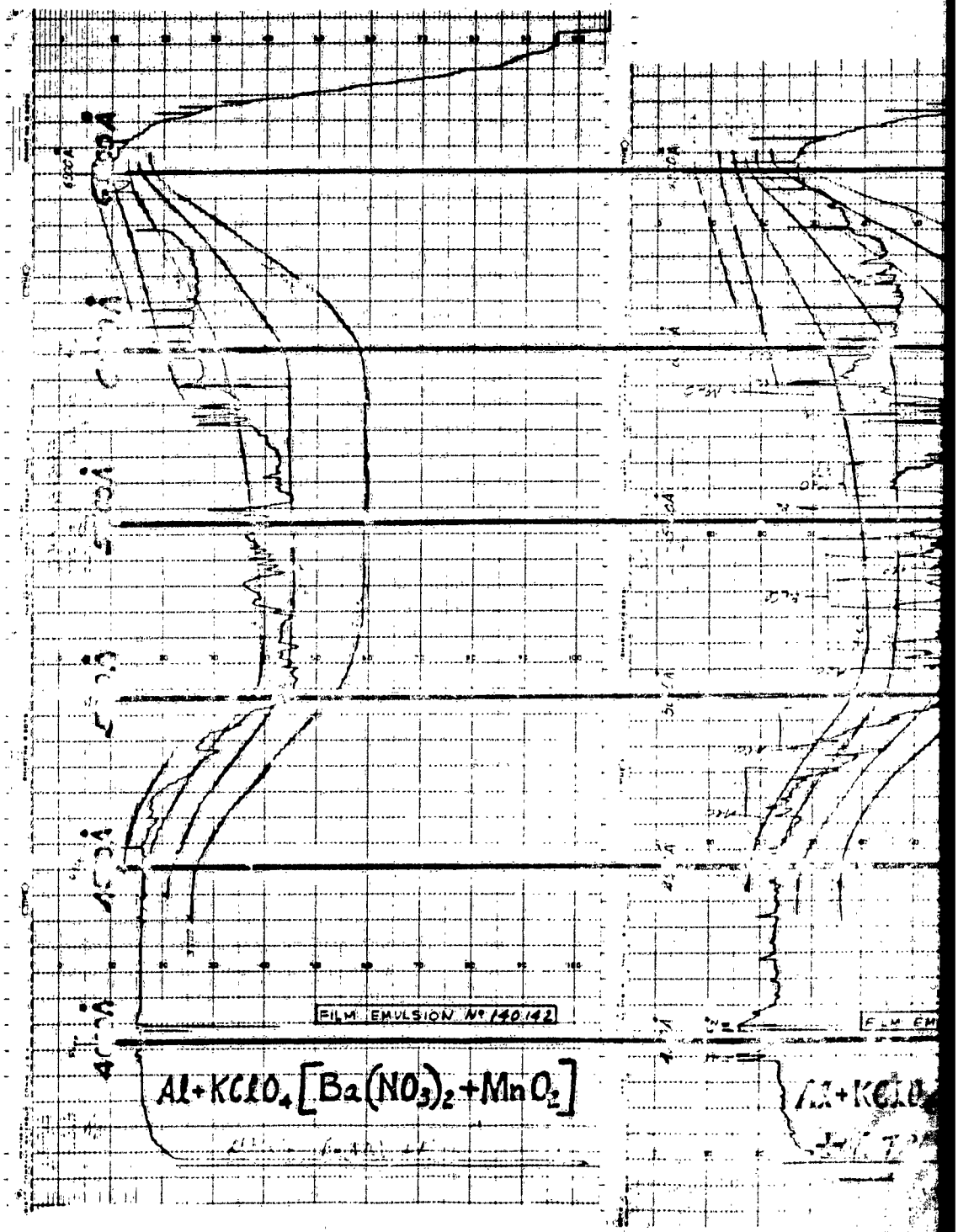

1

A

B

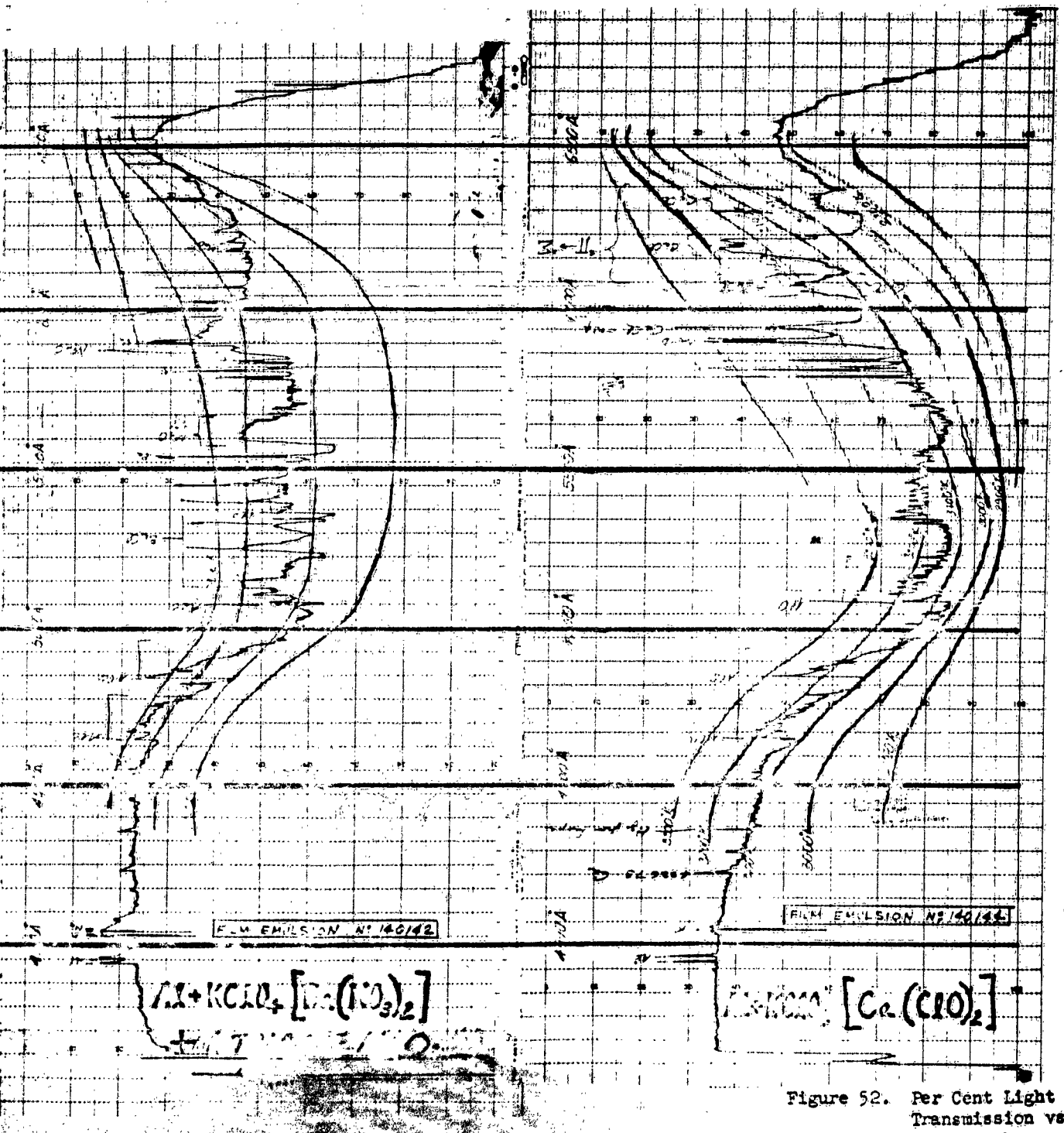

Figure 52. Per Cent Light Transmission vs. Wavelength

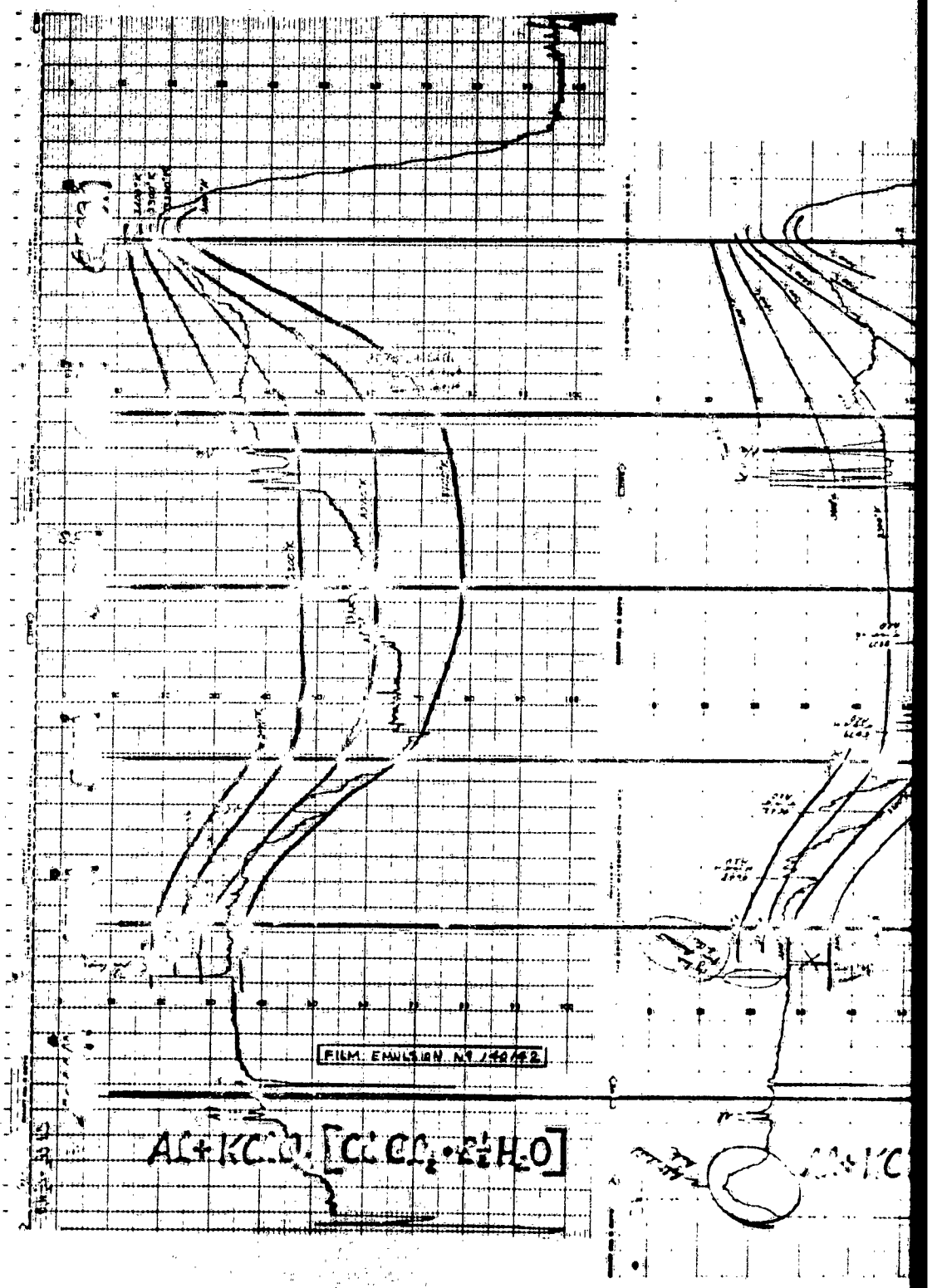

1

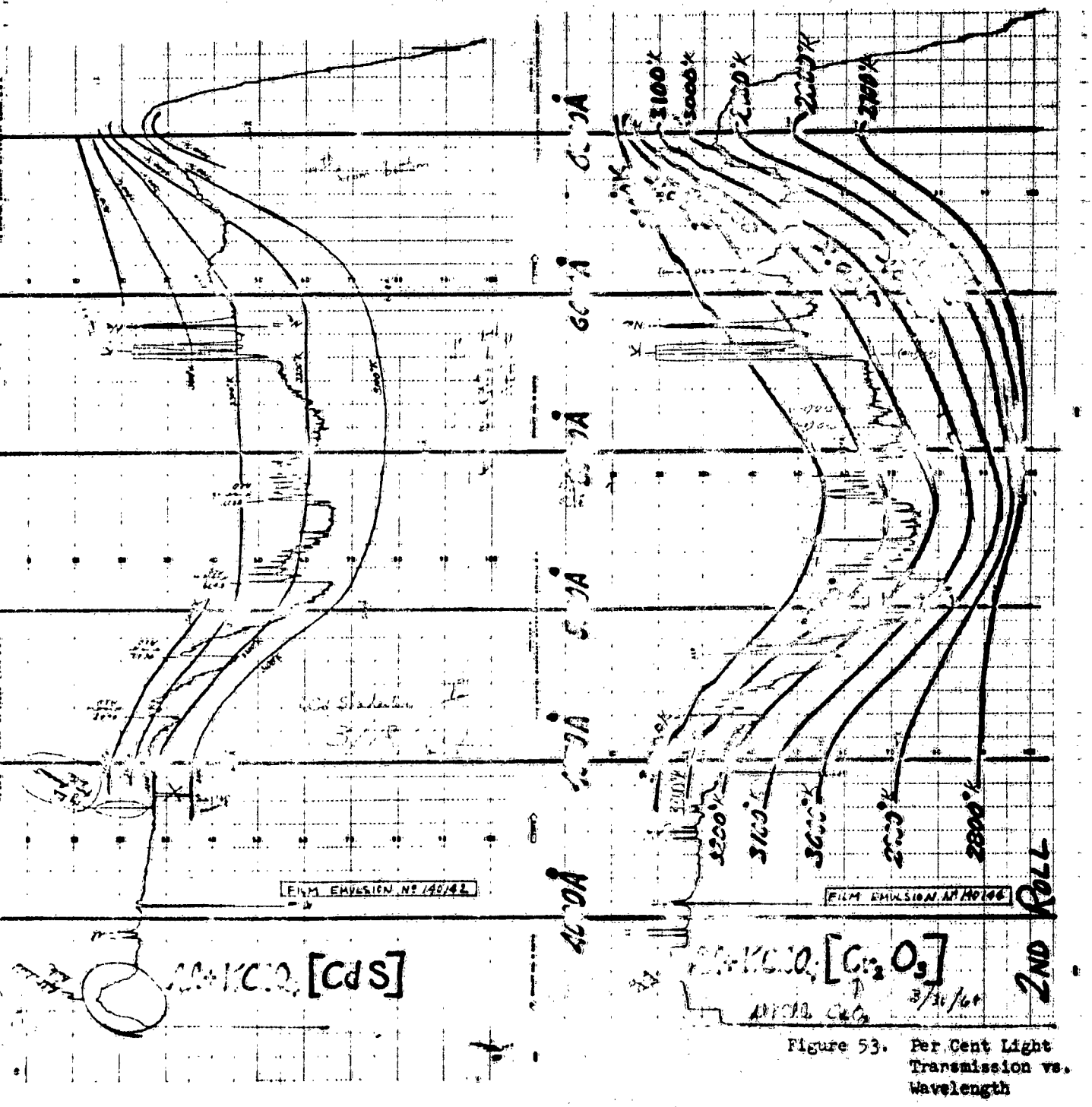

Figure 53. Per Cent Light Transmission vs. Wavelength

B C

1.

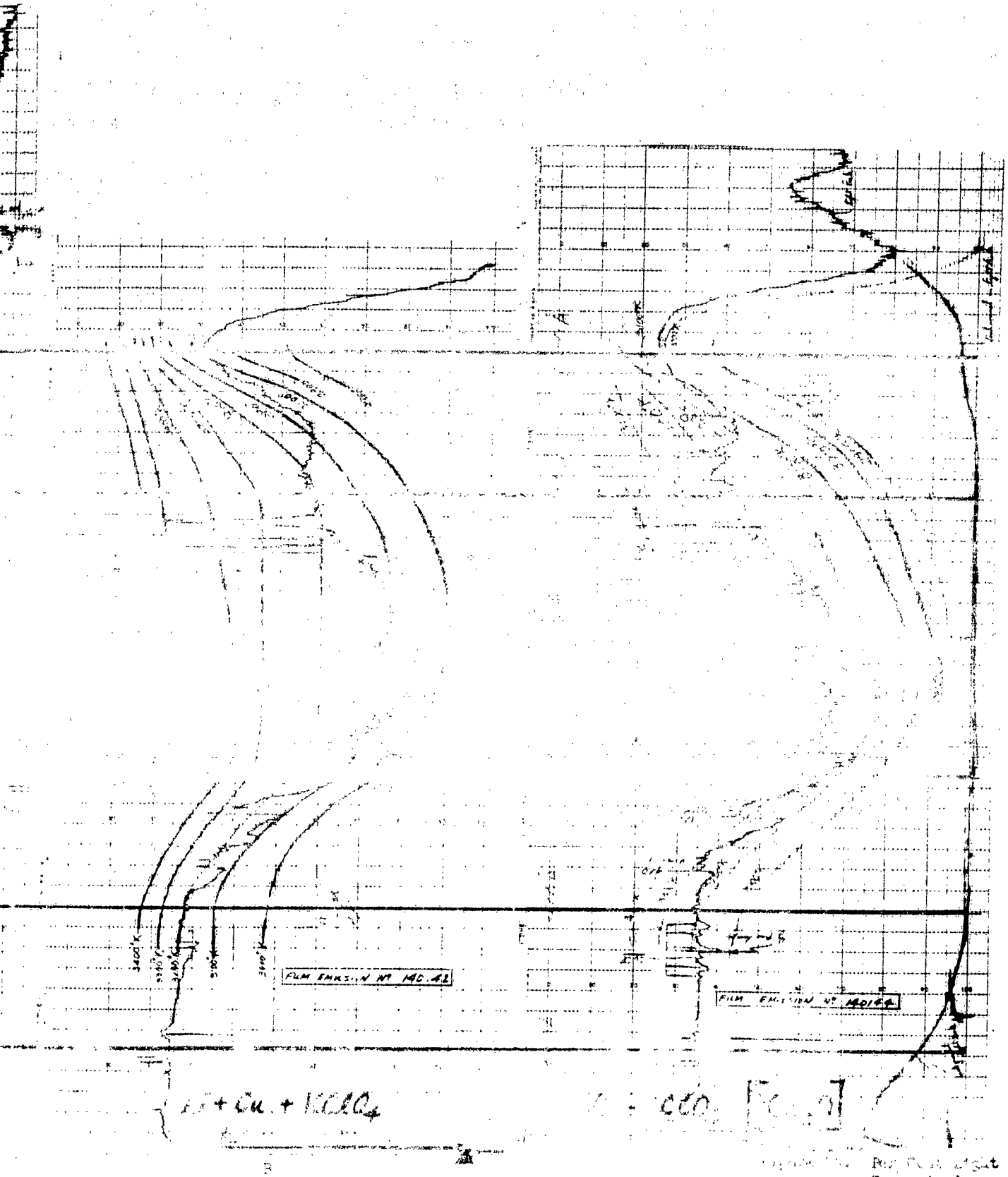

2

Fig. 2. Infrared Transmission vs. Wavelength

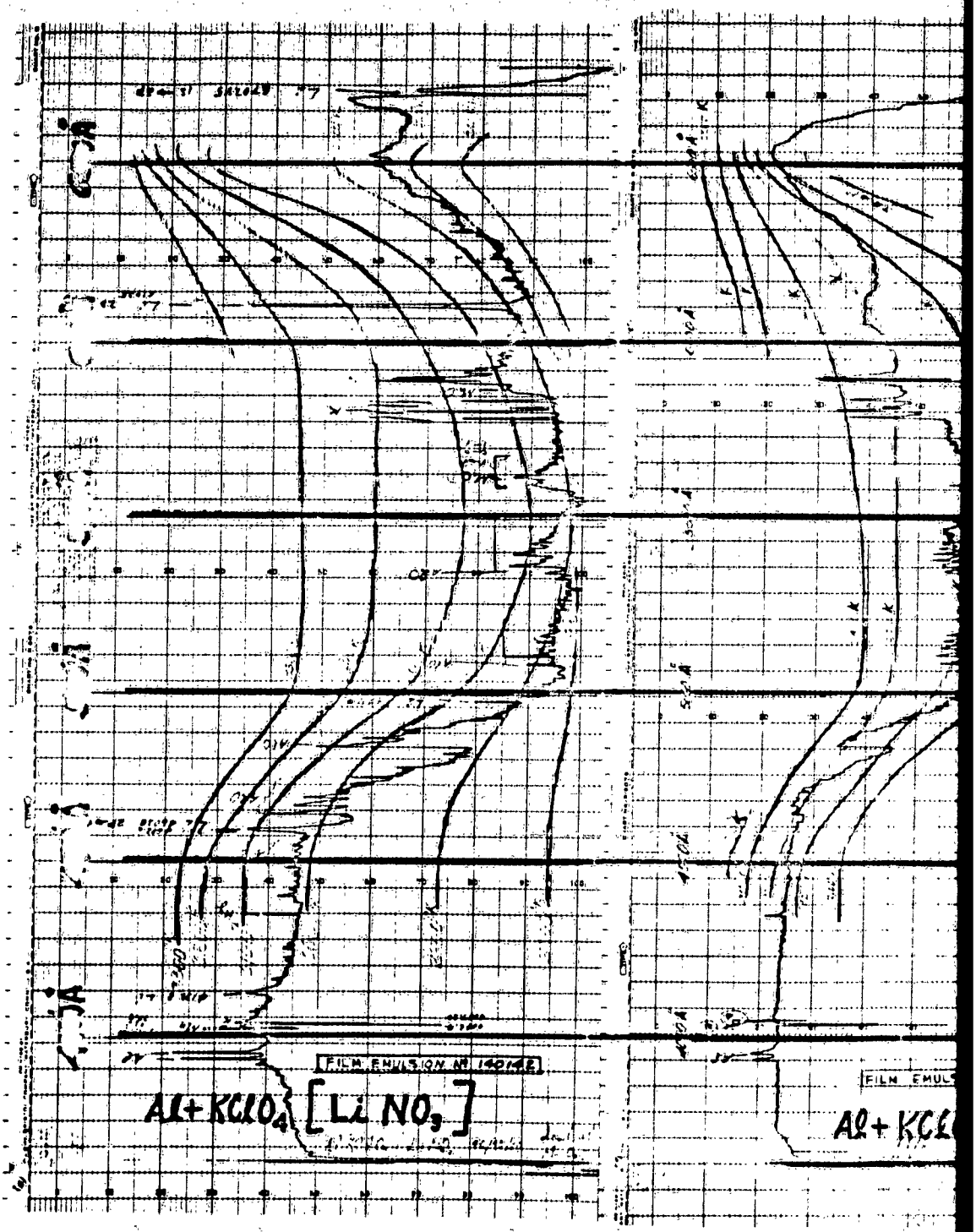

1

A

B

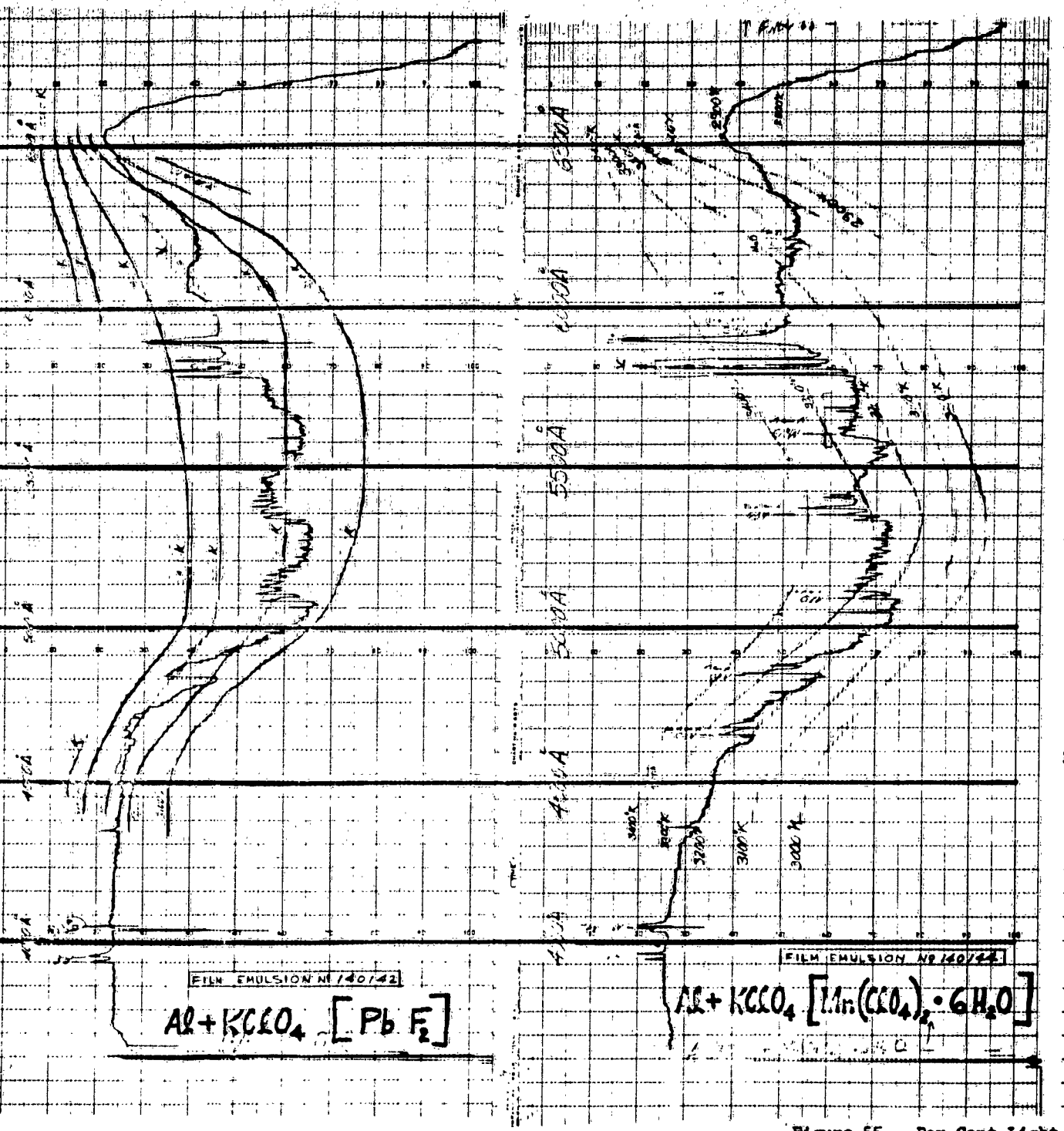

Figure 55. Per Cent Light Transmission Vs. Wavelength

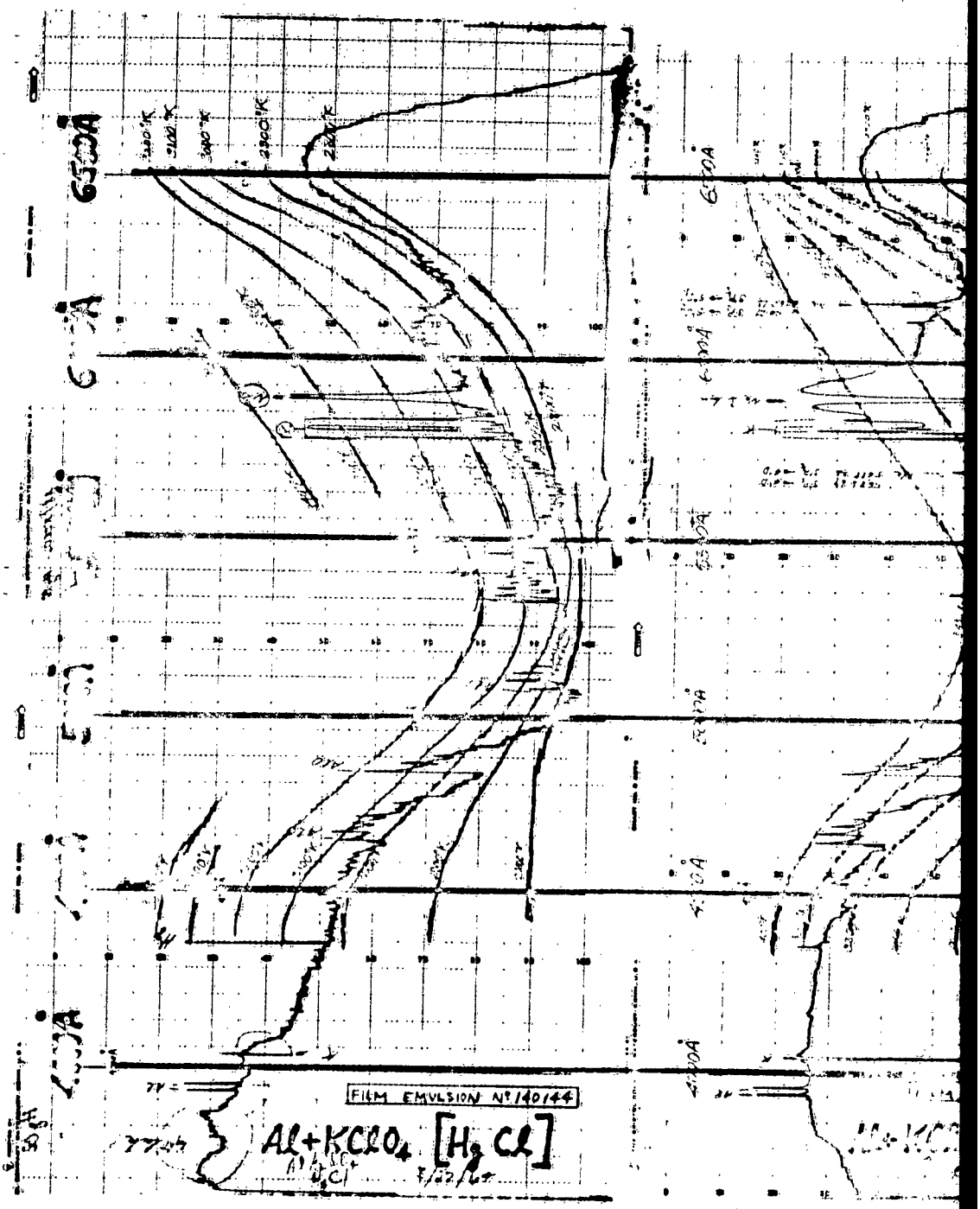

1

A

B

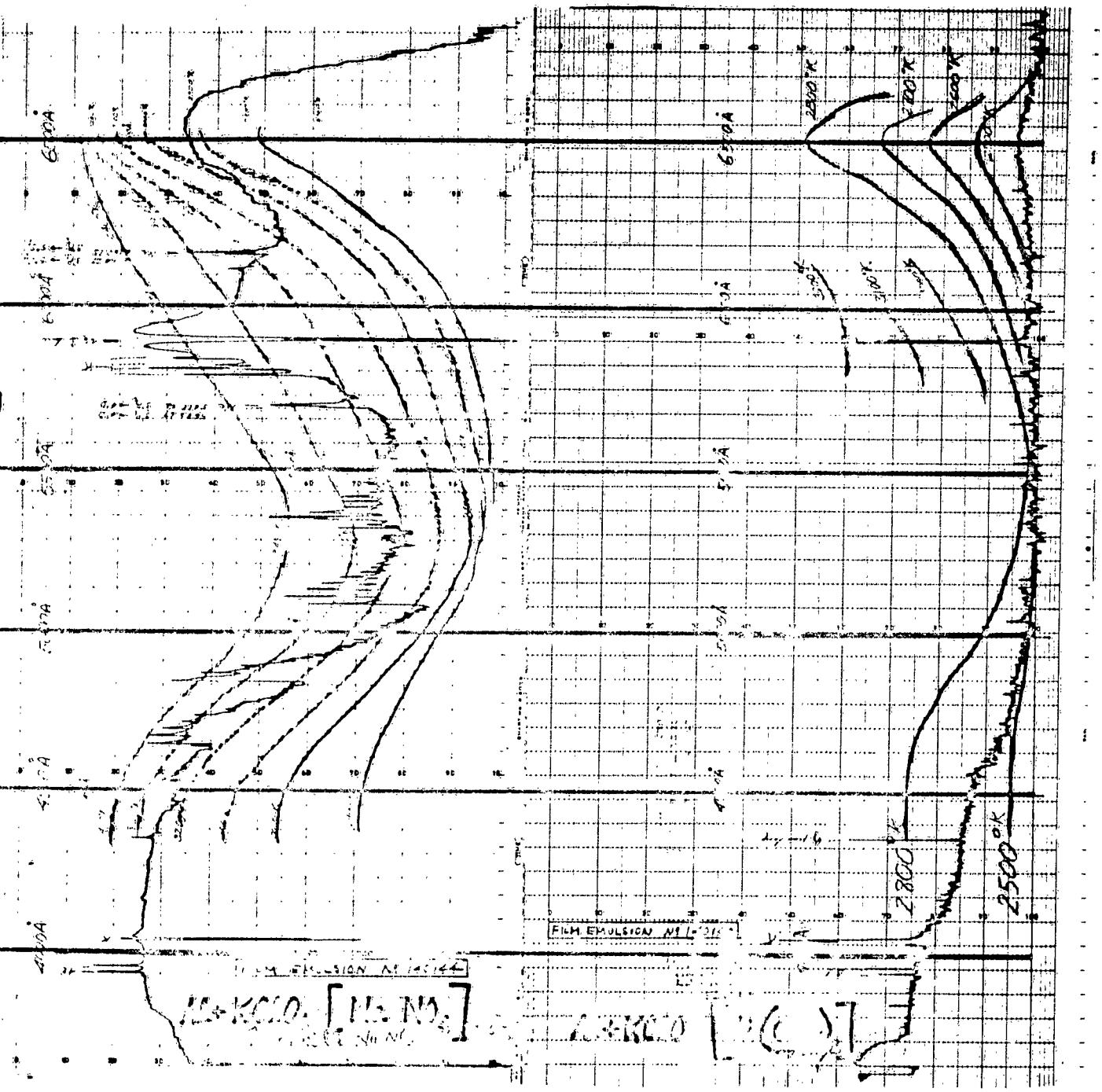

Figure 56. Per Cent Light Transmission vs. Wavelength

B C

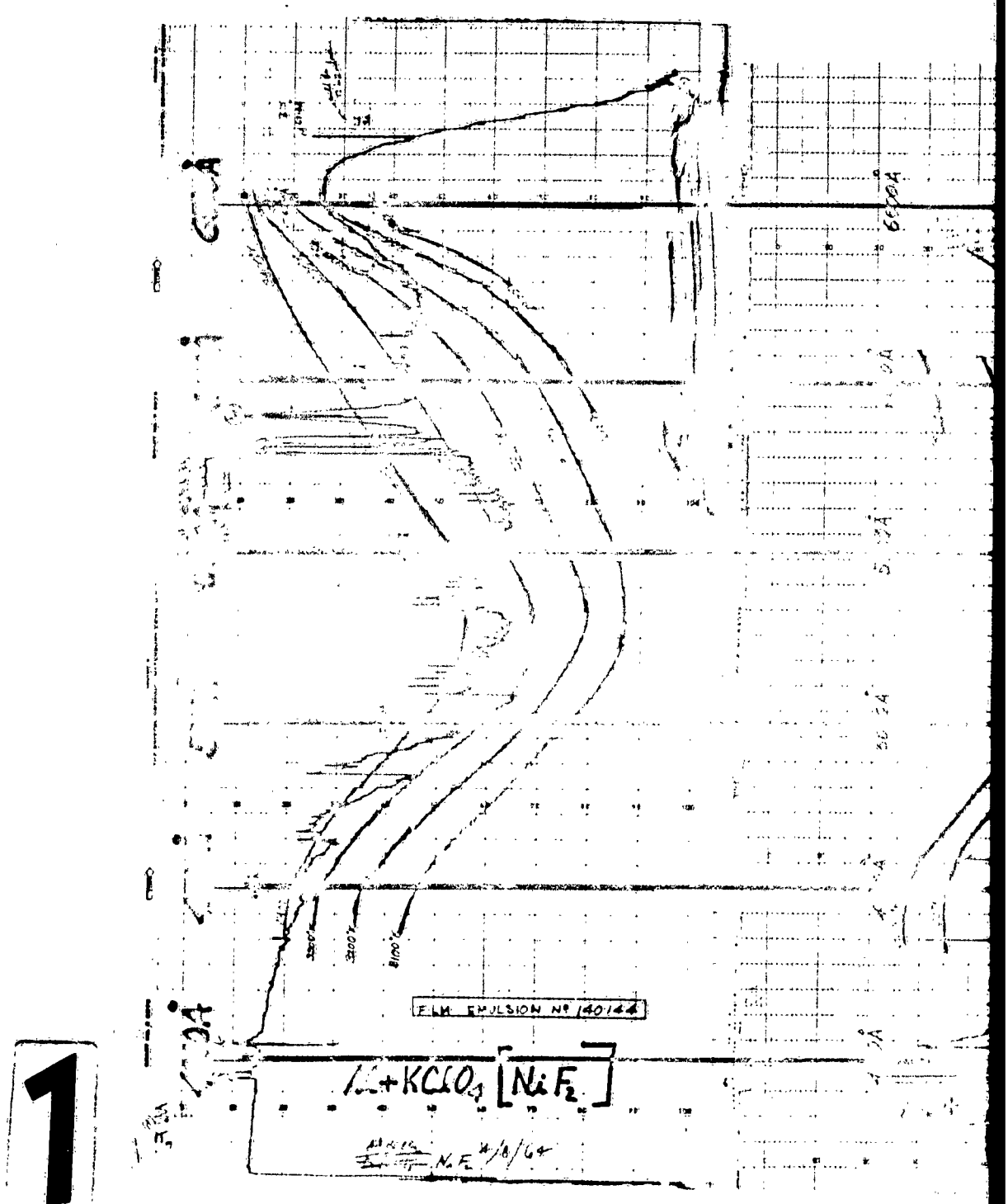

1

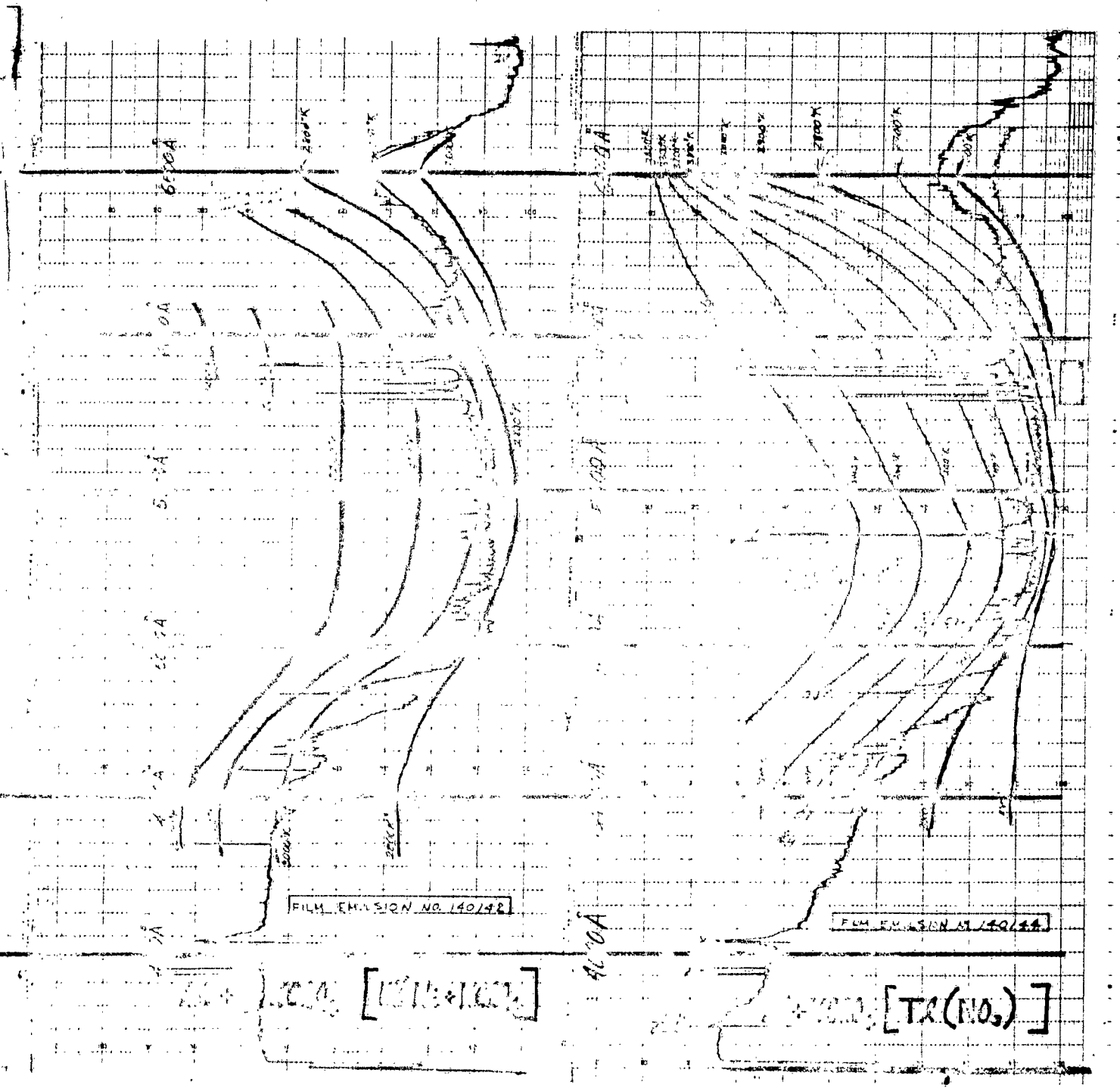

Figure 57. Per Cent Light Transmission vs. Wavelength

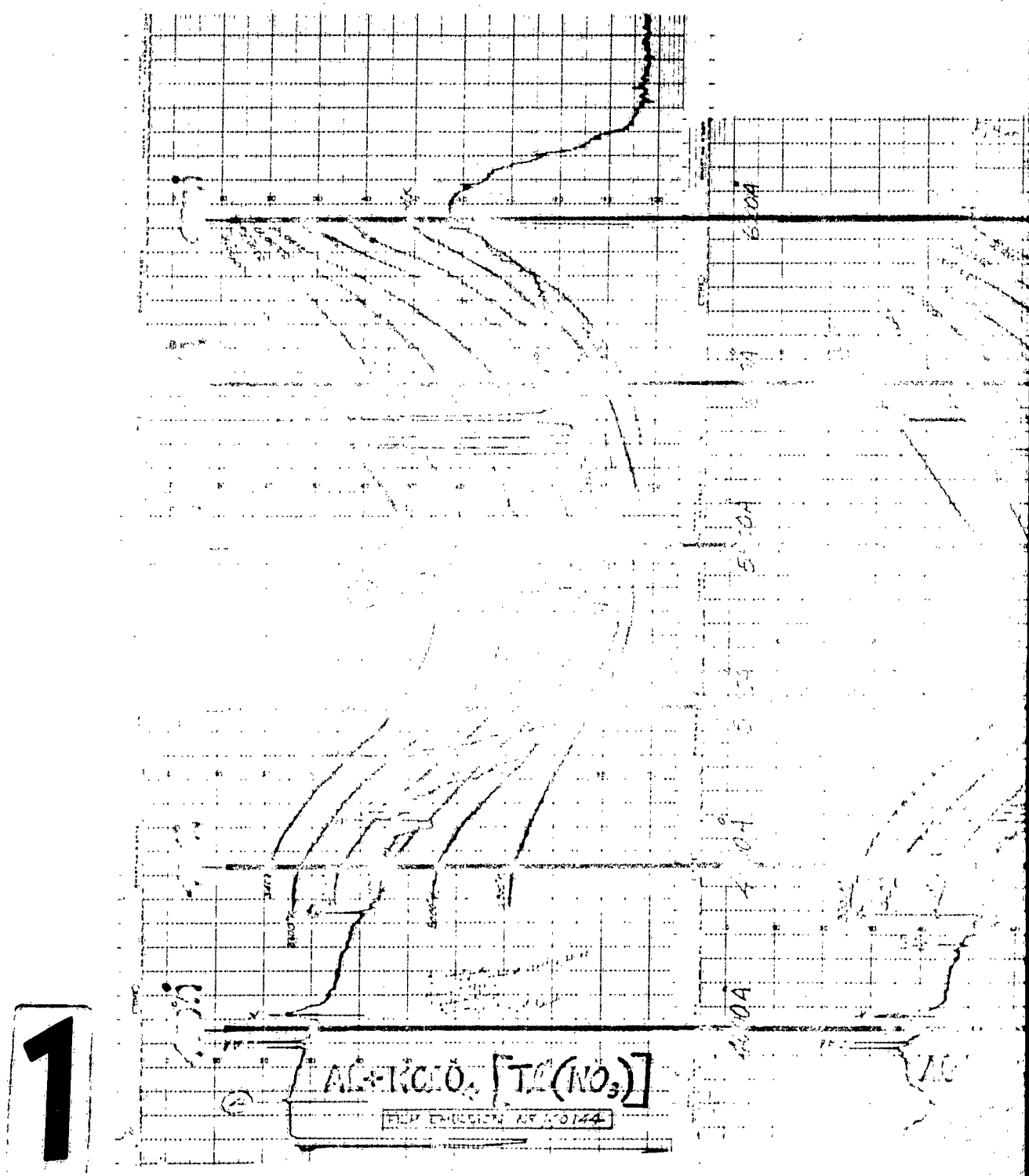
1
Al-Ka1,2 [Tl(NO3)]
FILM EMISSION No. 0144
A
B

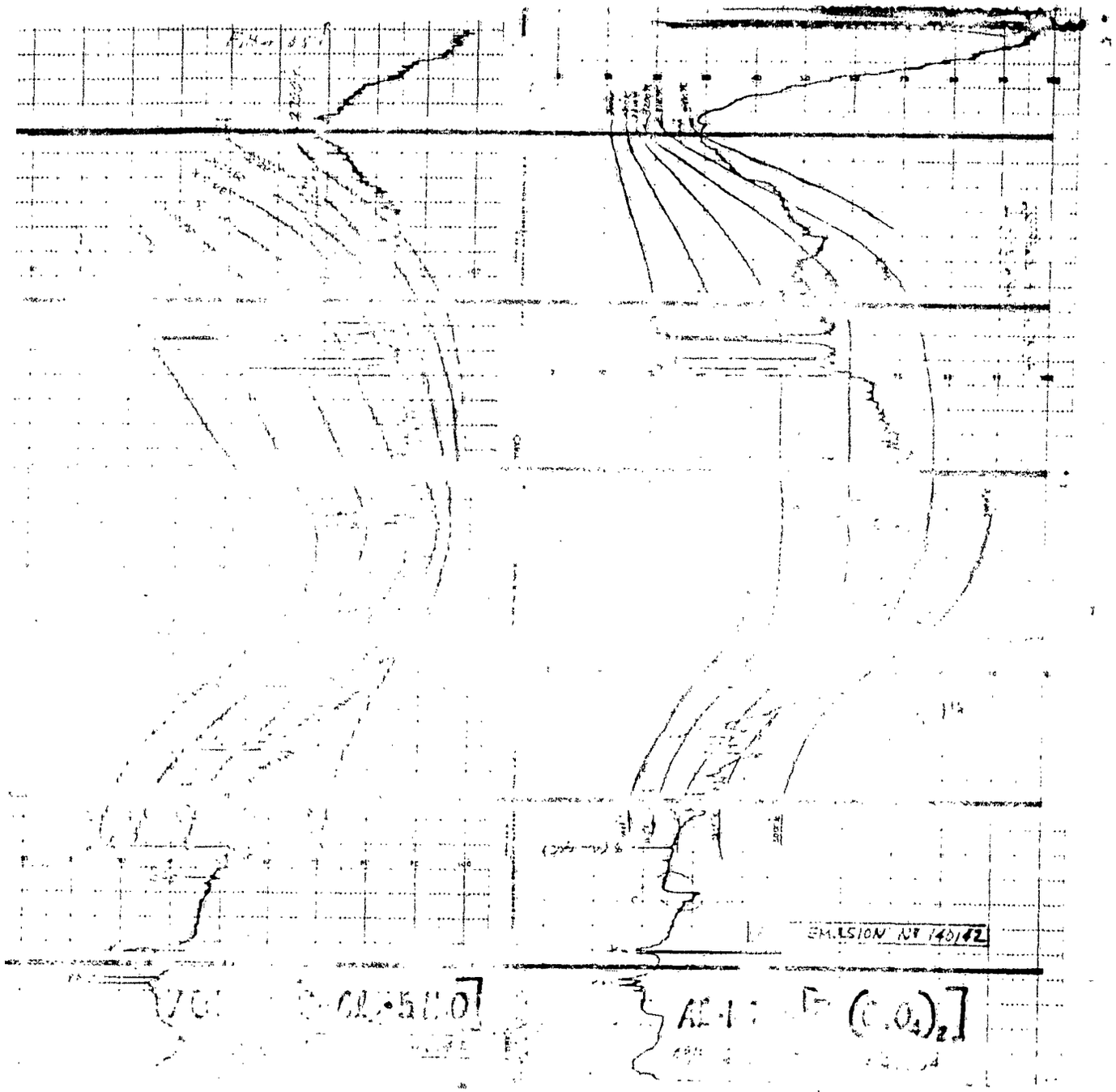

Figure [illegible] Per Cent Light Transmission vs. Wavelength

2

B C

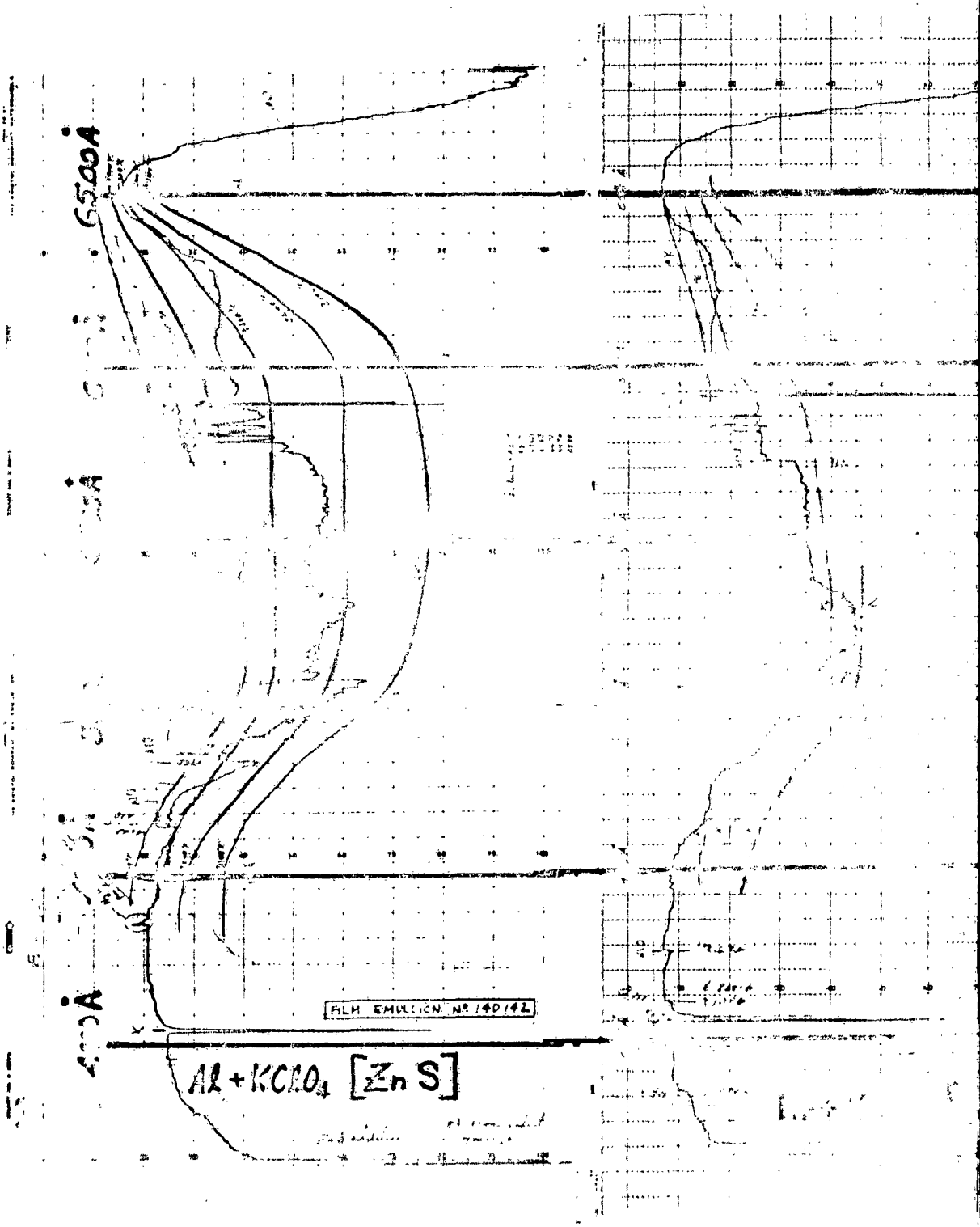

1

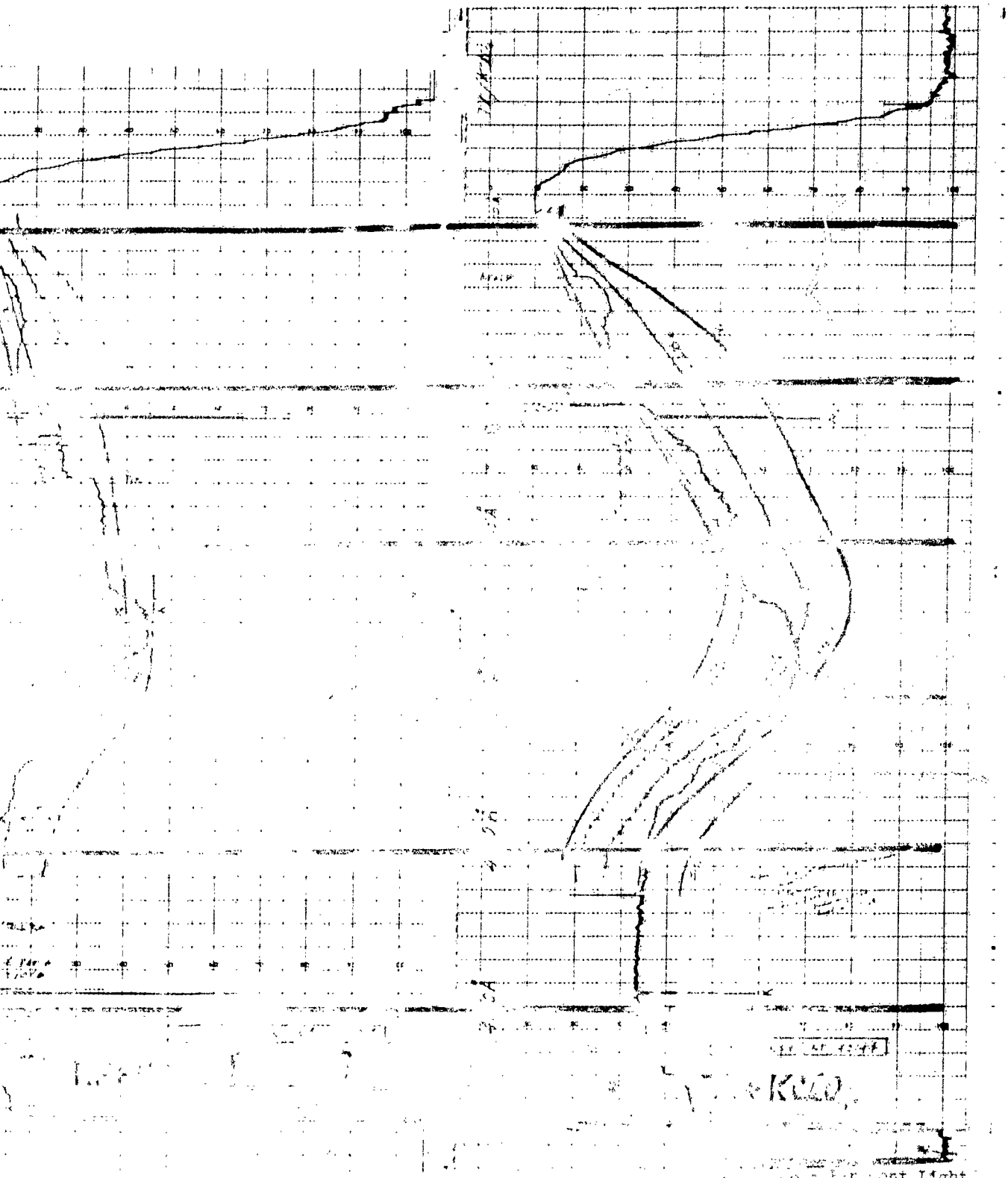

2

B

Curve 50- [illegible] Light Transmission vs. Wavelength

151

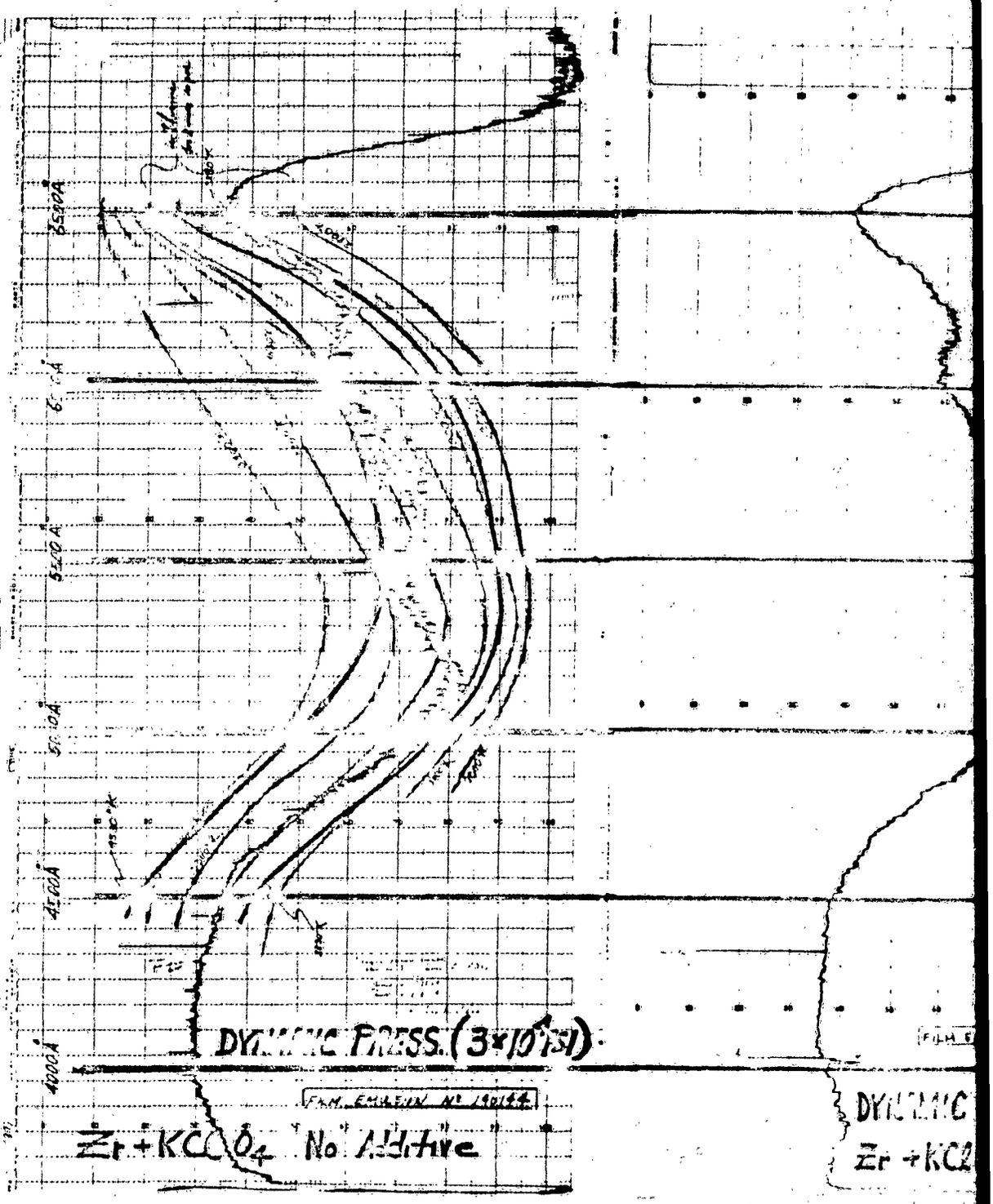
6500Å
5200Å
4100Å
4000Å
DYNAMIC PRESS. (3×10⁴ PSI)
FILM EMULSION Nº 19144
Zr + KClO4 "No Additive"
DYNAMIC
Zr + KCl

1

A

B

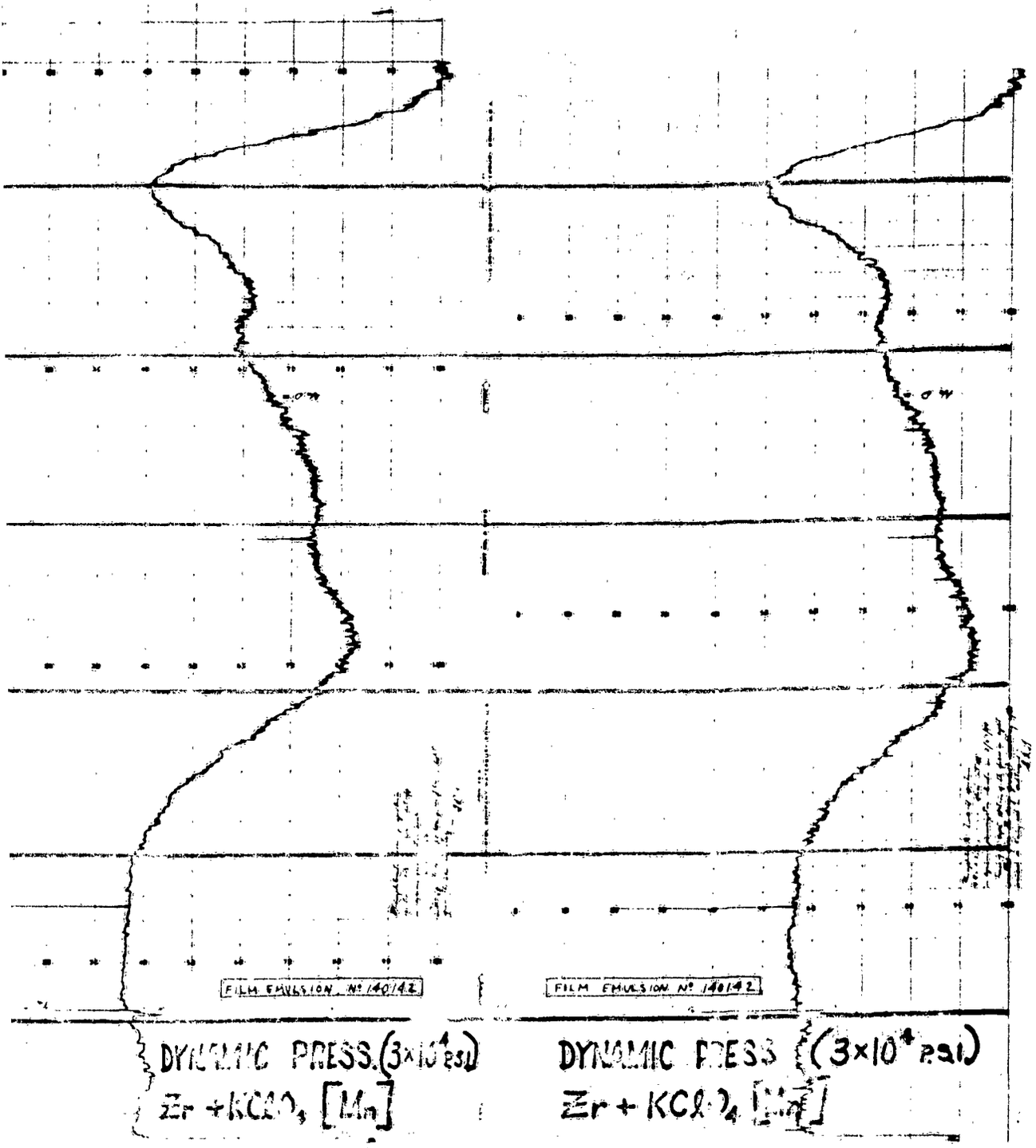

Figure 60. Per Cent Light Transmission vs. Wavelength